



Part A

Results of the benchmark for blade structural models

D. J. Lekou, D. Chortis (CRES)

With the contribution of: A. Belen Fariñas (CENER), C. Amézqueta (CENER), I. Nuin (CENER), C. Pavese (DTU), P. Berring (DTU), K. Branner (DTU), C. L. Bottasso (PoliMi), A. Croce (PoliMi), F. Gualdoni (PoliMi), T. P. Philippidis (UPAT), I. T. Masmanidis (UPAT), G. A. Roukis (UPAT), G. D. de Winkel (WMC), H. Dekker (WMC)

Contribution to deliverable 2.21

October, 2013

Agreement n.:	308974
Duration	60 months from 1st November 2012
Co-ordinator:	Mr Peter Hjuler Jensen
Supported by:	EU 7th Framework Programme

Support by:



PROPRIETARY RIGHTS STATEMENT

This document contains information, which is proprietary to the "INN WIND.EU" Consortium. Neither this document nor the information contained herein shall be used, duplicated or communicated by any means to any third party, in whole or in parts, except with prior written consent of the "INN WIND.EU" consortium.

Document information

Document Name:	Part A: Results of the benchmark for blade structural models
Confidentiality Class	CO
Document Number:	D2.21 Benchmarked aerodynamic-structural design methods
Author:	D. J. Lekou, D. Chortis (CRES)
Review:	XXXXXXXXXXXXXXXX
Date:	9 October 2013
WP:	WP2: Lightweight Rotor
Task:	Task 2.2: Lightweight structural design

TABLE OF CONTENTS

INTRODUCTION	5
2.1 Short description of the benchmark performed by partners	5
GLOBAL BLADE PROPERTIES AND SECTIONAL PROPERTIES	6
2.1 Global blade properties	6
2.2 Sectional properties	6
Mass properties	6
Stiffness properties	9
BLADE STIFFNESS	14
3.1 Natural frequencies analysis	14
3.2 Deflection analysis	14
Deflection analysis for simple load case	15
Deflection for reference load case	18
BLADE STRENGTH	21
4.1 Buckling analysis	21
4.2 Extreme load carrying capacity analysis	21
STRESSES –STRAINS RESULTS	23
5.1 Simple load case	24
5.2 Reference Load Case	31
CONCLUSIONS	34
REFERENCES	35
ANNEX 1: CENER Contribution on the Benchmark of blade structural models.....	36
ANNEX 2: CRES Contribution on the Benchmark of blade structural models.....	57
ANNEX 3: DTU Contribution on the Benchmark of blade structural models.....	79
ANNEX 4: PoliMi Contribution on the Benchmark of blade structural models.....	97
ANNEX 5: UPAT Contribution on the Benchmark of blade structural models.....	111
ANNEX 6: WMC Contribution on the Benchmark of blade structural models.....	122

INTRODUCTION

A benchmark on structural design methods for blades was performed within the InnWind.Eu project under WP2 “Lightweight Rotor” Task 2.2 “Lightweight structural design”. The present document describes the results of the comparison simulation runs that were performed by the partners involved within Task 2.2 of the InnWind.Eu project. The benchmark is based on the reference wind turbine and the reference blade provided by DTU [1]. "Structural Concept developers/modelers" of WP2 were provided with the necessary input for a comparison numerical simulation run, upon definition of the reference blade [2]. Output is compared in here in terms of weight, stiffness, natural frequencies, deflection (extreme load) and strength & stability (extreme load).

2.1 Short description of the benchmark performed by partners

CENER, CRES, DTU, PoliMi, UPAT and WMC (in alphabetical order) participated in the benchmark on structural analysis tools for wind turbine blades. Within the benchmark results on blade model data were provided as well as results of modal analysis, static analysis and extreme strength analysis. These will be presented in comparison in the following. The individual reports of the partners are available in the respective annexes.

The results provided by each participant in the benchmark were estimated by different tools by the partners, as shown in Table 1. All partners used commercial finite element software indicated by FEM in the table to provide part (or all) of the data. In the table by 3D FEM finite element models using shell elements are implied, 2D FEM implies the use of beam elements and 4D FEM implies use of solid elements. The FE software used by the partners was for CRES NISA II (EMRC), for CENER MSC.Patran was used for modelling in combination with MSC. Nastran solver, DTU also used MSC.Patran for modelling in combination with the in-house tool BMT, but MSC.Marc was used as the solver. MSC.Marc was also used as a solver for the buckling analysis using commercial FE software by WMC. PoliMi used MSC Nastran 2011 for data extracted by FE models, while UPAT used ANSYS. In house developed tools which were used for extraction of data by the partners are explicitly mentioned in the following table. Details of the tools used by each partner are provided in the relevant Annexes containing reports from each participant in the benchmark.

Table 1. *Tools used by partners*

Results for	CRES	CENER	DTU	POLIMI	UPAT	WMC
Global blade properties	3D FEM	2D FEM	4D FEM	3D FEM	3D FEM	FOCUS6
Natural frequencies	3D FEM	2D FEM	4D FEM	3D FEM	3D FEM	FOCUS6
Buckling analysis	3D FEM		4D FEM	3D FEM	3D FEM	3D FEM+ FOCUS6
Section properties	THIN	BASSF		ANBA	PROBUST	FOCUS6
Displacements	3D FEM	2D FEM	4D FEM	3D FEM	3D FEM	FOCUS6
Strength analysis	3D FEM + THIN	BASSF	4D FEM	3D FEM	3D FEM + PROBUST	FOCUS6
Strains	3D FEM	BASSF	4D FEM	3D FEM	3D FEM	FOCUS6
Stresses	3D FEM + THIN	BASSF	4D FEM	3D FEM	3D FEM	FOCUS6

GLOBAL BLADE PROPERTIES AND SECTIONAL PROPERTIES

2.1 Global blade properties

The results provided by the partners for the global blade properties are shown in the following table. Results for the total blade mass and the centre of gravity along the length of the blade are in good agreement. The three last columns of the table show the mean value, the standard deviation and the coefficient of variation, i.e. the standard deviation over the average value in per cent, of the data provided by the partners. A coefficient of variation of less than 1% is obtained for the total mass and of 1.5% for the centre of gravity with respect to the blade length. The results for the centre of gravity relative to the flap direction show a standard deviation of 0.03m (30mm) and in the edge direction 0.005m (5mm).

Taking into account the different modelling approaches employed the results are in very good agreement.

Table 2. *Global blade properties*

Property	CRES	CENER	DTU	POLIMI	UPAT	WMC	Average	StDev	COV (%)
Mass (kg)	42362.7	41880.4	42894.0	42262.4	42379.0	42649.4	42405.13	345.430	0.8
C.G. z (m)	28.802	28.518 ¹	28.153	29.421 ¹	28.802	28.912	28.769	0.4220	1.5
C.G. x (m)	-0.157	-	-0.167	-0.086	-0.158	-0.137	-0.141	0.0326	-23.2
C.G. y (m)	0.035	-	0.047	0.034	0.035	0.036	0.037	0.0054	14.5

2.2 Sectional properties

Mass and stiffness sectional properties were requested to compare data that are provided for performing an aeroelastic analysis upon structural design information of the blade. The data should be provided with respect to the global coordinate system, although each participant uses its own reference system. This request lead to larger deviations for properties that are affected by the selection of reference points and coordinate systems, such as the coordinates of the mass and/or elastic centre on the section and the properties incorporating the 2nd moment of inertias. Mass and stiffness properties were submitted for 5 reference sections dispersed along the blade length. Reference section 1 (Sec_1) is the circular root of the blade. In this part the results of three sections are compared, namely reference section 1, i.e. the root section, section 2, which is close to the maximum chord section, and section 4, which is at about 60% of the blade length.

Mass properties

The mass related properties of reference blade sections 1, 2 and 4 are presented in Table 3 to Table 5, respectively. PoliMI for the computation of the mass properties has modelled the core as a concentrated non-structural mass placed on the reference z-axis, therefore the mass moment of inertia accounts for the contribution only of the structural mass. DTU provided the data for the mass moment of inertia on the centre of gravity, while UPAT provided the data for the mass moment of inertia on axis parallel to the global, but on the elastic centre of the section. Thus, differences were shown in comparison to the results of the other partners. Therefore, the results in the following

¹ Shown value in global coordinate system

tables have been transformed to the global coordinate system, using the parallel axis theorem for the data provided by DTU and UPAT. This transformation brings the results closer; yet, still differences due to the different reference point and coordinate system used by all partners are evident.

Table 3. Mass properties of reference blade section 1 (Sec_1)

Property		CRES	CENER	DTU	POLIMI	UPAT	WMC
Z-position	(m)	2.8	2.8000	2.8000	2.8000	2.8000	2.8000
Mass/Length	(kg/m)	1210.00	1213.40	1232.40	1209.38	1201.00	1202.70
Mass Centre	x (m)	-0.0032	-0.0247	0.0070	-0.0107	-0.0032	0.0000
	y (m)	0.0010	0.0071	0.0270	-0.0002	0.0010	0.0010
Mass moment of inertia w.r.t. Global CS	ρI_{xx} (kg-m)	4140.01	4045.70	4177.06	3855.36	4051.01	4060.00
	ρI_{yy} (kg-m)	3803.00	3815.90	3815.90	3675.47	3716.00	3730.00
	ρI_{xy} (kg-m)	-0.7616	-20.8864	-0.5391	24.26	-1.1878	-4.8380
Polar mass inertia w.r.t. Global CS	ρI_p (kg-m)	7943.01	7861.63	7992.96	7530.69	7767.013	7789.00

Table 4. Mass properties of reference blade section 2 (Sec_2)

Property		CRES	CENER	DTU	POLIMI	UPAT	WMC
Z-position	(m)	26.694	26.6940	26.6940	26.6940	26.6940	26.6940
Mass/Length	(kg/m)	640.8	642.91	639.70	659.44	632.2000	647.47
Mass Centre	x (m)	-0.2981	-0.3283	-0.3110	-0.0734	-0.2872	-0.2710
	y (m)	0.0803	0.0849	0.0870	0.0431	0.0821	0.0810
Mass moment of inertia w.r.t. Global CS	ρI_{xx} (kg-m)	608.24	515.04	577.87	498.21	549.27	523.60
	ρI_{yy} (kg-m)	1684.13	1765.80	1648.84	1199.75	1634.82	1693.00
	ρI_{xy} (kg-m)	-229.20	-240.32	215.59	-120.58	-238.06	-225.40
Polar mass inertia w.r.t. Global CS	ρI_p (kg-m)	2292.376	2280.80	2226.71	1693.17	2184.09	2216.00

Table 5. Mass properties of reference blade section 4 (Sec_4)

Property		CRES	CENER	DTU	POLIMI	UPAT	WMC
Z-position	(m)	54.149	54.1490	54.1490	54.1490	54.1490	54.1490
Mass/Length	(kg/m)	342.6	333.43	328.40	351.03	336.90	345.20
Mass Centre	x (m)	-0.1653	-0.1746	-0.1420	-0.0124	-0.1818	-0.1430
	y (m)	0.0319	0.0275	0.0350	0.0243	0.0378	0.0350
Mass moment of inertia w.r.t. Global CS	ρI_{xx} (kg-m)	77.82	57.93	65.39	59.75	61.50	61.82
	ρI_{yy} (kg-m)	366.75	346.12	323.20	275.34	363.3746	360.80
	ρI_{xy} (kg-m)	-19.51	-18.69	15.69	-7.99	-20.02	-17.47
Polar mass inertia w.r.t. Global CS	ρI_p (kg-m)	444.5699	404.05	388.59	334.83	424.87	422.60

In graphical form a comparison of the mass related properties of all sections provided is shown in the following figures. It is clearly seen that whenever the property depends on the coordinate system and the point of reference differences are greater. The difference sign for ρI_{xy} could be due to an erroneous interpretation of the reference coordinate system DTU delivered data during the transformation for the comparison.

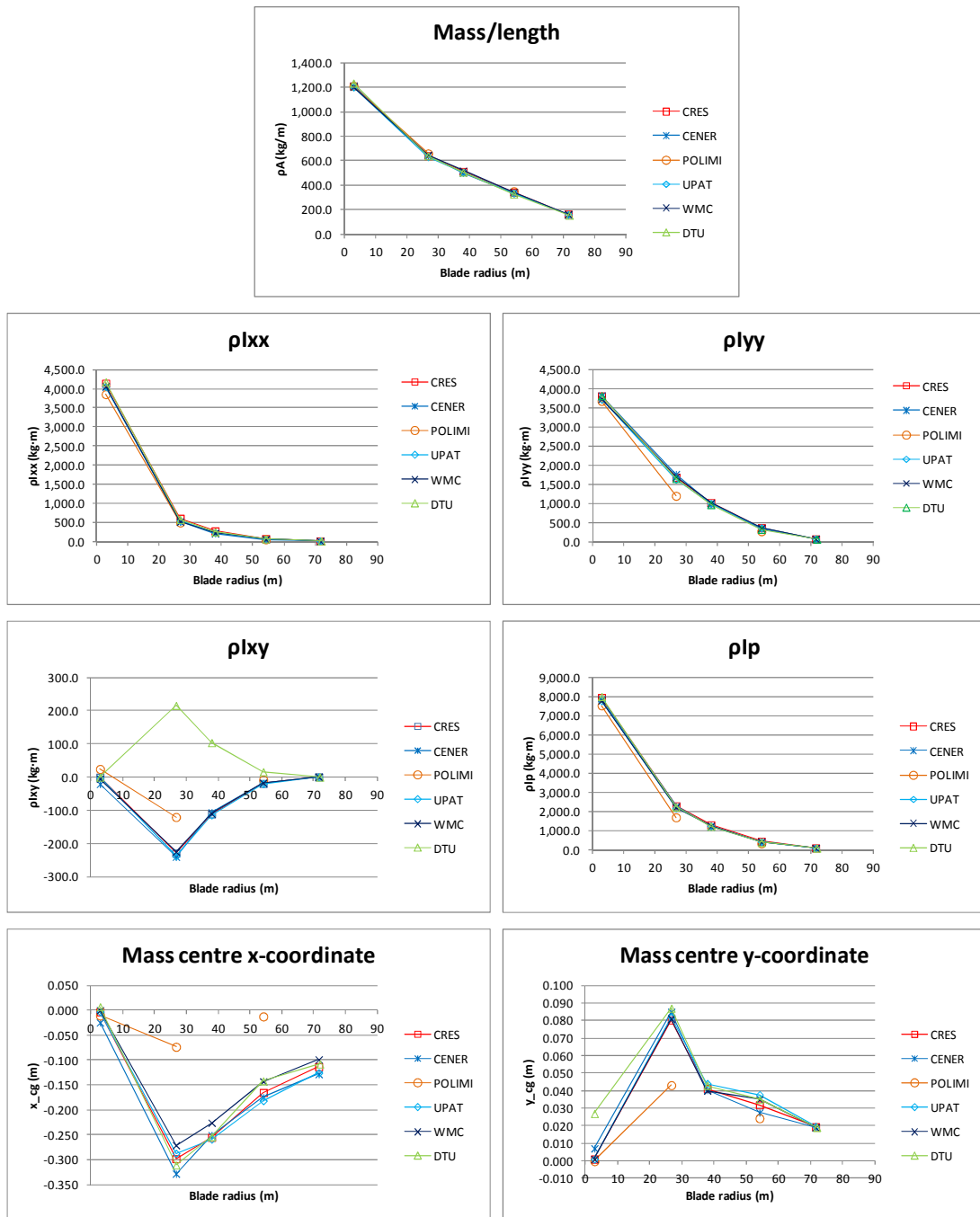


Figure 1. Mass related properties of reference sections (from top to bottom: Linear mass, mass moment of inertia with respect to the global x and y axis and coupling term, polar mass moment of inertia and mass centre in x and y axis of global coordinate system)

Table 6 shows the average value and the coefficient of variation among the partners' data, as a measure of dispersion, for the mass related properties of three reference sections (Sec_1, Sec_2 and Sec_4). The coefficient of variation for the linear mass ranges from below 1% to 2.5%, while the range for the coefficient of variation of the mass moment of inertia in the flap and edge direction is 2% to 13%. As already noted the dispersion of the mass centre coordinates and the coupling term of the mass moment of inertia, which depend on the coordinate system and are small values, is larger. The standard deviation of the mass centre in the edge (chord) direction reaches 0.094m for

reference section 2, while the standard deviation on the same section in the flap (thickness) direction reaches 0.017m.

Table 6. Average and dispersion of mass properties on Reference Sec_1, 2 & 4

Property		Average			Coefficient of variation		
		Sec_1	Sec_2	Sec_4	Sec_1	Sec_2	Sec_4
Z-position	(m)	2.800	26.694	54.149	2.800	26.694	54.149
Mass/Length	(kg/m)	1211.481	643.754	339.593	0.9%	1.4%	2.4%
Mass moment of inertia w.r.t. Global CS	ρI_{xx} (kg·m)	4054.857	545.373	64.034	2.7%	7.6%	11.2%
	ρI_{yy} (kg·m)	3759.378	1604.391	339.265	1.6%	12.7%	10.4%
	ρI_{xy} (kg·m)	-0.659	-139.663	-11.333	-2197.4%	-128.8%	-123.3%
Polar mass inertia w.r.t. Global CS	ρI_p (kg·m)	7814.051	2148.858	403.253	2.1%	10.6%	9.6%
Mass Centre	x (m)	-0.0058	-0.2615	-0.1365	-187.7%	-36.0%	-46.1%
	y (m)	0.0062	0.0764	0.0319	171.3%	21.6%	16.1%

Stiffness properties

Sectional stiffness properties of reference blade sections are presented in Table 7 to Table 9 for reference sections 1, 2 and 4, respectively. As for the mass properties, UPAT provided all data except for the coordinates of the elastic centre on an axis parallel to the global, but on the elastic centre of the section. Again, differences were noted in the provided values of all partners. To facilitate data comparison the data of UPAT were transformed to the global coordinate system, as in the case of the mass properties. Still, as with the mass related properties, the properties with the largest dispersion are the coordinates for elastic centre and shear centre, as well as the coupling term of the bending stiffness. This is clearer seen in Figure 2 and Figure 3, where the properties are compared for all sections.

Table 7. Stiffness properties of reference blade section 1 (Sec_1)

Property		CRES	CENER	DTU	POLIMI	UPAT	WMC
Z-position	(m)	2.800	2.800	NA	2.800	2.800	2.800
Axial Stiffness	EA (N)	1.81E+10	1.81E+10		1.81E+10	1.80E+10	1.78E+10
Elastic Centre	x (m)	-0.0035	-0.0275		-0.0112	-0.0035	0.0040
	y (m)	0.0010	0.0077		-0.0002	0.0010	-0.0006
Bending Stiffness w.r.t Global CS	$E I_{xx}$ (Nm ²)	6.44E+10	6.30E+10		6.35E+10	6.30E+10	6.26E+10
	$E I_{yy}$ (Nm ²)	6.29E+10	6.26E+10		6.21E+10	6.14E+10	6.08E+10
	$E I_{xy}$ (Nm ²)	-1.22E+07	-3.50E+08		1.64E+08	-1.63E+07	2.07E+07
Shear Centre	x (m)	-0.0025	0.0362		0.0188	0.0035	0.0270
	y (m)	0.0009	-0.0130		0.0012	-0.0090	-0.0010
Torsional Stiffness	GJ (Nm ²)	2.85E+10	2.70E+10		2.79E+10	2.81E+10	2.63E+10
Shear Stiffness	S_x (N)				2.53E+09		1.95E+09
	S_y (N)				1.95E+09		2.57E+09

Table 8. Stiffness properties of reference blade section 2 (Sec_2)

Property		CRES	CENER	DTU	POLIMI	UPAT	WMC
Z-position	(m)	26.694	26.694		26.694	26.694	26.694
Axial Stiffness	EA (N)	9.34E+09	9.51E+09		9.69E+09	9.23E+09	9.29E+09
Elastic Centre	x (m)	-0.1482	-0.1672		-0.0368	-0.1343	-0.1420
	y (m)	0.0535	0.0581		0.0405	0.0558	0.5600
Bending Stiffness w.r.t Global CS	El _{xx} (Nm ²)	9.77E+09	9.12E+09		9.37E+09	9.06E+09	8.91E+09
	El _{yy} (Nm ²)	2.18E+10	2.40E+10		1.94E+10	2.11E+10	2.17E+10
	El _{xy} (Nm ²)	-3.04E+09	-3.34E+09		-1.71E+09	-3.01E+09	-2.92E+09
Shear Centre	x (m)	0.4537	0.4440		0.5160	0.4747	0.5820
	y (m)	0.0653	0.0689		0.0754	0.0678	0.0560
Torsional Stiffness	GJ (Nm ²)	2.05E+09	1.69E+09		2.17E+09	1.90E+09	1.73E+09
Shear Stiffness	S _x (N)				7.27E+08		7.03E+08
	S _y (N)				5.60E+08		4.72E+08

Table 9. Stiffness properties of reference blade section 4 (Sec_4)

Property		CRES	CENER	DTU	POLIMI	UPAT	WMC
Z-position	(m)	54.149	54.149		54.149	54.149	54.149
Axial Stiffness	EA (N)	5.46E+09	5.37E+09		5.51E+09	5.37E+09	5.39E+09
Elastic Centre	x (m)	-0.0111	-0.0190		0.0461	-0.0282	-0.0100
	y (m)	0.0200	0.0118		0.0217	0.0200	0.0260
Bending Stiffness w.r.t Global CS	El _{xx} (Nm ²)	1.28E+09	1.09E+09		1.15E+09	1.09E+09	1.12E+09
	El _{yy} (Nm ²)	4.68E+09	4.54E+09		4.26E+09	4.68E+09	4.62E+09
	El _{xy} (Nm ²)	-2.43E+08	-2.31E+08		-7.38E+07	-2.25E+08	-2.14E+08
Shear Centre	x (m)	0.3058	0.2533		0.3544	0.2918	0.3910
	y (m)	0.0184	0.0465		0.0524	0.0220	0.0260
Torsional Stiffness	GJ (Nm ²)	2.49E+08	1.86E+08		2.59E+08	2.25E+08	2.08E+08
Shear Stiffness	S _x (N)				3.43E+08		3.43E+08
	S _y (N)				2.29E+08		1.84E+08

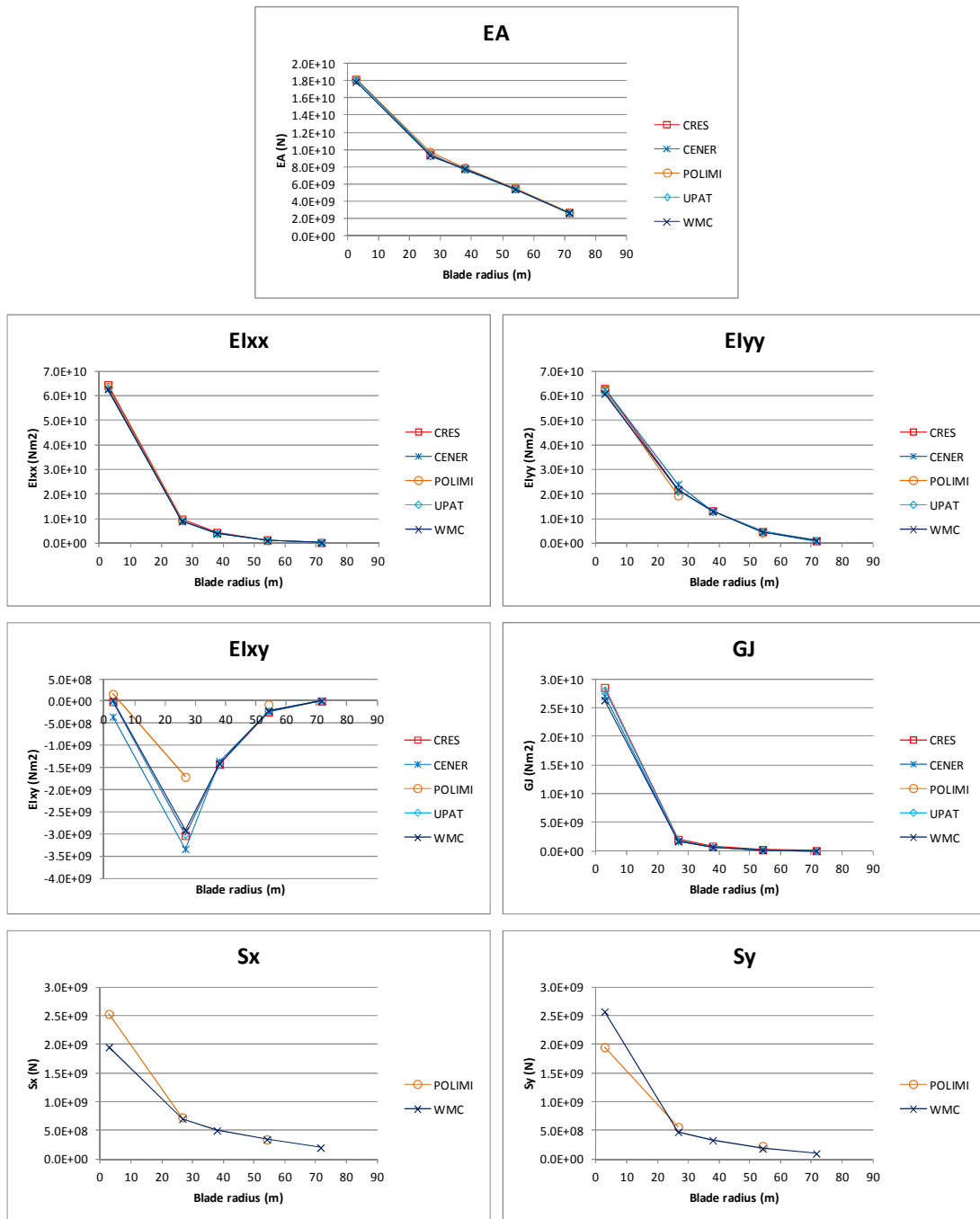


Figure 2. Stiffness related properties of reference sections (from top to bottom: Axial stiffness, bending stiffness with respect to the global x and y axis and coupling term, torsional stiffness and shear stiffness in global x and y axis)

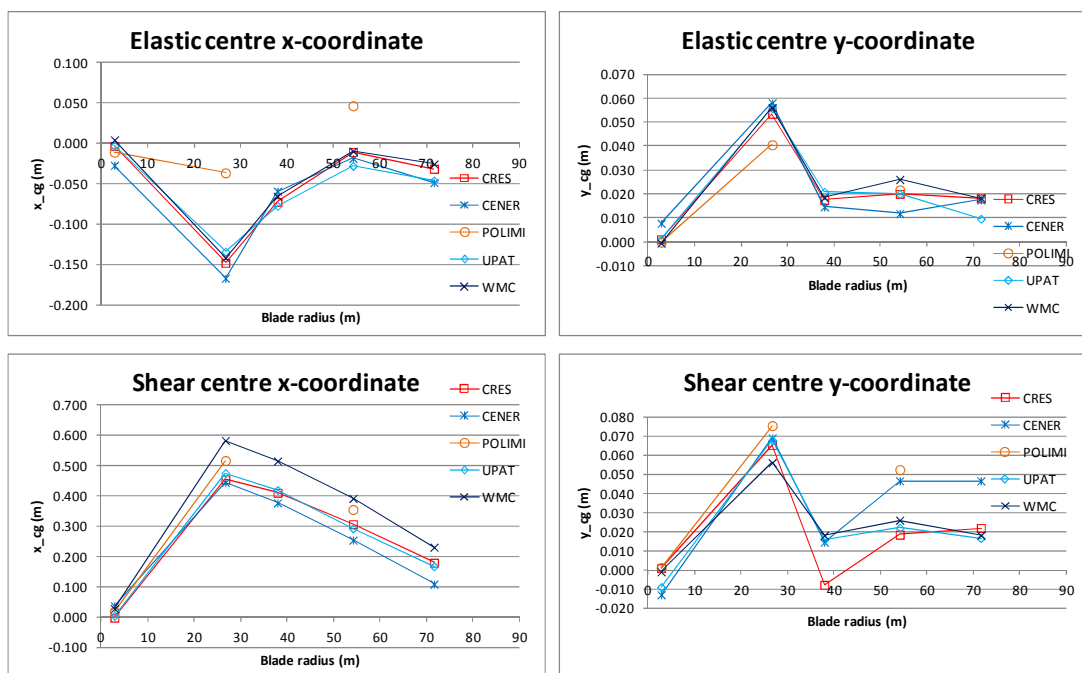


Figure 3. Stiffness related properties of reference sections (from top to bottom: elastic and shear centre location in x and y axis of global coordinate system)

Table 10 presents the average and dispersion of the data provided by the participants regarding the stiffness properties of reference sections 1, 2 and 4. From the table it can be concluded that the axial stiffness has a dispersion ranging from 1% to 2% around the mean value, the bending stiffness in the flap and edge direction and the torsional stiffness show a coefficient of variation between 1% and 13%, with the maximum dispersion in these cases being the torsional stiffness. Only two participants reported on shear stiffness. The values differ for the root section, but for the other sections their difference is close to the difference of the torsional stiffness.

Regarding the location of the elastic centre on the section, the standard deviation of the reported values is less than 0.05m in the x direction (chord) and less than 0.01m in the y direction (thickness). A strong deviation from the other partners is noted in the x-location for PoliMi.

For the shear centre, the dispersion of results is a little larger than that of the elastic centre, but comparable. The standard deviation in this case is less than 0.06m (for the x direction).

Table 10. Average and dispersion of stiffness properties on Reference Sec_1, 2 & 4

Property		Average			Coefficient of variation (%)		
		Sec_1	Sec_2	Sec_4	Sec_1	Sec_2	Sec_4
Z-position	(m)	2.800	26.694	54.149	2.800	26.694	54.149
Axial Stiffness	EA (N)	1.802E+10	9.412E+09	5.422E+09	0.7%	2.0%	1.1%
Bending Stiffness w.r.t Global CS	El _{xx} (Nm ²)	6.329E+10	9.245E+09	1.146E+09	1.1%	3.6%	6.7%
	El _{yy} (Nm ²)	6.196E+10	2.161E+10	4.557E+09	1.4%	7.6%	3.9%
	El _{xy} (Nm ²)	-3.875E+07	-2.803E+09	-1.973E+08	-487.4%	-22.5%	-35.4%
Torsional Stiffness	GJ (Nm ²)	2.757E+10	1.908E+09	2.253E+08	3.2%	10.7%	13.2%
Shear Stiffness	S _x (N)	2.240E+09	7.150E+08	3.430E+08	18.3%	2.4%	0.0%
	S _y (N)	2.260E+09	5.160E+08	2.065E+08	19.4%	12.1%	15.4%
Elastic Centre	x (m)	-0.0083	-0.1257	-0.0044	-143.6%	-40.7%	-656.8%
	y (m)	0.0018	0.0528	0.0199	190.2%	13.4%	25.9%
Shear Centre	x (m)	0.0166	0.4941	0.3193	97.0%	11.4%	16.9%
	y (m)	-0.0042	0.0667	0.0331	-154.6%	10.5%	46.3%

The location of the mass, elastic and shear centre is shown in Figure 4 for reference section 2 and Figure 5 for reference section 4 with respect to the section's dimensions. The dispersion in prediction of the location of the shear centre is clearly evident in these figures, in relation to the elastic centre, where estimations are closer and mass centre, where data are in good agreement.

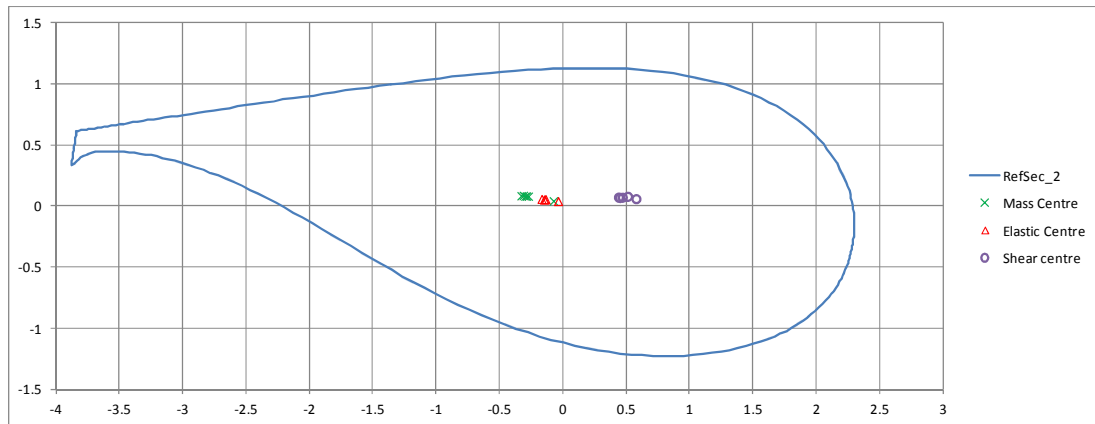


Figure 4. Location of mass, elastic and shear centre on reference section 2

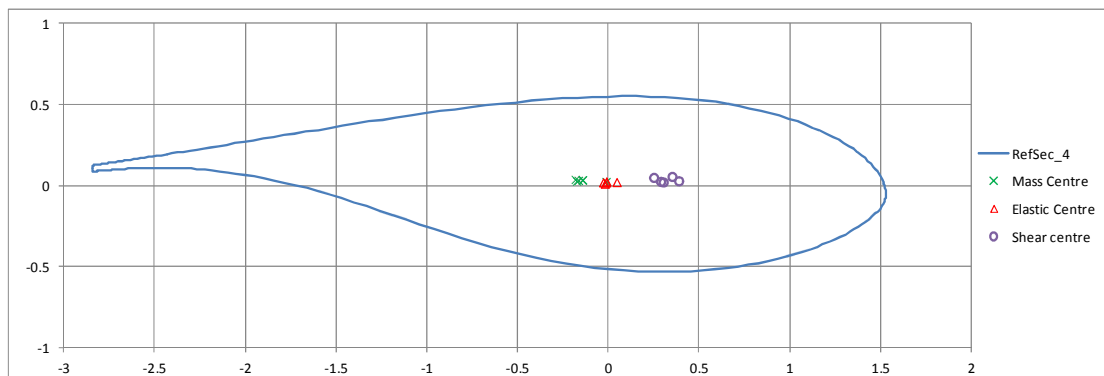


Figure 5. Location of mass, elastic and shear centre on reference section 4

BLADE STIFFNESS

3.1 Natural frequencies analysis

The first six natural frequencies of the blade are presented in Table 1. Results are in very good agreement up to and including the 5th mode of vibration. For most of the partners modes 1, 3 and 5 correspond to the first three bending natural frequencies in the flap direction, whereas modes 2, 4 refer to the first two bending natural frequencies in the edge direction of the structure. Results of CRES, DTU and WMC, where the mode shapes are presented with respect to both x and y axis for each mode reveal the existence of a small coupling between the flapwise and the edgewise mode-shapes of the blade. For DTU, the 6th mode is a torsional mode and judging from the mode shapes provided, so is this for UPAT and WMC. CRES provided also the 7th mode, which corresponds to the torsional mode of the blade, according to the partner's results. CENER provided modes normalized in each direction, thus, no conclusions can be made on coupling in the edge and flap direction.

Table 11. *Natural frequencies of the blade (all frequencies in Hz)*

Mode (#)	CRES	CENER	DTU	POLIMI	UPAT	WMC	Average	StDev	COV (%)
1	0.640	0.624	0.615	0.612	0.609	0.616	0.619	0.0113	1.8
2	0.959	1.013	0.980	0.912	0.948	0.974	0.964	0.0339	3.5
3	1.849	1.804	1.750	1.743	1.749	1.798	1.782	0.0421	2.4
4	2.863	3.023	2.889	2.769	2.833	2.975	2.892	0.0933	3.2
5	3.764	3.770	3.531	3.552	3.571	3.774	3.660	0.1201	3.3
6	5.823	6.239	5.492	5.669	5.551	6.170	5.824	0.3165	5.4
7	6.011								

For the first mode of vibration (flap direction) the coefficient of variation among the partners' results is 1.8%, while for the second mode of vibration (in the edge direction) the coefficient of variation is 3.5%. The coefficient of variation for the modes 3-5 are in between the first two modes. The results for the 6th mode of vibration lead to a coefficient of variation of 5.4%. A similar coefficient of variation (5.8%) and a comparable average value (5.806Hz) is obtained if the torsional modes of vibration (of CRES, DTU, UPAT and WMC) are treated disregarding the mode number.

3.2 Deflection analysis

Deflection analysis has been performed for two load cases. The first refers to the simple load case, which was used for comparing the overall stiffness of the modeling. The second refers to the reference load case, which was mainly employed to reveal differences in the modeling of the loads acting on the blade, as these are provided to the partners after aeroelastic analysis. For the two loading cases, the tip deflection and the deflection at 4 specific reference sections was asked to be provided by the benchmark participants. In turn it was requested to provide for each reference section the deflections on 4 key points.

Deflection analysis for simple load case

Table 12 to Table 14 present the results for the simple load case and, respectively, for key points 1 (on the trailing edge of the blade), 5 (on the pressure side on the location of the shear web) and 9 (on the leading edge) of the section at the tip of the blade.

It should be noted POLIMI reported the displacement only for a centre node on the tip section, while the analysis tool used by CENER (FE model using beam elements) only provides the displacement in the x and y axis.

For load application in the simple case, DTU used multi-point constraints of type RB3, with the master node located at the centre of the load carrying box of each section. Further to that, DTU performed a non-linear geometric analysis and for comparison purposes reported also the values at 5% load scaled to full load.

The results for displacement in the z-direction of DTU stand out, with the linear case, being one order of magnitude larger than the other participants and for the non-linear case, the displacement in the z-direction approaches in magnitude that in the x-direction.

Table 12. Tip deflection for simple load case (key point 1)

Partner	X (m)	Y (m)	Z (m)	Notes
CRES	3.242	18.323	0.046	
CENER	3.250	20.661		2D beam
DTU (linear)	3.417	20.906	-0.166	Load applied through MCP
DTU (non-linear)	3.341	18.885	-3.829	Non-linear analysis
POLIMI	2.671	19.378	0.011	Center node
UPAT	3.425	20.508	0.051	
WMC	3.373	20.077	0.052	

Table 13. Tip deflection for simple load case (key point 5)

Partner	X (m)	Y (m)	Z (m)	Notes
CRES	3.241	18.318	0.045	
CENER	3.250	20.661		2D beam
DTU (linear)	3.417	20.903	-0.178	Load applied through MCP
DTU (non-linear)	3.340	18.873	-3.837	Non-linear analysis
POLIMI	2.671	19.378	0.011	Center node
UPAT	3.424	20.504	0.052	
WMC	3.372	20.057	0.039	

Table 14. Tip deflection for simple load case (key point 9)

Partner	X (m)	Y (m)	Z (m)	Notes
CRES	3.242	18.316	-0.012	
CENER	3.250	20.661		2D beam
DTU (linear)	3.417	20.900	-0.242	Load applied through MCP
DTU (non-linear)	3.340	18.851	-3.891	Non-linear analysis
POLIMI	2.671	19.378	0.011	Center node
UPAT	3.425	20.501	-0.013	
WMC	3.376	20.044	-0.011	

Table 15 shows the displacement under the simple load case for key point 5 of reference section 2. For this case the results are in very good agreement. Table 16 collects the results of the displacement in the y-direction (flap) at key point 13 for all reference sections along the blade. Results are in good agreement, with a coefficient of variation of 4.6% for the reference section 5. Similar in Table 17 the results for the displacement in the x-direction (edge) are shown for all reference sections. The differences are in the order of 8% for reference section 5.

Table 15. Deflection for simple load case (key point 5), RefSection_2

Partner	X (m)	Y (m)	Z (m)
CRES	0.167	0.387	0.054
CENER	0.169	0.403	0.000
DTU (linear)	0.161	0.383	0.057
DTU (non-linear)	0.160	0.378	0.050
POLIMI	0.162	0.402	0.054
UPAT	0.173	0.397	0.057
WMC	0.175	0.402	0.057

Table 16. Deflection in flap direction for simple load case (key point 13)

Section	Position (m)	CRES	CENER	DTU	DTU (non-linear)	POLIMI	UPAT	WMC
RefSection_2	26.694	0.387	0.403	0.384	0.375	0.392	0.400	0.402
RefSection_3	37.907	1.221	1.259	1.285	1.240	1.230	1.282	1.292
RefSection_4	54.149	3.868	4.132	4.239	4.036	3.970	4.180	4.167
RefSection_5	71.592	9.503	10.505	10.903	10.229	9.960	10.680	10.532
Tip	89.166	18.318	20.661	20.902	18.850	19.378	20.504	20.057

Table 17. Deflection in edge direction for simple case (key point 13)

Section	Position (m)	CRES	CENER	DTU	DTU (non-linear)	POLIMI	UPAT	WMC
RefSection_2	26.694	0.197	0.169	0.196	0.189	0.184	0.206	0.210
RefSection_3	37.907	0.486	0.440	0.496	0.482	0.441	0.509	0.514
RefSection_4	54.149	1.165	1.106	1.208	1.180	1.030	1.225	1.230
RefSection_5	71.592	2.148	2.114	2.281	2.229	1.840	2.292	2.281
Tip	89.166	3.243	3.250	3.418	3.341	2.671	3.426	3.377

The results in graphical form are presented in following figures. Specifically on Figure 6 the displacement in the x-direction of key point 13 is shown using the data provided by the partners on the reference sections, while on Figure 7 the same information is provided for the flap direction. The non-linear geometric solution provided by DTU is also shown in both figures using dotted lines. CRES results are stiffer in the flap direction, while PoliMi's results have a similar trend in the edge direction. All other results are in good agreement. The non-linear solution falls also within the estimation of the other (linear) predictions.

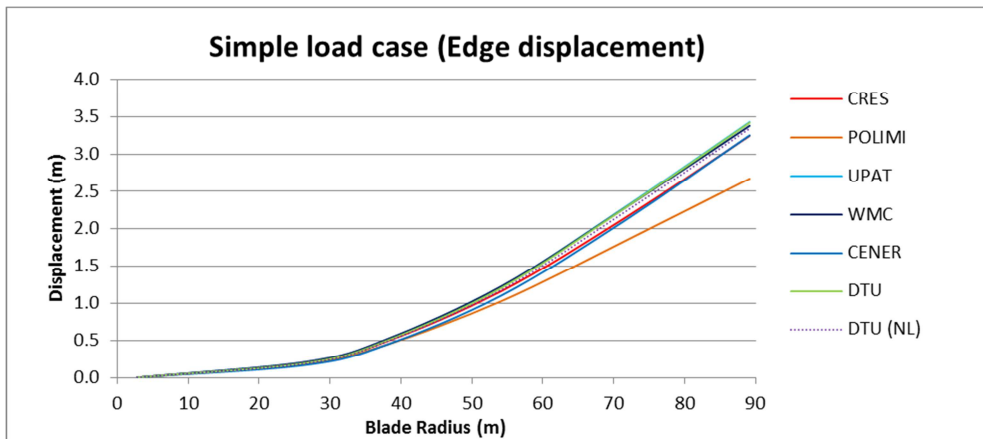


Figure 6. Displacement in the x-direction (edgewise) for simple load case and key point 13

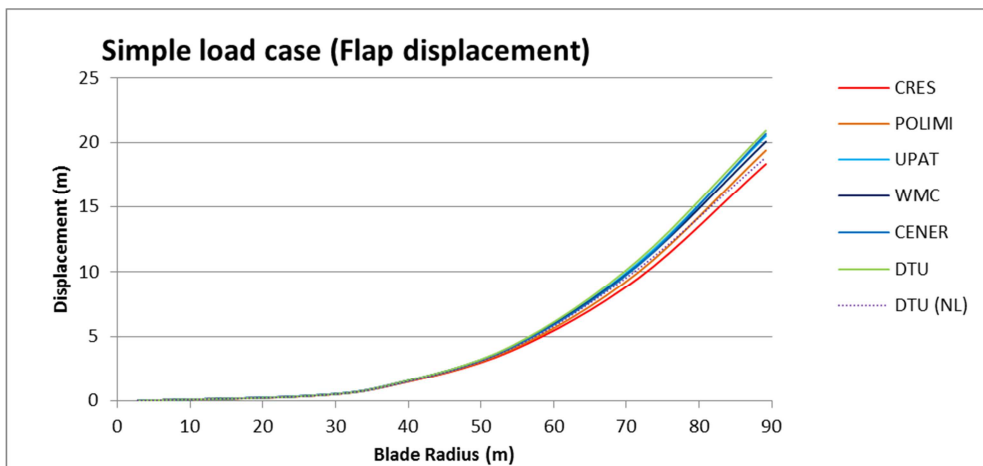


Figure 7. Displacement in the y-direction (flapwise) for simple load case and key point 13

The results provided allow for a simplified estimation of torsion along the blade length due to the application of the simple load case. Since the displacements are provided for 4 key points on the section, which more or less form a rhombus, the difference between the rhombus's diagonals before and after loading can be used as a measure of torsion on the sections. In Figure 8 the results of this procedure are shown for the torsion along the blade length estimated at the 5 reference sections. The estimation is performed between results for key points 1 and 9, shown on the left and key points 5 and 13, shown on the right of the figure. CENER did not provide data on the key points, while PoliMi did not provide the data for section on the tip of the blade. The non-linear analysis results performed by DTU are also presented in the figure. The non-linear solution clearly differs in this case from the results of linear models, revealing a softer torsional response. Yet there are also differences in the estimation using key points 1 and 9 and 5 and 13. Further to that, the results for WMC are also different, approaching the non-linear solution when checking key points 1 and 9. In this case, nevertheless the differences between estimations using key points 1 and 9 and 5 and 13 are not so pronounced.

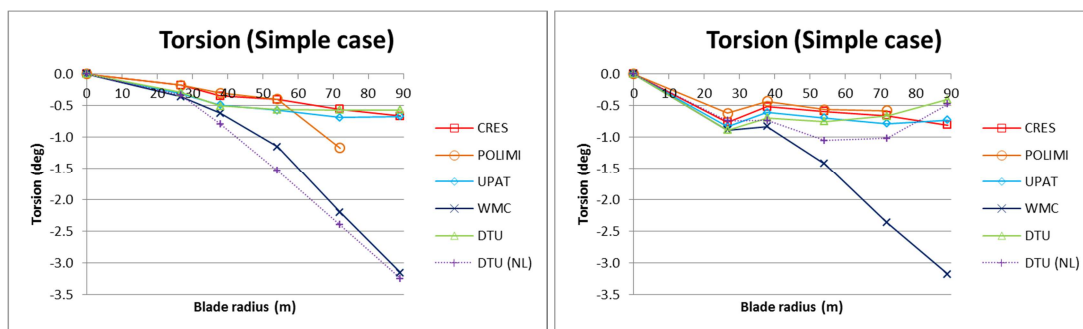


Figure 8. Simplified torsion for simple load case (calculated between key points 1 & 9, left and key points 5 & 13, right)

Deflection for reference load case

The results for the reference load case are presented in the current section, similar to the previous analysis corresponding to the simple load case. CENER and DTU did not provide displacement results for the reference load case. As for the previous case, PoliMi provided for the tip the displacement only at the centre node of the section.

For this case, results are also in good agreement, despite the differences in modeling assumptions for the load case and differences in the model itself. To be more specific, CRES and UPAT apply the load distributed on the blade directly on the nodes of the finite element model. PoliMi and WMC use multipoint constraints to apply the loads.

Table 18. *Tip deflection for reference load case (key point 1)*

Partner	X (m)	Y (m)	Z (m)	Notes
CRES	2.330	19.341	0.043	
POLIMI	2.674	19.609	0.015	Center node
UPAT	3.394	20.593	0.056	
WMC	3.313	20.004	0.055	

Table 19. *Tip deflection for reference load case (key point 5)*

Partner	X (m)	Y (m)	Z (m)	Notes
CRES	2.329	19.338	0.057	
POLIMI	2.674	19.609	0.015	Center node
UPAT	3.393	20.589	0.058	
WMC	3.313	19.995	0.043	

Table 20. *Tip deflection for reference load case (key point 9)*

Partner	X (m)	Y (m)	Z (m)	Notes
CRES	2.330	19.336	-0.005	
POLIMI	2.674	19.609	0.015	Center node
UPAT	3.394	20.586	-0.009	
WMC	3.314	19.990	-0.007	

Table 21 presents the displacement results for key point 5 of reference section 2. Again the results are in good agreement, with CRES presenting lower results for both x and y displacements, indicating the use of a stiffer model.

Collective results for the displacements in y and x direction (flap and edge direction, respectively) are presented in Table 22 Table 23 for all reference sections along the blade. For this loading case (reference load case) the coefficient of variation is larger than the simple load case, approaching 5.3% for reference section 5 in the flap direction (y-direction) and 16% in the edge direction.

Table 21. Deflection for reference load case (key point 5), RefSection_2

Partner	X (m)	Y (m)	Z (m)
CRES	0.117	0.385	0.054
POLIMI	0.163	0.404	0.056
UPAT	0.178	0.411	-0.029
WMC	0.178	0.404	0.059

Table 22. Deflection in flap direction for reference load case (key point 13)

Section (#)	Position (m)	CRES	POLIMI	UPAT	WMC
RefSection_2	26.694	0.385	0.394	0.403	0.404
RefSection_3	37.907	1.216	1.240	1.292	1.301
RefSection_4	54.149	3.830	4.000	4.191	4.183
RefSection_5	71.592	9.493	10.000	10.683	10.539
Tip	89.166	19.338	19.609	20.589	19.995

Table 23. Deflection in edge direction for reference load case (key point 13)

Section (#)	Position (m)	CRES	POLIMI	UPAT	WMC
RefSection_2	26.694	0.146	0.186	0.203	0.208
RefSection_3	37.907	0.367	0.450	0.510	0.511
RefSection_4	54.149	0.894	1.050	1.227	1.219
RefSection_5	71.592	1.621	1.860	2.286	2.250
Tip	89.166	2.331	2.674	3.395	3.315

In graphical form the results for the reference load case are presented in Figure 9 for the displacement in the edge direction (x-direction) and Figure 10 for the displacement in the flap direction (y-direction). Results by UPAT and WMC are in very close agreement for both directions, while CRES reports the lowest displacements.

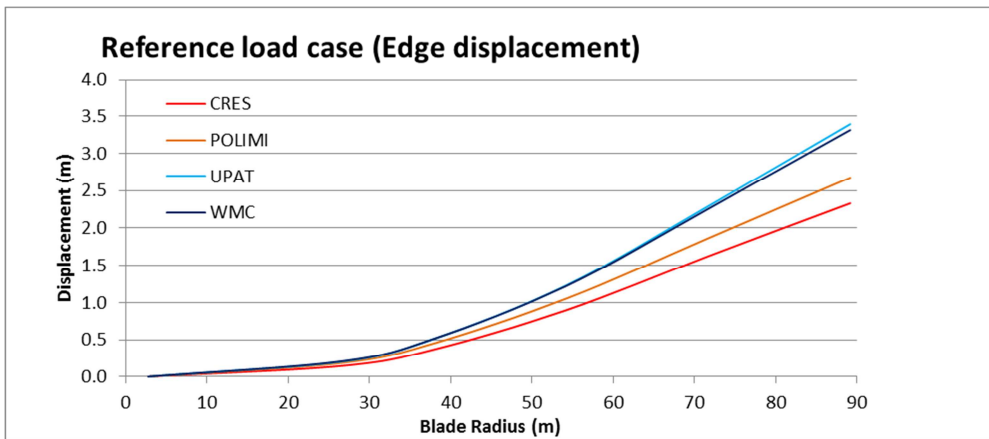


Figure 9. Displacement in edge direction for the reference load case

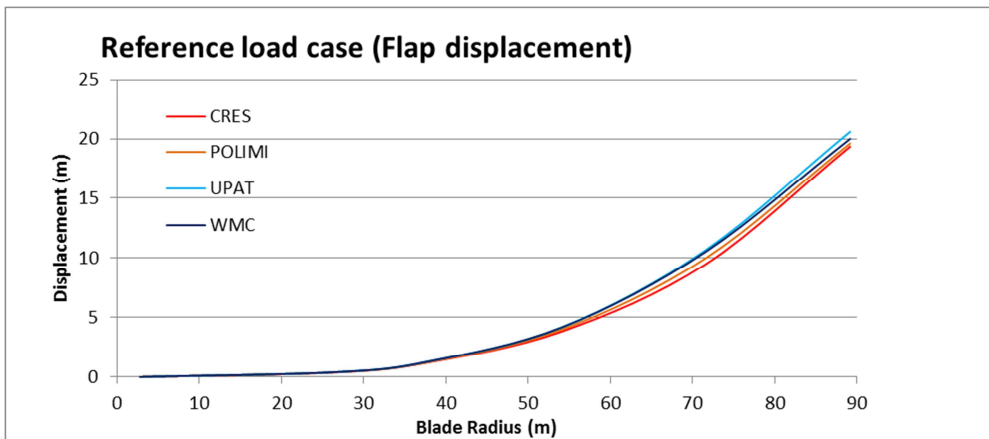


Figure 10. Displacement in flap direction for the reference load case

From the results provided, the torsion of the blade section can also be deduced in a simplified way as for the simple load case presented earlier in the current report. In Figure 11 results estimated by use of key points 1 & 9 on the reference sections along the blade length are shown on the left, while the corresponding results using key points 5 and 13 are shown on the right. As with the simple load case, results of CRES, PoliMi and UPAT follow the same trend up to reference section 4, while the values are different. For the reference load case (unlike the simple load case discussed earlier in the present report), results by WMC also follow the trend of the other participants.

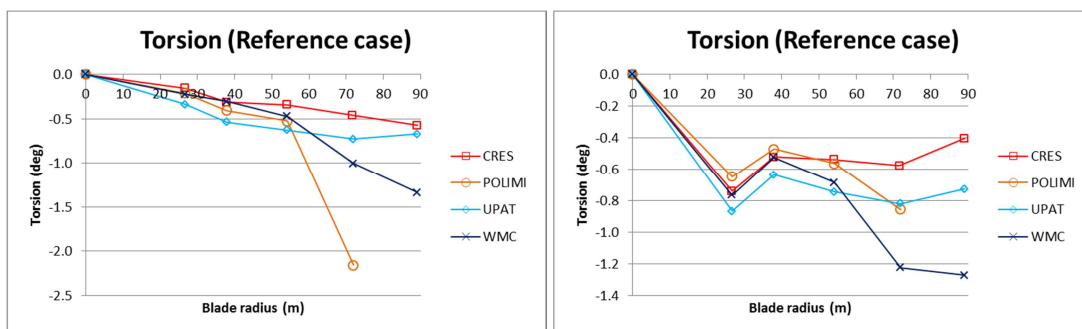


Figure 11. Simplified torsion for reference load case (calculated between key points 1 & 9, left and key points 5 & 13, right)

BLADE STRENGTH

4.1 Buckling analysis

Buckling load factor over reference load case is shown for all partners in Table 24. CENER did not provide data for buckling analysis. CRES and UPAT applied the safety factor against buckling on the elastic material properties. Further to that, CRES, as an alternative solution, applied the safety factor on the load. Results of the two analyses were identical. DTU has not applied the safety factor on the buckling analysis and the buckling results refer to the simple load case. A geometrical non-linear buckling analysis has been performed by DTU. PoliMi provided results for both loading cases (simple and reference). WMC performed two buckling analysis, namely one using the in-house developed FOCUS6 based on the finite strip method and the other using the finite element model and MARC solver.

From Table 24 it is evident that the results of buckling analysis show a large dispersion. This is true not only regarding the buckling load factor, but also the location of the buckling, both with respect to the blade length and the position on the section (Cap, trailing panel, etc.). All partners predicted buckling in the suction side of the blade, while more specific location on the section is indicated on Table 24.

In an attempt to reduce dispersion, the results of partners (CRES, PoliMi and UPAT), reporting buckling load factor and using buckling safety factor, were transformed to remove the buckling safety factor. WMC provided results both using and not using the buckling safety factor. Still in this case the difference between participants' results is in the order of 40%, PoliMi presenting the most conservative results and WMC through Marc analysis the least conservative.

Table 24. *Buckling load factor for reference case*

Partner	Load factor	Position on section	Position along the length	Homogenized buckling load factor
CRES	0.660	Trailing panel	~87.8m	1.348
DTU	2.698	Cap	Root	2.698
POLIMI	0.529	Trailing panel	~60-80m from blade root	1.080
POLIMI (simple case)	0.569	Trailing panel	~57-78m from blade root	1.162
UPAT	0.967	Cap+web	~65m from the root	1.974
WMC (FOCUS6)	1.222	Cap	24.2m	2.496
WMC (MARC)	1.511	Cap	25.9m	3.085

4.2 Extreme load carrying capacity analysis

Extreme load carrying capacity multiplication factor (static strength under reference case) is shown in Table 25, along with the failure criterion employed and information on location of failure. Some notes regarding the participants' data are necessary:

- Several partners (CRES, CENER, DTU and UPAT) used the Tsai-Wu failure criterion, with the Tsai-Hahn expression for the coupling term. CENER provided data with several formulations of the Tsai-Wu criterion, the Tsai-Hahn, Hoffman and Hill failure criterion. Additionally, CENER provided data using the maximum strain and the Puck

criterion checking fibre failure. PoliMi provided data using the maximum strain and maximum stress criterion, while WMC employed the Puck failure criterion.

- CRES provided results using both commercial finite elements and in-house built THIN sectional analysis tool.
- DTU run the simple case for extreme load carrying capacity and used nominal values for the Balsa material strength.

Again, from results of Table 25 large dispersion of data is seen. However, all partners predict failure in the suction side of the blade and most of the partners report critical failure area near the section with the largest chord (25-30m from the blade root). Specific location on the section, the location of the critical section along the blade and the most critical layer on the lamination sequence are presented on the table.

Table 25. Extreme load carrying capacity for reference case

Partner	Failure criterion	Load factor	Location on section	Location along the blade	Layer
CRES	Tsai – Wu	0.520	Shear web A	~37.500m	Balsa
CRES (THIN)	Tsai – Wu	0.720	Leading panel	26.694m	Balsa
CENER	Hill	0.341	Leading panel	54.149m	Triax ply
	Hoffman	0.357	Leading panel	54.149m	Triax ply
	Tsai - Wu	0.345	Leading panel	54.149m	Triax ply
	Max. Strain	0.366	Leading panel	54.149m	Triax ply
	Puck (fibre)	NA	Leading panel	54.149m	Triax ply
DTU	Tsai – Wu	0.500	Leading panel	25.4m (radial)	Uniax
POLIMI	Max Strain & Stress	0.648	Leading panel	26.694m	Uniax
POLIMI (simple case)	Max Strain & Stress	0.682	Leading panel	26.694m	Uniax
UPAT	Tsai - Hahn	0.545	Leading panel	25.200m	Uniax
WMC	Puck (compression)	0.450	Nose panel	~29.800m	Balsa
	Puck IFF_A	0.500	Shear Web	~29.800m	Biax
	Puck IFF_B	0.530	Nose panel	~29.800m	Triax
	Puck IFF_C	0.530	Nose + trailing edge	~29.800m	Uniax

Through data provided by CENER on various failure criteria, the dispersion only due to the failure criterion is about 3%. If one compares the results obtained through use of the Tsai-Hahn failure criterion (although not all appear at the same position on the blade) the dispersion increases to 25%. If all data are taken into account (the minimum reported value for each participant) then the dispersion again reduces to 20%.

The most conservative results are provided by CENER on Reference Section 5 using the Hill failure criterion and the in-house BASSF sectional analysis tool, followed by WMC using the Puck failure criterion in in-house developed FOCUS6. The least conservative results are given by CRES using the in-house THIN sectional analysis tool.

STRESSES –STRAINS RESULTS

All partners provided data on the calculation of the stress and the respective strain values at specific keypoints of the reference cross-sections, according to [2]. In the present document, the data are compared both for the simple and the reference load cases and focus:

- Around the reference sections 1, 2 and 4
- Along the blade length based on the position of the five reference sections and
- Through-the-thickness at specific segments (laminates) of reference sections 1 and 2.

Table 26 summarizes the contribution of each partner in terms of stress and strain values for both the reference and the simple case. It should be noted that the data provided by DTU refer to the non-linear solution performed.

Table 26. *Summary of the data provided by the task members*

Partner	Simple Load case		Reference Load Case		Comments
	Stress	Strain	Stress	Strain	
CRES	x	x	x	x	
CRES (THIN)	x		x		
CENER			x	x	
DTU (non-linear)	x ^a	x ^b			a: Only for Key points 9 & 12 b: Not for reference section 1
POLIMI	x	x	x	x	
UPAT	x	x	x	x	
WMC	x	x	x	x	

The key points (KP) and the segments where the stress-strain values results are compared are better illustrated in Figure 12. For sake of consistency, KP1 corresponds to the pressure side Trailing Edge (TE) segment, called “Tail A” and consequently KP5, KP9 and KP12 are numbered counter-clockwise around the section.

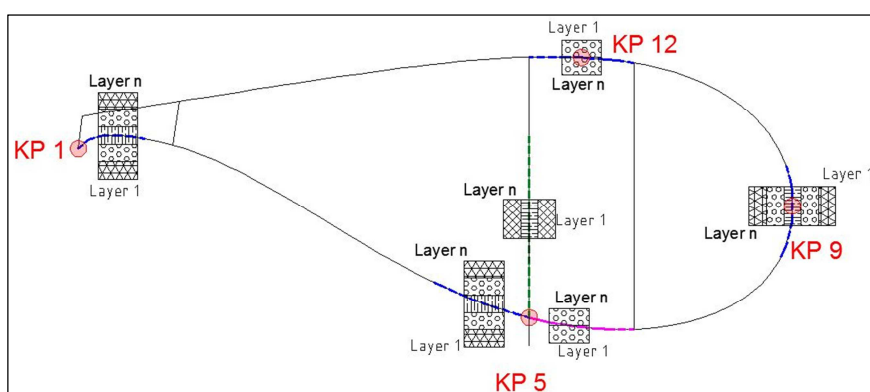


Figure 12. Key point numbering definition and lamination sequence direction in the present report

The exact coordinates of each key point, as provided by each partner, on each one of the five reference sections, is shown in graphs of Fig. 11 for reference sections 1, 2 and 4. The relative position of the key points is similar for reference sections 3 and 5 not shown in here.

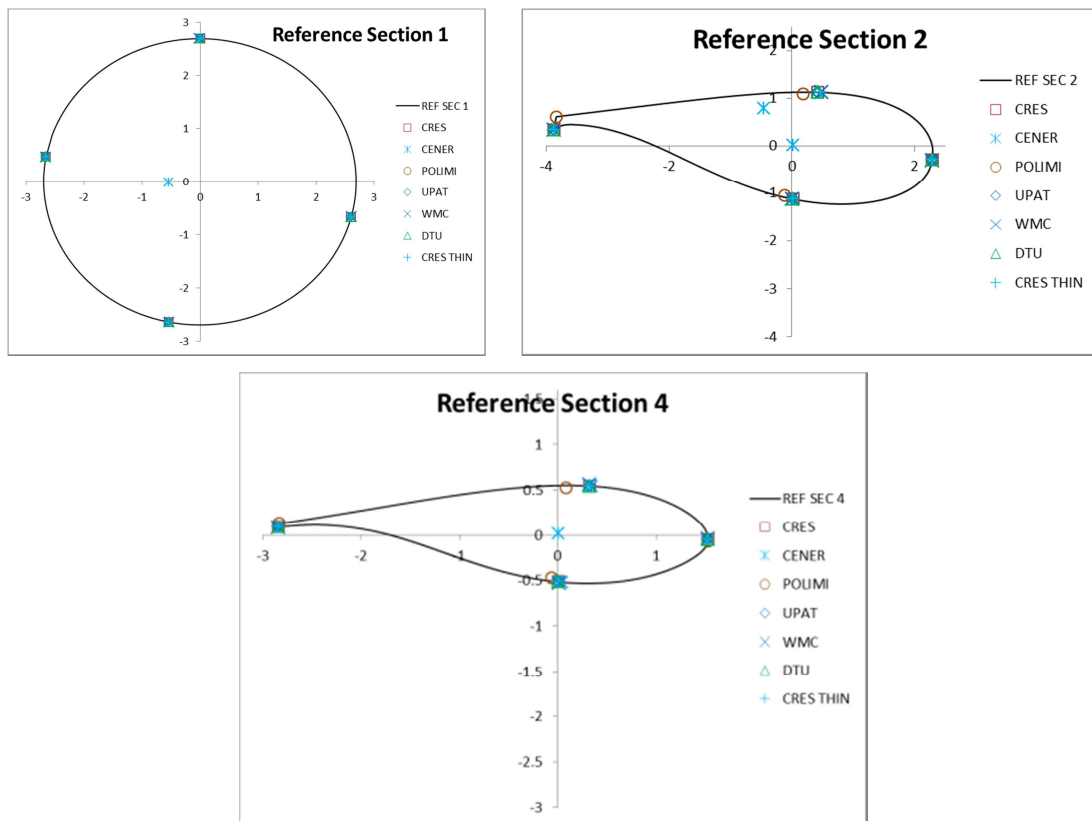


Figure 13. Position of each key point on partners results at reference section 1, 2 and 4

5.1 Simple load case

The simple loading case dealt with the application of specific loads on the reference sections of the blade in the flap and edge direction [2]. The stress and strains results were calculated for six different lamination sequences at four key points around the section, resulting in 6 points of comparison (numbered from 1 to 6) as shown in Table 27. Each comparison point corresponds to a different lamination sequence and refers to the outer layer of the each laminate, i.e.: triaxial layer (TRIAx) for key points 1, 2 and 5, uniaxial layer (UNIAX) for key points 3 and 6 and biaxial layer (BIAX) for key point 4.

Table 27. Relation between graphs points and key points

Lamination sequence	Point on Graph	Key points			
		KP1	KP5	KP9	KP12
Tail A	1	X			
Trailing Panel (pressure side)	2		X		
CAP (pressure side)	3		X		
Shear Web B	4		X		
NOSE	5			X	
CAP (suction side)	6				X

Figure 14 presents the distribution of normal stress along the blade length (σ_x) and in-plane shear stress (σ_{xy}) at the six comparison points of reference sections 1, 2 and 4. It is obvious that there is a good agreement for the normal stress values, with the exception

of WMC data on reference section 1 at comparison points 2, 3, 4 (key point 5) and 6 (key point 12). This difference may be caused by the use of different boundary conditions at the blade root; for the shell finite element analyses, WMC restrained only the displacements at the blade root nodes, but the rotation degrees of freedom were free. Other partners restrained both displacement and rotations. POLIMI gives somewhat lower values for the lower CAP also at KP5 (Graph point 3) and KP12 (Graph point 6) for reference sections 2 and 4.

The scatter regarding the shear strains is larger, although the absolute values are about one order of magnitude less than that of the normal stress along the blade length. The reason for that is attributed to the local coordinate system defined by each participant on their analysis tools. Figure 15 presents the absolute values of the shear stress data provided by each partner at reference section 2. It turns out that all values, now having the same sign, are in good agreement, with the exception of some outliers as e.g. CRES results for key point 5 being larger than the rest.

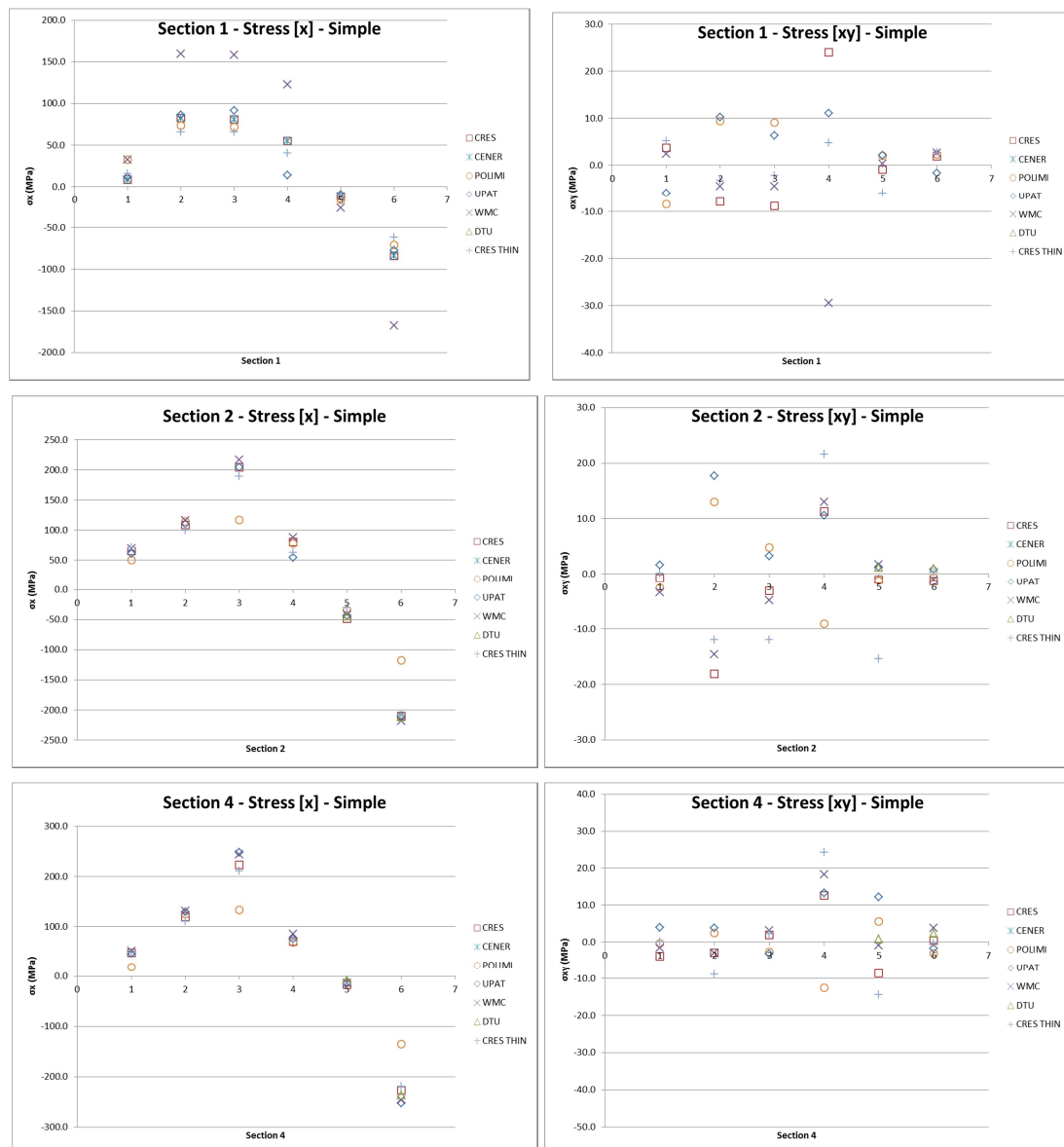


Figure 14. Normal and shear stress values for the outer layer of reference sections 1, 2 and 4

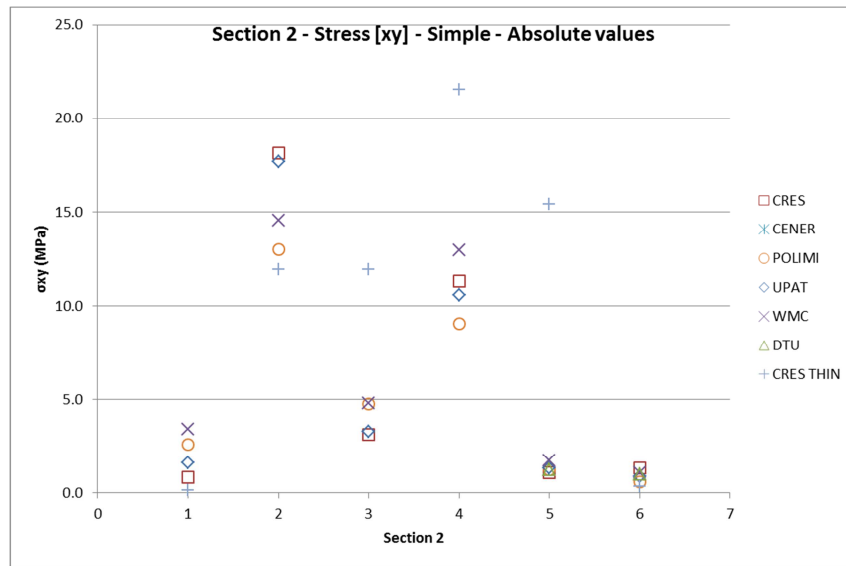


Figure 15. Absolute shear stress values for the outer layer of reference section 2

Regarding the strain values, the same trend as for the stresses is observed in Figure 16, which shows the respective normal and shear strain values on reference section 2 and 4. Normal strains (strain along the blade) as expected are in better agreement than shear strains. Wherever available also strains provided by DTU for the non linear solution are in good agreement with the linear solution results provided by the other partners.

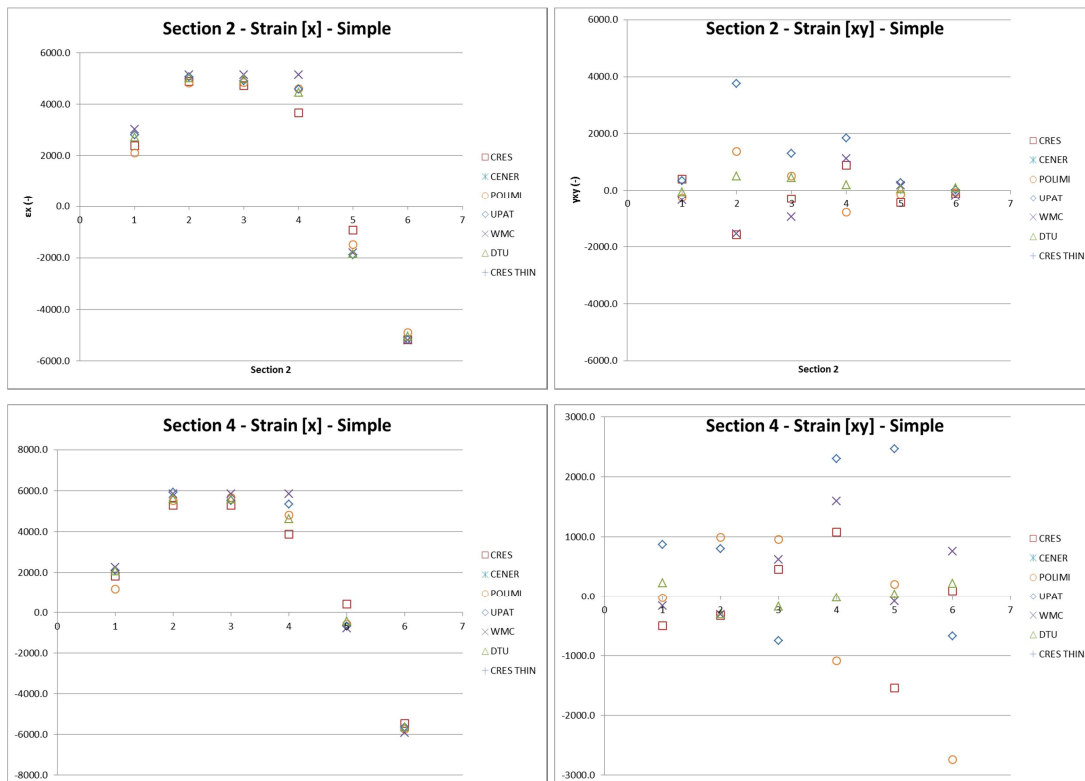


Figure 16. Normal and shear strain values for the outer layer of reference section 2 and 4

Figure 17 presents the distribution of the normal stress of the outer layer on the left and the first UNIAX layer on the right along the blade length for KP1 (Tail A), KP5 (CAP – pressure side), KP9 (NOSE) and KP12 (CAP – suction side) using the data provided at the

5 reference sections. Generally, the results are in good agreement and the trends are the same for all partners. Nevertheless, some notes should be made:

- POLIMI has included TRIAX layers in the CAP segments of both the pressure and the suction side, whereas the rest of the participants modelled the CAPS by just two UNIAX layers. Consequently, POLIMI gives out significant lower values at KP5 and KP12 for the outer layer of the CAPS. This effect is eliminated for the case of first UNIAX layer.
- POLIMI has introduced a UNIAX layer at KP9 – NOSE segment of reference section 5. Other partners did not include in their model an UNIAX layer at this specific section.
- WMC provides significant higher values for reference section 1 at the lower and upper CAP segments both for the outer (TRIAX) and the first unidirectional (UNIAX) layer. As discussed earlier for Figure 14 this difference at section 1 may be caused by using different boundary conditions at the blade root.

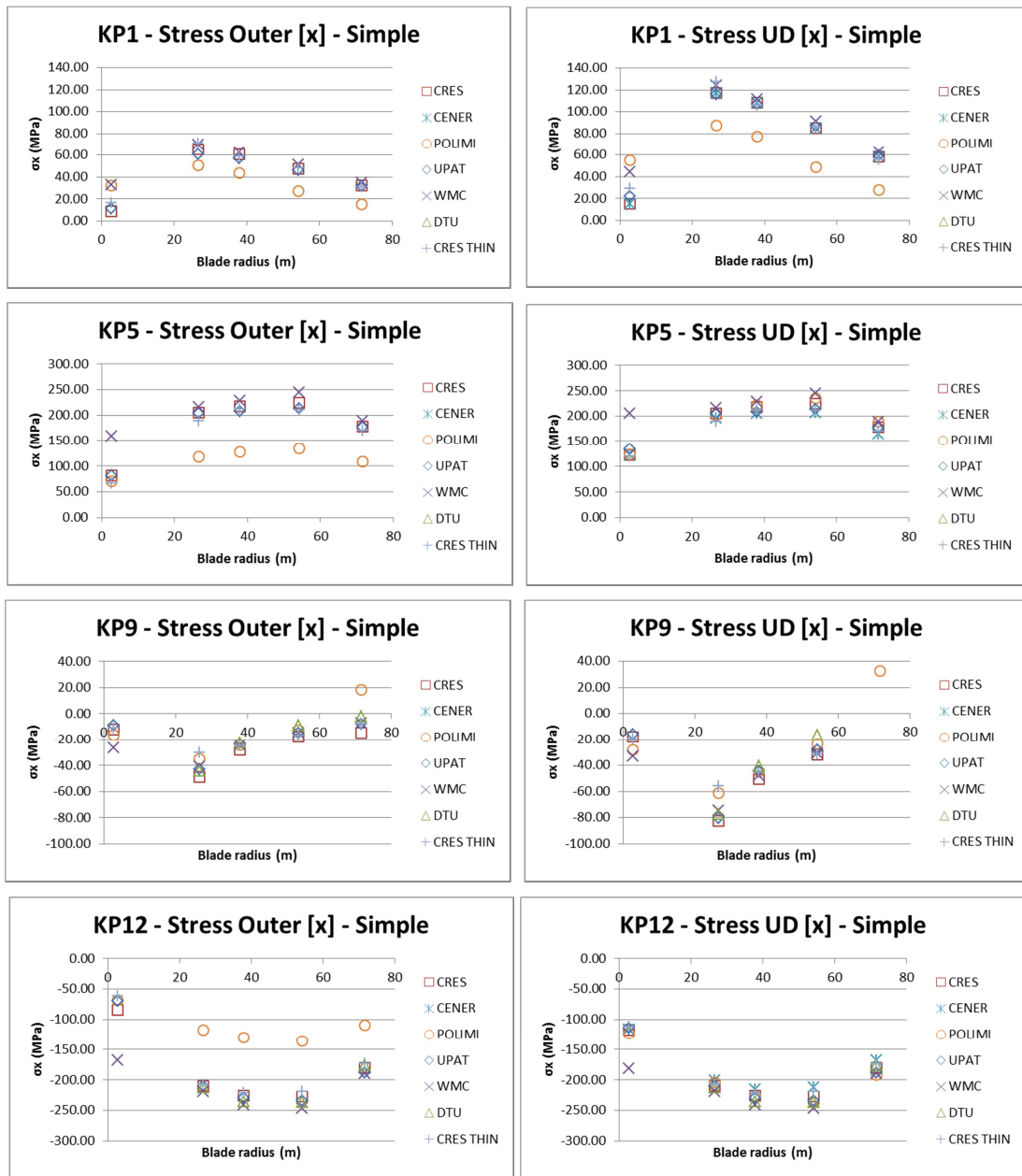


Figure 17. Normal stresses distribution of the outer (left) and the first UNIAX layer (right) along the blade length

Figure 18 presents the shear stresses on key points 1, 5, 9 and 12 along the blade length. Absolut values are only presented for reasons explained earlier. The differences in predictions are larger than the normal stresses.

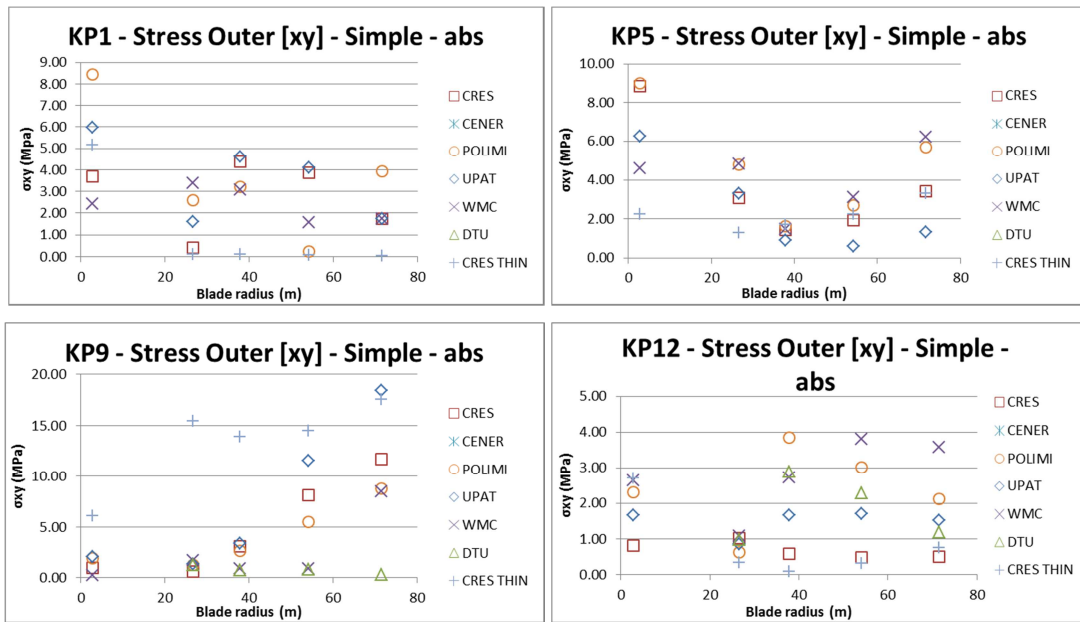


Figure 18. Absolute values of shear stresses distribution of the outer layer along the blade length for key points 1, 5, 9 and 12

Looking into more detail on the data provided, stress and strain data are discussed in the following for some specific lamination sequences focusing on reference section 2, which was indicated as close to the critical location of failure in the strength prediction by most of the partners. In the following graphs numbers refer to layer number in a lamination sequence TRIAX, UNIAX, BALSA, UNIAX, TRIAX. Whenever a specific material type is not included in the lamination sequence compared this is left out. The direction 1 to 5 is consistent with that shown in Figure 12, layer one being closer to the outer surface of the blade layer 5 being in the inner surface.

Based on this nomenclature, Figure 19 presents the normal (along the blade length), transverse (along the section) and in-plane stresses (on the left) and strains (on the right) for KP12 – middle point of upper CAP. The following remark can be made:

- POLIMI values for TRIAX layers (comparison points 1 and 5) should be discarded for CAPS regions, since at these locations TRIAX layers are not prescribed in the lamination sequence, as discussed previously.

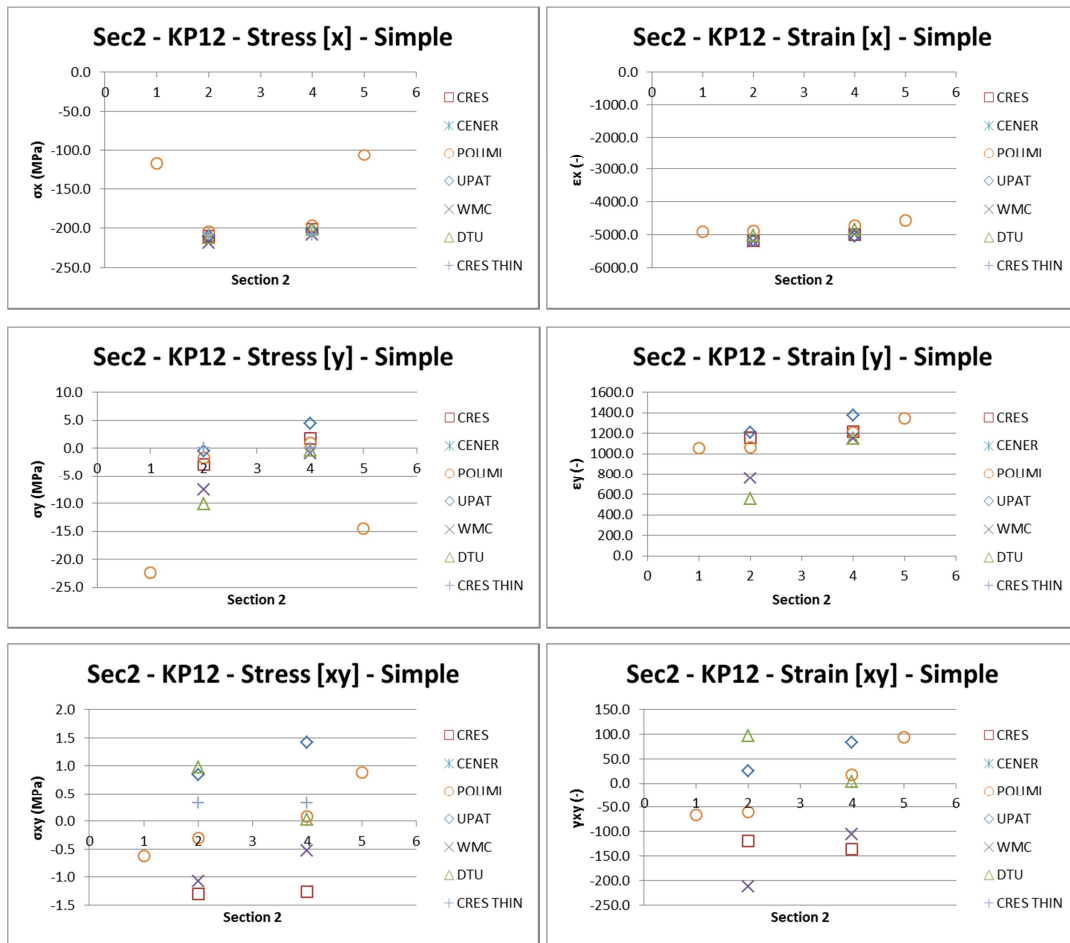


Figure 19. Normal, transversal and shear stress (left) and strain (right) for key point 12 of reference section 2

Respective results for KP5 – Shear Web B on reference section 2 are shown on Figure 20. Comparison points 1, 2, 3 on the graph correspond to layers in the lamination sequence BIAx, BALSA, BIAx, with layer 1 being the layer towards the leading edge (Figure 12).

The results are in good agreement for the normal stress and strains (along the blade length) as well as for the transverse stress (along the section), σ_y and shear stress. Again, there are significant differences regarding the shear strain data, even neglecting the direction of the local coordinated system that each partner adopted in the analysis tool.

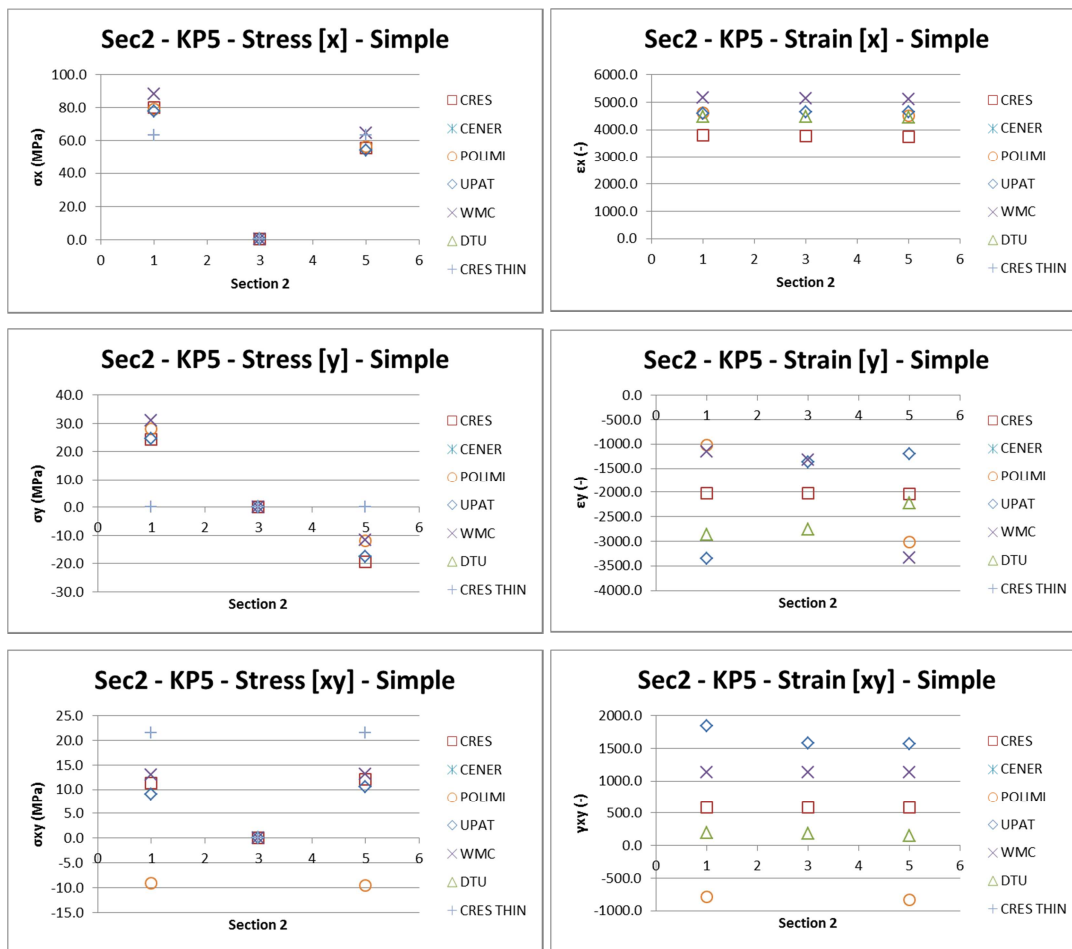


Figure 20. Normal, transversal and shear stress (left) and strain (right) for Shear Web B of reference section 2

5.2 Reference Load Case

In this load case scenario each partner used its own methodology to convert the sectional moments and forces provided by [2], into concentrated loads along the blade length. It should be outlined that each partner possibly uses:

- Different load values along the blade
- Different load application methods
- Different load location not only along the blade length but also on the airfoil

In comparison to the simple load case, for the reference load case stress and strain results were also provided by CENER, but not by DTU.

Figure 21 presents the normal and shear stress values for reference sections 2 and 4. Conclusions are similar with the respective graph for the simple load case shown in Figure 14. Likewise, Figure 22 presents the normal and shear strain data for reference section 2, with comments similar to those of the respective graphs of Figure 16.

A special note should be made for the stress values of CENER for comparison point 4, which corresponds to the key point 5 on the shear web B of each cross-section. It is obvious that this point exhibits significant lower values than the other partners (almost zero), which is attributed to the fact that CENER makes the calculations at the middle point of web B rather than at the joint of web B with Trailing Panel and lower CAP segments.

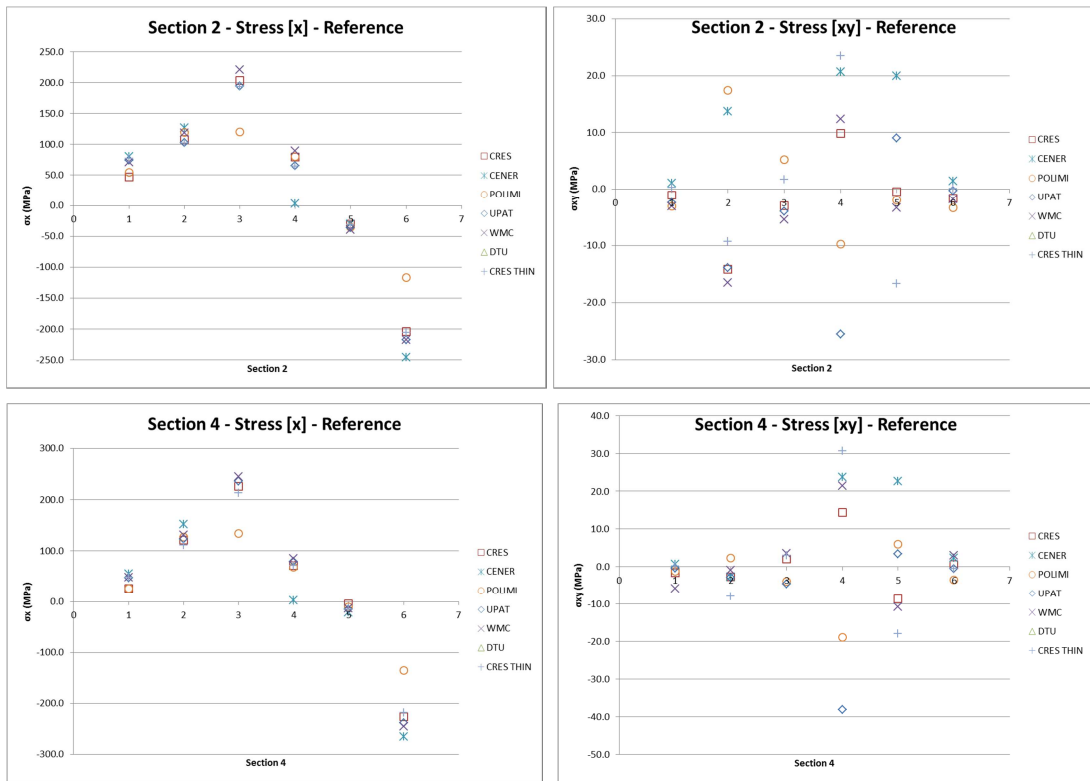


Figure 21. Normal (left) and shear (right) stresses on outer layer of key points for sections 2 and 4 (reference load case)

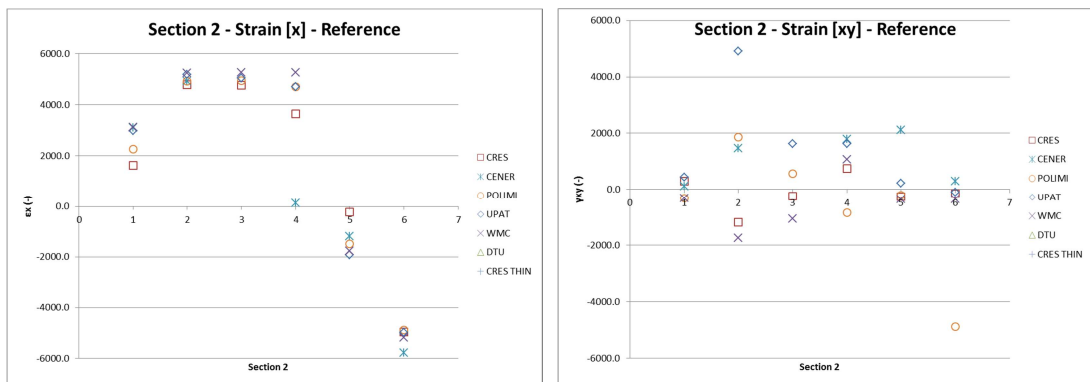


Figure 22. Normal and shear strains on outer layer of key points for section 2 (reference load case)

Figure 23 presents the normal stress distribution along the blade, based on the outer UNIAX layer values of key points 1, 5, 9 and 12 of the five reference cross-sections. Comparison notes are similar to the respective ones for the simple load case on Figure 17.

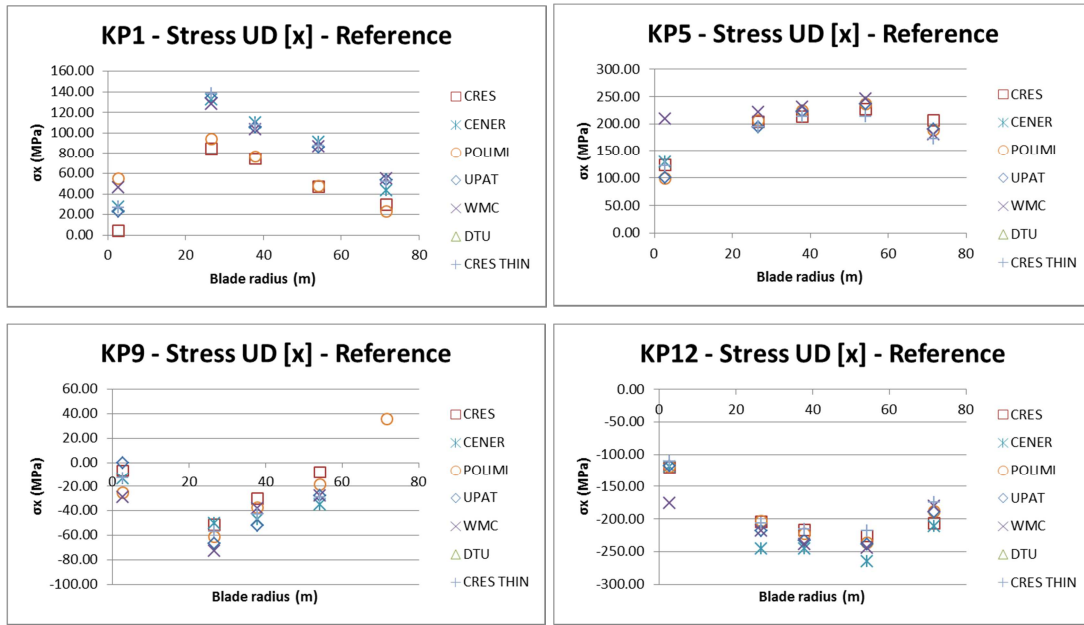


Figure 23. Normal stresses for the reference load case for the first UNIAX layer along the blade length

Similar observations can be made for other locations compared as for the simple case for both stress and strain results.

CONCLUSIONS

The benchmark results regarding the structural modeling and analysis tools of the participants within the InnWind.Eu project was presented in the current report. In general the data provided by the partners are in good agreement.

Especially regarding global blade properties, i.e. mass, centre of gravity, natural frequencies and displacement results are quite close, irrespective of the differences in the modeling assumptions and the analysis methods used by the participants.

Results regarding the strength of the blade, namely the strength against buckling and against extreme loading, need to be further discussed.

A closer look at the stresses and strains estimated along the blade on specific lamination sequences on the sections, also indicate differences. These differences are more pronounced for the reference load case, since this case for most of the participant's tools also involves the transformation of the internal stress resultants to external loads.

REFERENCES

- [1] Bak C, Zahle F, Bitsche R, Kim T, Yde A, Henriksen LC, Andersen PB, Natarajan A, Hansen MH, 2013, "Design and performance of a 10 MW wind turbine", submitted to J. Wind Energy.
- [2] Lekou DJ, "Information on the Benchmark of blade structural models", InnWind.EU Report, July 2013.

CENER contribution on the Benchmark of blade structural models

Ana Belen Fariñas

Carlos Amézqueta

Iñaki Nuin

CENER

SHORT DESCRIPTION OF STRUCTURAL ANALYSIS TOOL(S) USED

The analytical tool for a global blade structural pre-design used in CENER is called BASSF. BASSF is the acronym for Blade Analysis Strain Stress Failure. It is CENER in-house software which is based on 2D analytical formulation. Among its characteristics it is remarkable the direct Input/Output data communication with GH Bladed.

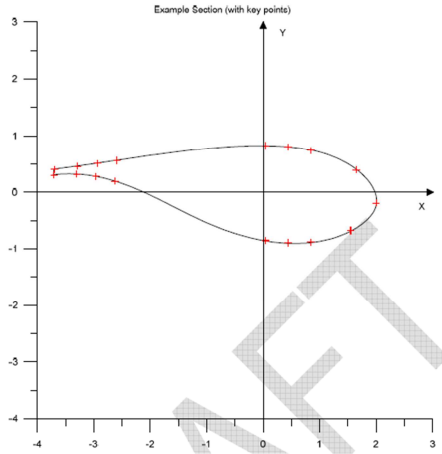


Figure 24. Coordinate system indicated for the benchmark (global z axis pointing from root to tip with starting point at rotor center).

1.1. For the analysis for the extraction of blade properties

BASSF:

The continuous aerodynamic airfoil is divided into finite segments/elements where the Classical Laminate Theory is applied, which implies the following assumptions, valid for small deformations:

- Laminate thickness much smaller than other dimensions.
- Laminae perfectly bonded one to each other, with linear elastic response.
- Perpendicular lines to the laminate surface remain perpendicular and straight after laminate deformation.
- Negligible variation in the through thickness deformation.

For each of the discrete segments, the stiffness matrix [Q] of each lamina is calculated and then taking into account the lamina orientation in the lay-up, the [A], [B] and [D] matrices, in order to obtain the laminate constitutive matrix. The laminate equivalent stiffnesses (E_x , E_y , G_{xy}) and Poisson's ratio (ν_{xy}) are inferred from the constitutive equations.

The global stiffness of the section to analyze with respect to the coordinate system located in the pitch axis is calculated as the summation of the partial stiffness of the different "i" segments, which as well results from the summation of the partial stiffness of each lamina "j" in the segment "i":

$$(E \cdot I)_{x,y}^{section} = \sum_{i=1}^n (E \cdot I)_{x,y}^i = \sum_{i=1}^n \sum_{j=1}^m (E \cdot I)_{x,y}^j$$

The section mass centre location is calculated as follows:

$$m.c._{x,y} = \frac{\sum_{i=1}^n m_i \cdot x, y}{m_{Section}}$$

The blade has been divided in 101 segments. Each segment starts at the r_start of the laminate and ends at the r_end of the laminate. BASSF performs the calculations at the

middle section of each segment. The r-location of these middle sections do not match those provided in "DTU10MWRReferenceWindTurbine.xls", version 1.04 neither those where the external blade geometry points are defined. Thus it is assumed the aerodynamic profile closer to the before mentioned middle section, and the aerodynamic values (chord, twist, etc.) in "DTU10MWRReferenceWindTurbine.xls", version 1.04 in the fine N=200 data closer to the aerodynamic profile selected.

Afterwards the blade has been modelled in MSC. Patran software (FEM) with 2D beam elements. The beams connect the nodes located at each r-location calculated in the software BASSF. The mass (kg/m) and stiffness values (bending and torsional) calculated by BASSF have been assigned to each beam property at both nodes (tapered beams). This Finite Element model has been calculated with MSC. Nastran solver to obtain both the blade properties and natural frequencies and mode shapes.

In the case of the tip deflection calculation under the simple load case, additional intermediate nodes (and consequently beams) at the r-locations where the simple loads are applied, have been modelled. The mass and stiffness properties at those nodes have been interpolated from the values calculated by the software BASSF.

1.2. For the natural frequencies (modal) analysis

The model used is the FE bar model, as explained in 1.1.

1.3. For the extreme load carrying capacity analysis (static analysis)

This analysis has been performed with the software BASSF only at the five reference sections loaded under the Reference Load Case. Therefore failure arising at other r-locations different from the ones of the reference sections is not assessed.

The analysis is based on the calculation in each of the segments of the reference section of the following variables: axial strain (ϵ_z) and shear flow (q). Both are used to obtain the laminate strains in each segment. Therefore the software is capable to identify the most critical segments and sectors of the section.

The flap-wise & edge-wise bending moments (M_y , M_x) and the blade axial load (F_z) lead to the following **axial strain (ϵ_z)** in each of the segments of the section:

$$\epsilon_z^i = \frac{F_z}{(EA)^{section}} + \frac{M_x' \cdot Y^i}{(E \cdot I)_x^{section}} + \frac{M_y' \cdot X^i}{(E \cdot I)_y^{section}}$$

With

$$M_x' = \frac{M_x - M_y \cdot (E \cdot I)_{xy}^{section} / (E \cdot I)_y^{section}}{1 - (E \cdot I)_{xy}^{2,section} / ((E \cdot I)_x^{section} (E \cdot I)_y^{section})}$$

$$M_y' = \frac{M_y - M_x \cdot (E \cdot I)_{xy}^{section} / (E \cdot I)_x^{section}}{1 - (E \cdot I)_{xy}^{2,section} / ((E \cdot I)_x^{section} (E \cdot I)_y^{section})}$$

equations used because the BASSF (x , y) coordinate system doesn't match the principal axes of inertia (x' , y').

Due to the Beam Euler - Bernoulli Theory in which the software BASSF is based, the strains in the direction towards the trailing edge (ϵ_y in GL2010 Fig 4.A.1 coordinate system; $-\epsilon_x$ in the global coordinate system of the present structural benchmark) are not calculated. It is assumed a plane strain state in which $\epsilon_x = 0$ and σ_x according to it (in the global coordinate system of the present structural benchmark).

The torque (M_z) and the shear forces (F_x , F_y) generate shear flows (q_i) around the section that are calculated based on the following assumptions:

- Thin wall, so that the flow remains constant through the laminate thickness, being this thickness negligible compared with the characteristic length of the aerodynamic section.
- Closed multi-cell torsional theory.
- Free warping of the section so that there are no axial strains due to torque ($\sigma_z = 0$).

The fraction of the shear flows in each cell (q_i) generated by the torque (M_z), the rotation angle θ and the torsion constant (J) are obtained from the Bredt's theory considering geometrical compatibility ($\theta_1 = \theta_2 = \theta_3 \dots = \theta_n$; same rotation angle in all cells):

$$M_z = \sum_{i=1}^n 2 \cdot S_i \cdot q_i \qquad \theta'_i = \frac{1}{2 \cdot S_i} \int_{C_i} \frac{q \cdot d_s}{G_{ref} \cdot t_{eq}}$$

with S_i the enclosed area of each cell.

The shear forces (F_x, F_y) generate the shear flows (q_i) as shown in **Σφάλμα! Το αρχείο προέλευσης της αναφοράς δεν βρέθηκε.** according to the following equations:

$$q(s) = q_0 + q_b(s)$$

$$q_b(s) = -\frac{\bar{F}_x}{I_y} \cdot Q_y - \frac{\bar{F}_y}{I_x} \cdot Q_x$$

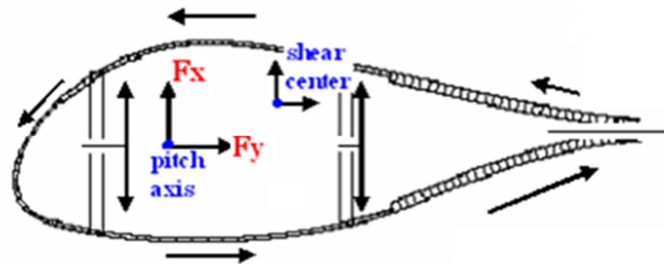


Figure 25: Shear flows q_i around the section (GL2010 Fig 4.A.1 coordinate system)

$$-F_x \cdot y + F_y \cdot x = \oint_c q(s) \cdot r_{t1}$$

$$Q_y = \int_0^s t \cdot x \cdot ds; \qquad Q_x = \int_0^s t \cdot y \cdot ds$$

$$\theta'_i = \frac{1}{2 \cdot S_i} \cdot \oint_c \frac{q \cdot ds}{G_{ref} \cdot t_{eq}}$$

$$\theta_1 = \theta_2 = \theta_3$$

In this way are calculated the total shear flows (q_i) in each of the section's cells and also the elastic and shear centers. These shear flows are introduced in the laminate constitutive equations in order to obtain the laminate in-plane shear strain (γ_{xz}).

The assumption of iso-deformation through the segment width and through the laminate thickness is followed so that all laminae within the laminate stack-up suffer the same axial strain (ϵ_z), in-plane shear strain (γ_{xz}) and "transverse" strain (ϵ_x). The stresses ($\sigma_z, \sigma_x, \tau_{xz}$; given in the global coordinate system of the present structural benchmark) in each type of lamina within the segment laminate are calculated based on the stiffness matrix $[Q]$ of each lamina type.

Failure criterion used

The comparison of the strains and stresses mentioned in the previous point with the material allowable turns out different failure indexes (FI) or strength ratios (SR, the roots of the failure indexes) according to the following composite First Ply Failure Criteria:

- Hill
- Hoffman
- Tsai-Wu
- Max strain
- Puck: only the Uniax plies have been analyzed under this criterion.

Modelling of the reference load case

The five reference sections have been loaded and calculated with BASSF software. Input loads to BASSF shall be given with reference to the blade coordinate system of GL2010 - Fig 4.A.1 [1]. This coordinate system differs from the one in which the reference loads in Table-5 from the document "Information on the Benchmark of blade structural models_ver2.pdf" [2] are given. Not only the axis directions differ but also the origin: GL 2010 coordinate system [1] is centered at the pitch axis and not at the elastic centre.

Therefore loads in Table 5 from [2] have been transformed to GL 2010 coordinate system [1]. The location of the elastic centre is needed for the transformation. In order to avoid "noise" in this transformation, it has been used the elastic centre coordinates given by DTU in Table 4.10 from "DTU_Wind_Energy_Report-I-0092.pdf" [3]. These coordinates are shown in sections located at different r-locations than the ones in Table-5 from [2]. Consequently loads in Table-5 from [2] have been interpolated to the r-location of sections in Table 4.10 from [3] and then they have been transformed to GL 2010 coordinate system [1].

For the transformation explained before, the coordinates of the elastic centre with reference to GL 2010 coordinate system [1] must also be calculated. The twist, chord and "pitch axis aft LE" values are used in this calculation. The values are taken from Table called "Blade planform properties (Fine N=200)" within the excel file "DTU10MWReferenceWindTurbine.xls", version 1.04. Again, interpolation between sections in the excel sheet table have been carried out to obtain those aerodynamic properties at the same r-locations as in Table 4.10 from [3] (elastic centre coordinate sections).

Finally the transformed loads calculated at the r-location of sections in Table 4.10 from [3] have been interpolated to obtain the loads at the benchmark Reference Sections, which are shown in the following table.

Table 1. Reference Load Case according to GL coordinate system

Reference Sections	Reference Load case						
	GL 2010 coordinate system - Fig 4.A.1 [1]						
n°	z [m]	Fx [kN]	Fy [kN]	Fz [kN]	Mx [kNm]	My [kNm]	Mz [kNm]
1	2.8	1299.1770	-667.8640	978.8800	25458.8609	65745.2037	457.9357
2	26.694	1218.2533	-490.6334	873.3602	13604.3349	34952.3723	336.3447
3	37.907	932.6271	-229.9550	521.1405	6785.5232	24461.7919	208.8791
4	54.149	725.0681	-135.6836	240.3196	2201.4222	11875.8862	116.4645
5	71.592	352.7386	-31.5754	46.6085	357.1515	3090.8372	17.6090

1.4. For the buckling analysis

Not implemented in the tool.

1.5. For the variable load carrying capacity analysis (fatigue analysis)

NA

Failure criterion used

NA

DATA OUTPUT

2.1 Global blade properties

Overall mass of blade: 41880.43 kg

Location of centre of gravity of blade: x: - (m), y: - (m), z: 25.718 (m)*

* x and y coordinate for the centre of gravity is not calculated, as we use a FE bar model with the mass centred in the sections.

Natural frequencies analysis

Natural frequencies of the blade:

Table 2. *Natural frequencies of the blade*

Mode (#)	Frequency (Hz)
1	0.624
2	1.013
3	1.804
4	3.023
5	3.770
6	6.239

Following figures show mode shapes, normalizing to 1 the maximum displacement. The z-displacement is 0 in our model.

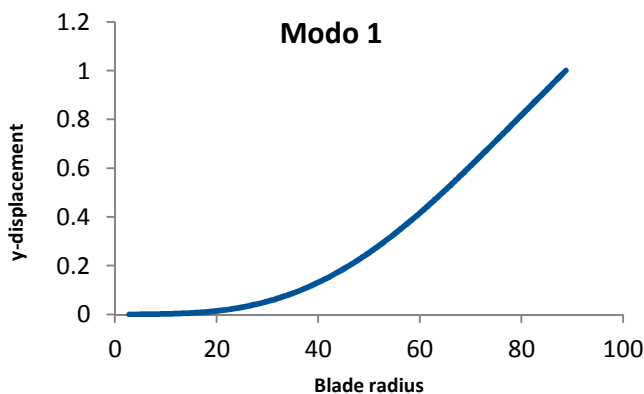
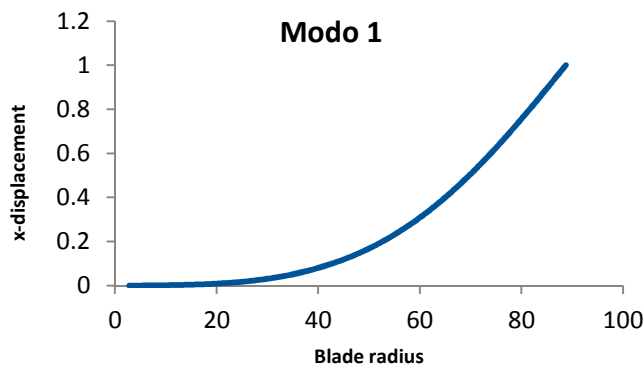


Figure 26. Mode shape for mode number 1

Table 3. *x* and *y* displacement for mode number 1

Blade radius (m)	x [m]	y [m]	Blade radius (m)	x [m]	y [m]
2.8311	0.00E+00	0.00E+00	46.9929	1.37E-01	2.12E-01
3.3211	0.00E+00	0.00E+00	47.71	1.44E-01	2.21E-01
4.3021	7.65E-05	0.00E+00	47.8073	1.45E-01	2.22E-01
4.7896	1.15E-04	0.00E+00	48.6178	1.53E-01	2.33E-01
5.7504	2.29E-04	3.06E-04	49.424	1.62E-01	2.45E-01
6.6819	4.21E-04	6.12E-04	51.0219	1.80E-01	2.68E-01
7.5842	6.12E-04	9.17E-04	51.8128	1.89E-01	2.80E-01
8.5169	8.80E-04	1.22E-03	52.029	1.92E-01	2.83E-01
9.4913	1.19E-03	1.53E-03	52.5977	1.99E-01	2.91E-01
9.9942	1.38E-03	1.83E-03	53.3764	2.09E-01	3.04E-01
11.0321	1.80E-03	2.45E-03	54.1485	2.19E-01	3.16E-01
12.1126	2.26E-03	3.06E-03	54.9136	2.30E-01	3.28E-01
12.6689	2.56E-03	3.67E-03	55.6714	2.40E-01	3.41E-01
13.8135	3.21E-03	4.59E-03	56.4216	2.51E-01	3.53E-01
14.4019	3.56E-03	4.89E-03	57.898	2.74E-01	3.78E-01
15.6103	4.40E-03	6.42E-03	58.6236	2.85E-01	3.91E-01
16.2303	4.86E-03	7.03E-03	59.3405	2.97E-01	4.04E-01
16.8606	5.39E-03	7.95E-03	60.0484	3.09E-01	4.17E-01
18.1521	6.58E-03	1.01E-02	61.4365	3.33E-01	4.42E-01
18.813	7.27E-03	1.13E-02	62.1163	3.45E-01	4.54E-01
19.4839	8.03E-03	1.28E-02	62.393	3.50E-01	4.60E-01
20.073	8.76E-03	1.41E-02	62.7863	3.57E-01	4.67E-01
20.1644	8.87E-03	1.44E-02	63.4463	3.69E-01	4.80E-01
21.554	1.08E-02	1.77E-02	64.7362	3.94E-01	5.04E-01
22.2627	1.19E-02	1.99E-02	65.3657	4.07E-01	5.17E-01
22.9803	1.31E-02	2.20E-02	65.847	4.17E-01	5.26E-01
23.7067	1.44E-02	2.45E-02	65.9848	4.19E-01	5.28E-01
25.1844	1.74E-02	3.00E-02	67.1914	4.44E-01	5.52E-01
25.9352	1.90E-02	3.30E-02	67.7789	4.57E-01	5.64E-01
26.6937	2.09E-02	3.61E-02	68.9218	4.82E-01	5.87E-01
27.4594	2.29E-02	3.98E-02	69.4772	4.94E-01	5.98E-01
28.232	2.50E-02	4.34E-02	70.5559	5.18E-01	6.20E-01
29.0112	2.73E-02	4.74E-02	71.592	5.42E-01	6.42E-01
29.7967	2.98E-02	5.20E-02	72.0941	5.54E-01	6.52E-01
30.437	3.20E-02	5.57E-02	73.0667	5.78E-01	6.72E-01
30.588	3.25E-02	5.66E-02	73.9977	6.00E-01	6.91E-01
31.3849	3.54E-02	6.12E-02	74.8878	6.22E-01	7.10E-01
32.9933	4.18E-02	7.19E-02	75.7376	6.44E-01	7.28E-01
33.028	4.19E-02	7.22E-02	76.211	6.56E-01	7.37E-01
33.8042	4.54E-02	7.77E-02	76.548	6.65E-01	7.44E-01
34.6188	4.91E-02	8.38E-02	77.3201	6.85E-01	7.61E-01
35.4369	5.31E-02	8.99E-02	78.4087	7.13E-01	7.83E-01
36.258	5.73E-02	9.66E-02	79.4171	7.40E-01	8.05E-01
37.0815	6.18E-02	1.04E-01	80.0467	7.57E-01	8.18E-01
37.9072	6.65E-02	1.11E-01	80.9305	7.81E-01	8.36E-01
38.7344	7.15E-02	1.19E-01	81.7449	8.03E-01	8.53E-01
39.5628	7.68E-02	1.27E-01	82.7303	8.31E-01	8.74E-01
40.3918	8.23E-02	1.35E-01	83.6098	8.55E-01	8.92E-01
41.2211	8.81E-02	1.43E-01	84.3929	8.77E-01	9.09E-01
42.0501	9.42E-02	1.52E-01	84.848	8.90E-01	9.18E-01
42.8784	1.01E-01	1.61E-01	85.25	9.01E-01	9.27E-01
43.7055	1.07E-01	1.71E-01	86.1217	9.26E-01	9.45E-01
44.5309	1.14E-01	1.81E-01	87.0597	9.52E-01	9.65E-01
45.3543	1.21E-01	1.91E-01	87.8686	9.75E-01	9.82E-01

Blade radius (m)	x [m]	y [m]	Blade radius (m)	x [m]	y [m]
46.1751	1.29E-01	2.01E-01	88.744	1.00E+00	1.00E+00

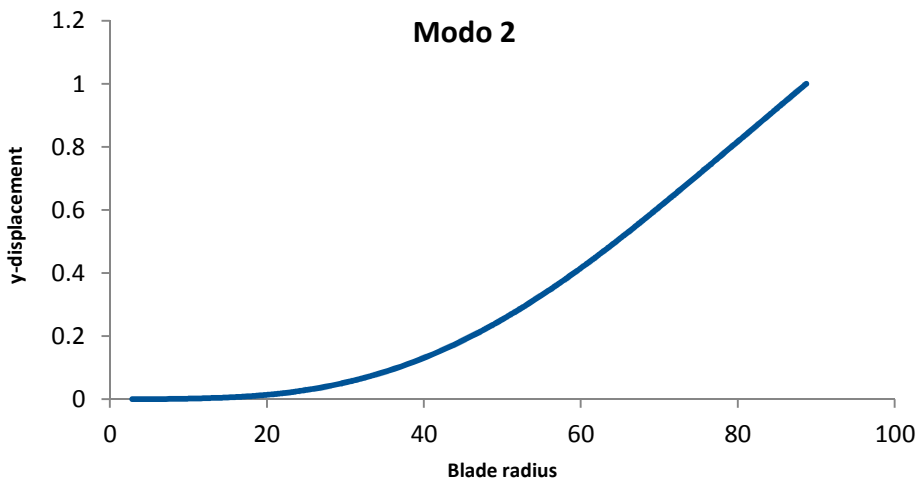
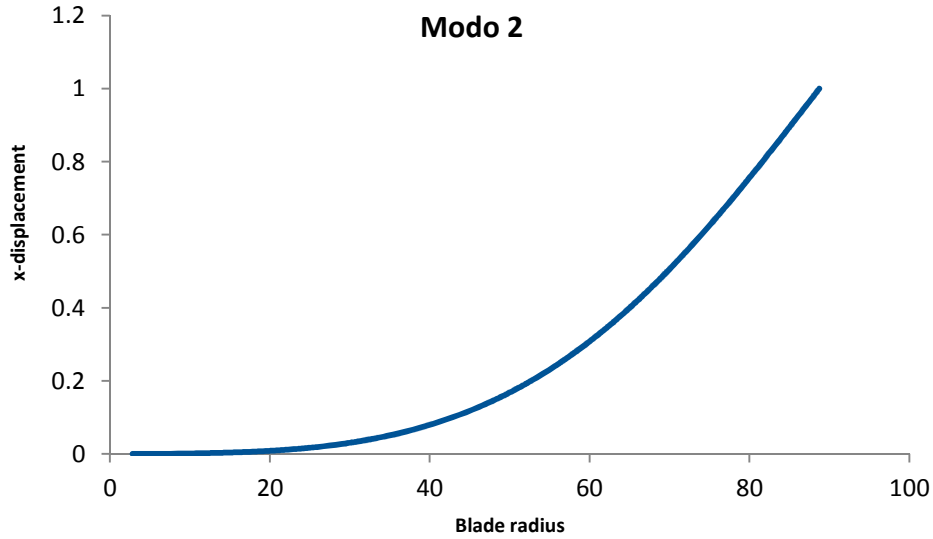


Figure 27. Mode shape for mode number 2

Table 4. *x and y displacement for mode number 2*

Blade radius (m)	x [m]	y [m]	Blade radius (m)	x [m]	y [m]
2.8311	0.00E+00	0.00E+00	46.9929	1.37E-01	2.12E-01
3.3211	0.00E+00	0.00E+00	47.71	1.44E-01	2.21E-01
4.3021	7.65E-05	0.00E+00	47.8073	1.45E-01	2.22E-01
4.7896	1.15E-04	0.00E+00	48.6178	1.53E-01	2.33E-01
5.7504	2.29E-04	3.06E-04	49.424	1.62E-01	2.45E-01
6.6819	4.21E-04	6.12E-04	51.0219	1.80E-01	2.68E-01
7.5842	6.12E-04	9.17E-04	51.8128	1.89E-01	2.80E-01
8.5169	8.80E-04	1.22E-03	52.029	1.92E-01	2.83E-01
9.4913	1.19E-03	1.53E-03	52.5977	1.99E-01	2.91E-01
9.9942	1.38E-03	1.83E-03	53.3764	2.09E-01	3.04E-01

Blade radius (m)	x [m]	y [m]	Blade radius (m)	x [m]	y [m]
11.0321	1.80E-03	2.45E-03	54.1485	2.19E-01	3.16E-01
12.1126	2.26E-03	3.06E-03	54.9136	2.30E-01	3.28E-01
12.6689	2.56E-03	3.67E-03	55.6714	2.40E-01	3.41E-01
13.8135	3.21E-03	4.59E-03	56.4216	2.51E-01	3.53E-01
14.4019	3.56E-03	4.89E-03	57.898	2.74E-01	3.78E-01
15.6103	4.40E-03	6.42E-03	58.6236	2.85E-01	3.91E-01
16.2303	4.86E-03	7.03E-03	59.3405	2.97E-01	4.04E-01
16.8606	5.39E-03	7.95E-03	60.0484	3.09E-01	4.17E-01
18.1521	6.58E-03	1.01E-02	61.4365	3.33E-01	4.42E-01
18.813	7.27E-03	1.13E-02	62.1163	3.45E-01	4.54E-01
19.4839	8.03E-03	1.28E-02	62.393	3.50E-01	4.60E-01
20.073	8.76E-03	1.41E-02	62.7863	3.57E-01	4.67E-01
20.1644	8.87E-03	1.44E-02	63.4463	3.69E-01	4.80E-01
21.554	1.08E-02	1.77E-02	64.7362	3.94E-01	5.04E-01
22.2627	1.19E-02	1.99E-02	65.3657	4.07E-01	5.17E-01
22.9803	1.31E-02	2.20E-02	65.847	4.17E-01	5.26E-01
23.7067	1.44E-02	2.45E-02	65.9848	4.19E-01	5.28E-01
25.1844	1.74E-02	3.00E-02	67.1914	4.44E-01	5.52E-01
25.9352	1.90E-02	3.30E-02	67.7789	4.57E-01	5.64E-01
26.6937	2.09E-02	3.61E-02	68.9218	4.82E-01	5.87E-01
27.4594	2.29E-02	3.98E-02	69.4772	4.94E-01	5.98E-01
28.232	2.50E-02	4.34E-02	70.5559	5.18E-01	6.20E-01
29.0112	2.73E-02	4.74E-02	71.592	5.42E-01	6.42E-01
29.7967	2.98E-02	5.20E-02	72.0941	5.54E-01	6.52E-01
30.437	3.20E-02	5.57E-02	73.0667	5.78E-01	6.72E-01
30.588	3.25E-02	5.66E-02	73.9977	6.00E-01	6.91E-01
31.3849	3.54E-02	6.12E-02	74.8878	6.22E-01	7.10E-01
32.9933	4.18E-02	7.19E-02	75.7376	6.44E-01	7.28E-01
33.028	4.19E-02	7.22E-02	76.211	6.56E-01	7.37E-01
33.8042	4.54E-02	7.77E-02	76.548	6.65E-01	7.44E-01
34.6188	4.91E-02	8.38E-02	77.3201	6.85E-01	7.61E-01
35.4369	5.31E-02	8.99E-02	78.4087	7.13E-01	7.83E-01
36.258	5.73E-02	9.66E-02	79.4171	7.40E-01	8.05E-01
37.0815	6.18E-02	1.04E-01	80.0467	7.57E-01	8.18E-01
37.9072	6.65E-02	1.11E-01	80.9305	7.81E-01	8.36E-01
38.7344	7.15E-02	1.19E-01	81.7449	8.03E-01	8.53E-01
39.5628	7.68E-02	1.27E-01	82.7303	8.31E-01	8.74E-01
40.3918	8.23E-02	1.35E-01	83.6098	8.55E-01	8.92E-01
41.2211	8.81E-02	1.43E-01	84.3929	8.77E-01	9.09E-01
42.0501	9.42E-02	1.52E-01	84.848	8.90E-01	9.18E-01
42.8784	1.01E-01	1.61E-01	85.25	9.01E-01	9.27E-01
43.7055	1.07E-01	1.71E-01	86.1217	9.26E-01	9.45E-01
44.5309	1.14E-01	1.81E-01	87.0597	9.52E-01	9.65E-01
45.3543	1.21E-01	1.91E-01	87.8686	9.75E-01	9.82E-01
46.1751	1.29E-01	2.01E-01	88.744	1.00E+00	1.00E+00

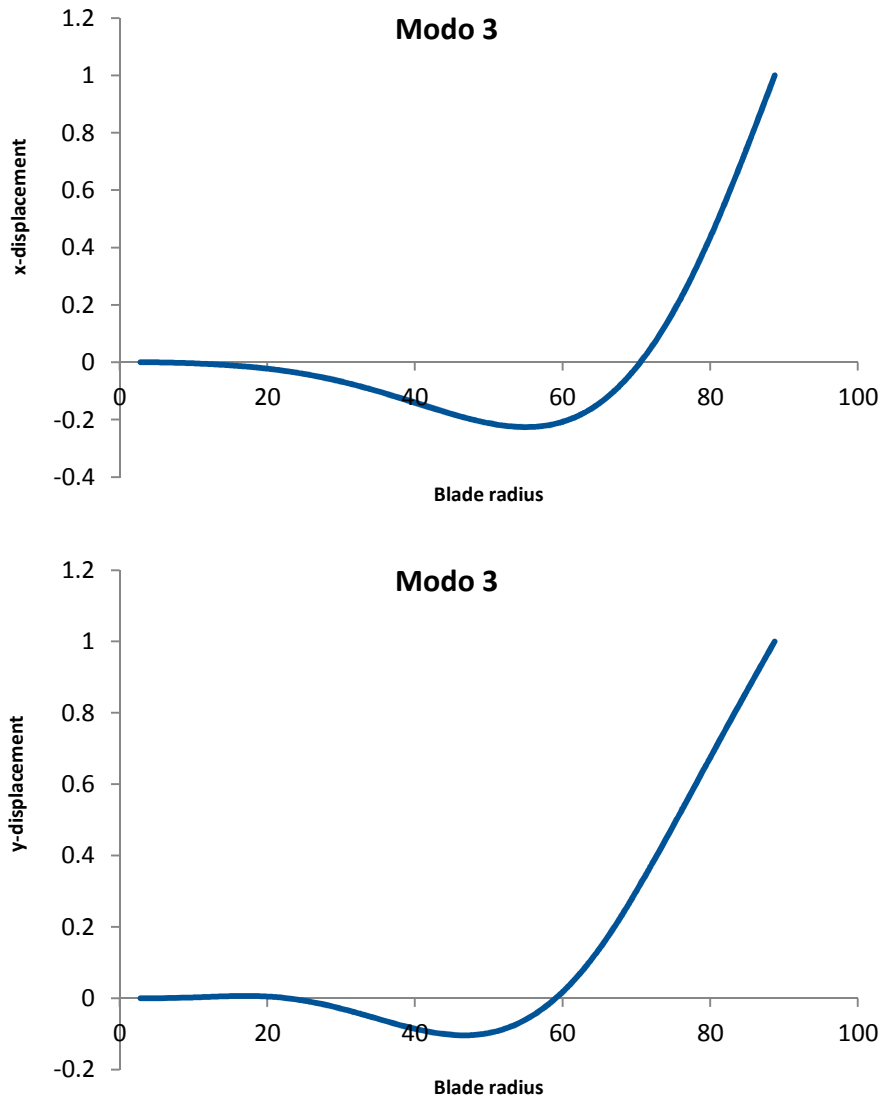


Figure 28. Mode shape for mode number 3

Table 5. *x* and *y* displacement for mode number 3

Blade radius (m)	x [m]	y [m]	Blade radius (m)	x [m]	y [m]
2.8311	0.00E+00	0.00E+00	46.9929	-1.95E-01	-1.04E-01
3.3211	-2.60E-05	0.00E+00	47.71	-1.99E-01	-1.03E-01
4.3021	-2.08E-04	0.00E+00	47.8073	-2.00E-01	-1.03E-01
4.7896	-3.38E-04	3.60E-04	48.6178	-2.05E-01	-1.01E-01
5.7504	-7.03E-04	3.60E-04	49.424	-2.09E-01	-9.92E-02
6.6819	-1.20E-03	7.19E-04	51.0219	-2.17E-01	-9.28E-02
7.5842	-1.77E-03	1.08E-03	51.8128	-2.20E-01	-8.81E-02
8.5169	-2.47E-03	1.80E-03	52.029	-2.21E-01	-8.67E-02
9.4913	-3.36E-03	2.16E-03	52.5977	-2.23E-01	-8.23E-02
9.9942	-3.85E-03	2.52E-03	53.3764	-2.24E-01	-7.62E-02
11.0321	-5.00E-03	3.24E-03	54.1485	-2.26E-01	-6.90E-02
12.1126	-6.32E-03	3.96E-03	54.9136	-2.26E-01	-6.08E-02
12.6689	-7.08E-03	4.67E-03	55.6714	-2.26E-01	-5.18E-02
13.8135	-8.77E-03	5.39E-03	56.4216	-2.25E-01	-4.21E-02
14.4019	-9.73E-03	5.75E-03	57.898	-2.20E-01	-2.01E-02

Blade radius (m)	x [m]	y [m]	Blade radius (m)	x [m]	y [m]
15.6103	-1.19E-02	6.47E-03	58.6236	-2.17E-01	-7.91E-03
16.2303	-1.31E-02	6.47E-03	59.3405	-2.13E-01	5.03E-03
16.8606	-1.44E-02	6.83E-03	60.0484	-2.07E-01	1.87E-02
18.1521	-1.74E-02	6.47E-03	61.4365	-1.95E-01	4.78E-02
18.813	-1.91E-02	6.11E-03	62.1163	-1.87E-01	6.36E-02
19.4839	-2.08E-02	5.75E-03	62.393	-1.84E-01	7.01E-02
20.073	-2.25E-02	5.03E-03	62.7863	-1.78E-01	7.98E-02
20.1644	-2.28E-02	5.03E-03	63.4463	-1.69E-01	9.64E-02
21.554	-2.72E-02	2.88E-03	64.7362	-1.48E-01	1.31E-01
22.2627	-2.97E-02	1.44E-03	65.3657	-1.36E-01	1.49E-01
22.9803	-3.24E-02	-3.60E-04	65.847	-1.26E-01	1.63E-01
23.7067	-3.52E-02	-2.52E-03	65.9848	-1.23E-01	1.68E-01
25.1844	-4.15E-02	-7.19E-03	67.1914	-9.62E-02	2.05E-01
25.9352	-4.50E-02	-1.01E-02	67.7789	-8.16E-02	2.24E-01
26.6937	-4.87E-02	-1.29E-02	68.9218	-5.05E-02	2.62E-01
27.4594	-5.27E-02	-1.62E-02	69.4772	-3.41E-02	2.82E-01
28.232	-5.69E-02	-1.98E-02	70.5559	0.00E+00	3.20E-01
29.0112	-6.13E-02	-2.37E-02	71.592	3.58E-02	3.57E-01
29.7967	-6.60E-02	-2.77E-02	72.0941	5.42E-02	3.75E-01
30.437	-6.99E-02	-3.13E-02	73.0667	9.20E-02	4.11E-01
30.588	-7.08E-02	-3.20E-02	73.9977	1.31E-01	4.46E-01
31.3849	-7.59E-02	-3.63E-02	74.8878	1.70E-01	4.79E-01
32.9933	-8.69E-02	-4.57E-02	75.7376	2.09E-01	5.11E-01
33.028	-8.71E-02	-4.57E-02	76.211	2.32E-01	5.29E-01
33.8042	-9.26E-02	-5.03E-02	76.548	2.48E-01	5.42E-01
34.6188	-9.85E-02	-5.50E-02	77.3201	2.88E-01	5.72E-01
35.4369	-1.05E-01	-6.01E-02	78.4087	3.45E-01	6.13E-01
36.258	-1.11E-01	-6.47E-02	79.4171	4.01E-01	6.52E-01
37.0815	-1.17E-01	-6.98E-02	80.0467	4.37E-01	6.76E-01
37.9072	-1.24E-01	-7.44E-02	80.9305	4.90E-01	7.09E-01
38.7344	-1.30E-01	-7.87E-02	81.7449	5.39E-01	7.40E-01
39.5628	-1.37E-01	-8.31E-02	82.7303	6.00E-01	7.77E-01
40.3918	-1.44E-01	-8.70E-02	83.6098	6.57E-01	8.10E-01
41.2211	-1.51E-01	-9.10E-02	84.3929	7.07E-01	8.40E-01
42.0501	-1.57E-01	-9.42E-02	84.848	7.37E-01	8.57E-01
42.8784	-1.64E-01	-9.71E-02	85.25	7.64E-01	8.72E-01
43.7055	-1.70E-01	-9.96E-02	86.1217	8.22E-01	9.04E-01
44.5309	-1.77E-01	-1.01E-01	87.0597	8.86E-01	9.38E-01
45.3543	-1.83E-01	-1.03E-01	87.8686	9.40E-01	9.68E-01
46.1751	-1.89E-01	-1.04E-01	88.744	1.00E+00	1.00E+00

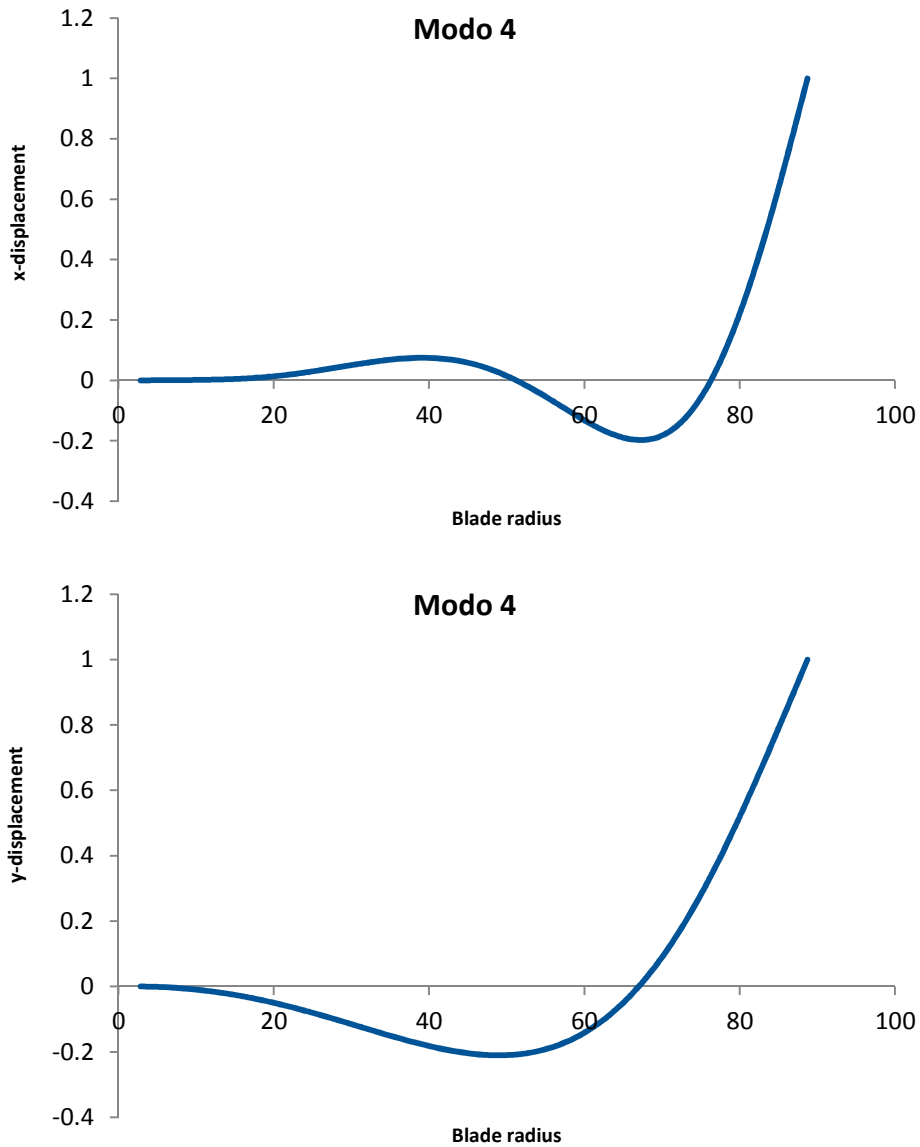


Figure 29. Mode shape for mode number 4

Table 6. *x* and *y* displacement for mode number 4

Blade radius (m)	x [m]	y [m]	Blade radius (m)	x [m]	y [m]
2.8311	0.00E+00	0.00E+00	46.9929	4.46E-02	-2.09E-01
3.3211	0.00E+00	-8.70E-05	47.71	3.84E-02	-2.10E-01
4.3021	1.15E-04	-5.22E-04	47.8073	3.75E-02	-2.10E-01
4.7896	1.15E-04	-8.70E-04	48.6178	2.98E-02	-2.10E-01
5.7504	2.31E-04	-1.80E-03	49.424	2.14E-02	-2.10E-01
6.6819	4.62E-04	-2.96E-03	51.0219	2.65E-03	-2.09E-01
7.5842	5.77E-04	-4.41E-03	51.8128	-7.50E-03	-2.07E-01
8.5169	8.08E-04	-6.15E-03	52.029	-1.04E-02	-2.06E-01
9.4913	1.15E-03	-8.26E-03	52.5977	-1.82E-02	-2.04E-01
9.9942	1.39E-03	-9.48E-03	53.3764	-2.93E-02	-2.01E-01
11.0321	1.85E-03	-1.22E-02	54.1485	-4.07E-02	-1.97E-01
12.1126	2.31E-03	-1.54E-02	54.9136	-5.24E-02	-1.93E-01
12.6689	2.65E-03	-1.71E-02	55.6714	-6.43E-02	-1.87E-01

Blade radius (m)	x [m]	y [m]	Blade radius (m)	x [m]	y [m]
13.8135	3.46E-03	-2.11E-02	56.4216	-7.62E-02	-1.81E-01
14.4019	3.92E-03	-2.33E-02	57.898	-9.97E-02	-1.67E-01
15.6103	5.19E-03	-2.82E-02	58.6236	-1.11E-01	-1.59E-01
16.2303	6.00E-03	-3.09E-02	59.3405	-1.22E-01	-1.50E-01
16.8606	6.93E-03	-3.38E-02	60.0484	-1.33E-01	-1.41E-01
18.1521	9.12E-03	-4.00E-02	61.4365	-1.53E-01	-1.20E-01
18.813	1.05E-02	-4.34E-02	62.1163	-1.61E-01	-1.08E-01
19.4839	1.20E-02	-4.69E-02	62.393	-1.65E-01	-1.03E-01
20.073	1.34E-02	-5.02E-02	62.7863	-1.69E-01	-9.61E-02
20.1644	1.36E-02	-5.07E-02	63.4463	-1.76E-01	-8.33E-02
21.554	1.75E-02	-5.87E-02	64.7362	-1.88E-01	-5.60E-02
22.2627	1.99E-02	-6.29E-02	65.3657	-1.92E-01	-4.16E-02
22.9803	2.23E-02	-6.74E-02	65.847	-1.95E-01	-3.00E-02
23.7067	2.48E-02	-7.20E-02	65.9848	-1.95E-01	-2.66E-02
25.1844	3.04E-02	-8.16E-02	67.1914	-1.98E-01	4.81E-03
25.9352	3.34E-02	-8.66E-02	67.7789	-1.97E-01	2.12E-02
26.6937	3.65E-02	-9.18E-02	68.9218	-1.93E-01	5.50E-02
27.4594	3.97E-02	-9.71E-02	69.4772	-1.88E-01	7.24E-02
28.232	4.29E-02	-1.02E-01	70.5559	-1.76E-01	1.08E-01
29.0112	4.63E-02	-1.08E-01	71.592	-1.58E-01	1.45E-01
29.7967	4.95E-02	-1.14E-01	72.0941	-1.48E-01	1.63E-01
30.437	5.22E-02	-1.18E-01	73.0667	-1.23E-01	2.01E-01
30.588	5.28E-02	-1.19E-01	73.9977	-9.41E-02	2.38E-01
31.3849	5.60E-02	-1.25E-01	74.8878	-6.18E-02	2.76E-01
32.9933	6.20E-02	-1.36E-01	75.7376	-2.62E-02	3.13E-01
33.028	6.21E-02	-1.37E-01	76.211	-4.50E-03	3.35E-01
33.8042	6.48E-02	-1.42E-01	76.548	1.19E-02	3.50E-01
34.6188	6.72E-02	-1.48E-01	77.3201	5.19E-02	3.86E-01
35.4369	6.95E-02	-1.53E-01	78.4087	1.15E-01	4.39E-01
36.258	7.13E-02	-1.59E-01	79.4171	1.80E-01	4.89E-01
37.0815	7.27E-02	-1.64E-01	80.0467	2.23E-01	5.21E-01
37.9072	7.38E-02	-1.70E-01	80.9305	2.88E-01	5.67E-01
38.7344	7.43E-02	-1.75E-01	81.7449	3.51E-01	6.11E-01
39.5628	7.43E-02	-1.79E-01	82.7303	4.33E-01	6.64E-01
40.3918	7.38E-02	-1.84E-01	83.6098	5.09E-01	7.12E-01
41.2211	7.26E-02	-1.88E-01	84.3929	5.79E-01	7.55E-01
42.0501	7.09E-02	-1.93E-01	84.848	6.21E-01	7.81E-01
42.8784	6.83E-02	-1.96E-01	85.25	6.59E-01	8.03E-01
43.7055	6.51E-02	-2.00E-01	86.1217	7.42E-01	8.52E-01
44.5309	6.12E-02	-2.03E-01	87.0597	8.33E-01	9.05E-01
45.3543	5.64E-02	-2.05E-01	87.8686	9.13E-01	9.51E-01
46.1751	5.09E-02	-2.07E-01	88.744	1.00E+00	1.00E+00

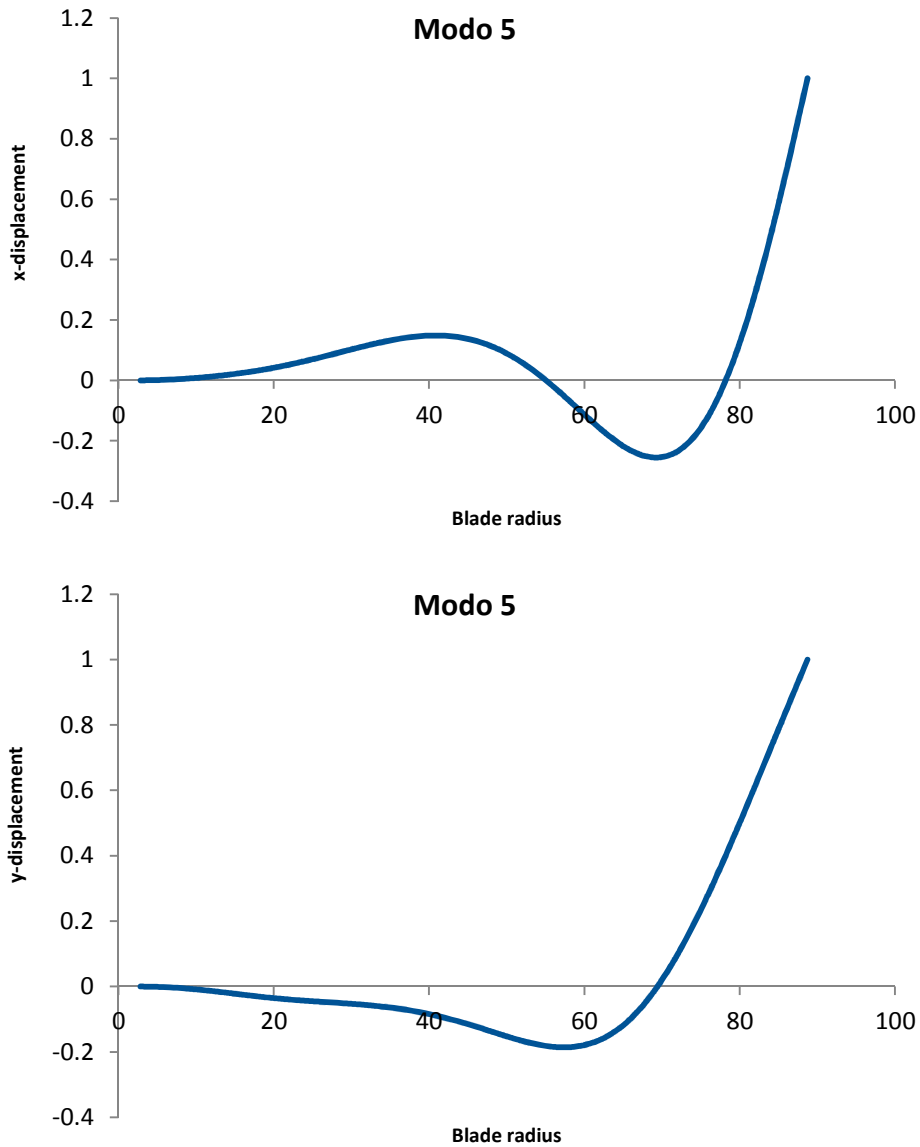


Figure 30. Mode shape for mode number 5

Table 7. *x* and *y* displacement for mode number 5

Blade radius (m)	x [m]	y [m]	Blade radius (m)	x [m]	y [m]
2.8311	0.00E+00	0.00E+00	46.9929	1.23E-01	-1.30E-01
3.3211	8.72E-05	-1.67E-04	47.71	1.16E-01	-1.35E-01
4.3021	4.58E-04	-5.01E-04	47.8073	1.15E-01	-1.36E-01
4.7896	7.63E-04	-8.35E-04	48.6178	1.07E-01	-1.42E-01
5.7504	1.53E-03	-1.67E-03	49.424	9.70E-02	-1.48E-01
6.6819	2.53E-03	-2.84E-03	51.0219	7.44E-02	-1.60E-01
7.5842	3.73E-03	-4.01E-03	51.8128	6.17E-02	-1.65E-01
8.5169	5.19E-03	-5.68E-03	52.029	5.81E-02	-1.66E-01
9.4913	6.95E-03	-7.68E-03	52.5977	4.82E-02	-1.70E-01
9.9942	7.98E-03	-8.68E-03	53.3764	3.38E-02	-1.74E-01
11.0321	1.02E-02	-1.12E-02	54.1485	1.87E-02	-1.78E-01
12.1126	1.28E-02	-1.39E-02	54.9136	2.99E-03	-1.81E-01
12.6689	1.43E-02	-1.54E-02	55.6714	-1.32E-02	-1.84E-01

Blade radius (m)	x [m]	y [m]	Blade radius (m)	x [m]	y [m]
13.8135	1.75E-02	-1.85E-02	56.4216	-2.98E-02	-1.85E-01
14.4019	1.94E-02	-2.02E-02	57.898	-6.37E-02	-1.86E-01
15.6103	2.34E-02	-2.37E-02	58.6236	-8.08E-02	-1.85E-01
16.2303	2.56E-02	-2.55E-02	59.3405	-9.77E-02	-1.82E-01
16.8606	2.80E-02	-2.72E-02	60.0484	-1.14E-01	-1.79E-01
18.1521	3.32E-02	-3.09E-02	61.4365	-1.46E-01	-1.69E-01
18.813	3.61E-02	-3.26E-02	62.1163	-1.62E-01	-1.62E-01
19.4839	3.92E-02	-3.42E-02	62.393	-1.68E-01	-1.59E-01
20.073	4.20E-02	-3.56E-02	62.7863	-1.76E-01	-1.54E-01
20.1644	4.25E-02	-3.57E-02	63.4463	-1.89E-01	-1.45E-01
21.554	4.96E-02	-3.87E-02	64.7362	-2.13E-01	-1.24E-01
22.2627	5.35E-02	-4.02E-02	65.3657	-2.23E-01	-1.12E-01
22.9803	5.75E-02	-4.16E-02	65.847	-2.30E-01	-1.01E-01
23.7067	6.18E-02	-4.27E-02	65.9848	-2.32E-01	-9.82E-02
25.1844	7.09E-02	-4.52E-02	67.1914	-2.46E-01	-6.81E-02
25.9352	7.56E-02	-4.64E-02	67.7789	-2.51E-01	-5.18E-02
26.6937	8.05E-02	-4.76E-02	68.9218	-2.55E-01	-1.65E-02
27.4594	8.56E-02	-4.88E-02	69.4772	-2.56E-01	2.00E-03
28.232	9.07E-02	-4.99E-02	70.5559	-2.51E-01	4.07E-02
29.0112	9.59E-02	-5.13E-02	71.592	-2.41E-01	8.11E-02
29.7967	1.01E-01	-5.26E-02	72.0941	-2.34E-01	1.02E-01
30.437	1.05E-01	-5.36E-02	73.0667	-2.15E-01	1.44E-01
30.588	1.06E-01	-5.39E-02	73.9977	-1.91E-01	1.86E-01
31.3849	1.11E-01	-5.54E-02	74.8878	-1.62E-01	2.29E-01
32.9933	1.21E-01	-5.89E-02	75.7376	-1.29E-01	2.71E-01
33.028	1.21E-01	-5.89E-02	76.211	-1.08E-01	2.95E-01
33.8042	1.26E-01	-6.09E-02	76.548	-9.18E-02	3.12E-01
34.6188	1.30E-01	-6.31E-02	77.3201	-5.19E-02	3.53E-01
35.4369	1.34E-01	-6.56E-02	78.4087	1.24E-02	4.12E-01
36.258	1.38E-01	-6.83E-02	79.4171	8.02E-02	4.67E-01
37.0815	1.41E-01	-7.13E-02	80.0467	1.26E-01	5.03E-01
37.9072	1.44E-01	-7.46E-02	80.9305	1.96E-01	5.53E-01
38.7344	1.46E-01	-7.81E-02	81.7449	2.66E-01	5.99E-01
39.5628	1.48E-01	-8.20E-02	82.7303	3.55E-01	6.56E-01
40.3918	1.48E-01	-8.63E-02	83.6098	4.40E-01	7.07E-01
41.2211	1.48E-01	-9.07E-02	84.3929	5.20E-01	7.52E-01
42.0501	1.48E-01	-9.55E-02	84.848	5.67E-01	7.78E-01
42.8784	1.46E-01	-1.01E-01	85.25	6.10E-01	8.01E-01
43.7055	1.43E-01	-1.06E-01	86.1217	7.04E-01	8.51E-01
44.5309	1.40E-01	-1.12E-01	87.0597	8.09E-01	9.04E-01
45.3543	1.35E-01	-1.18E-01	87.8686	9.00E-01	9.50E-01
46.1751	1.30E-01	-1.24E-01	88.744	1.00E+00	1.00E+00

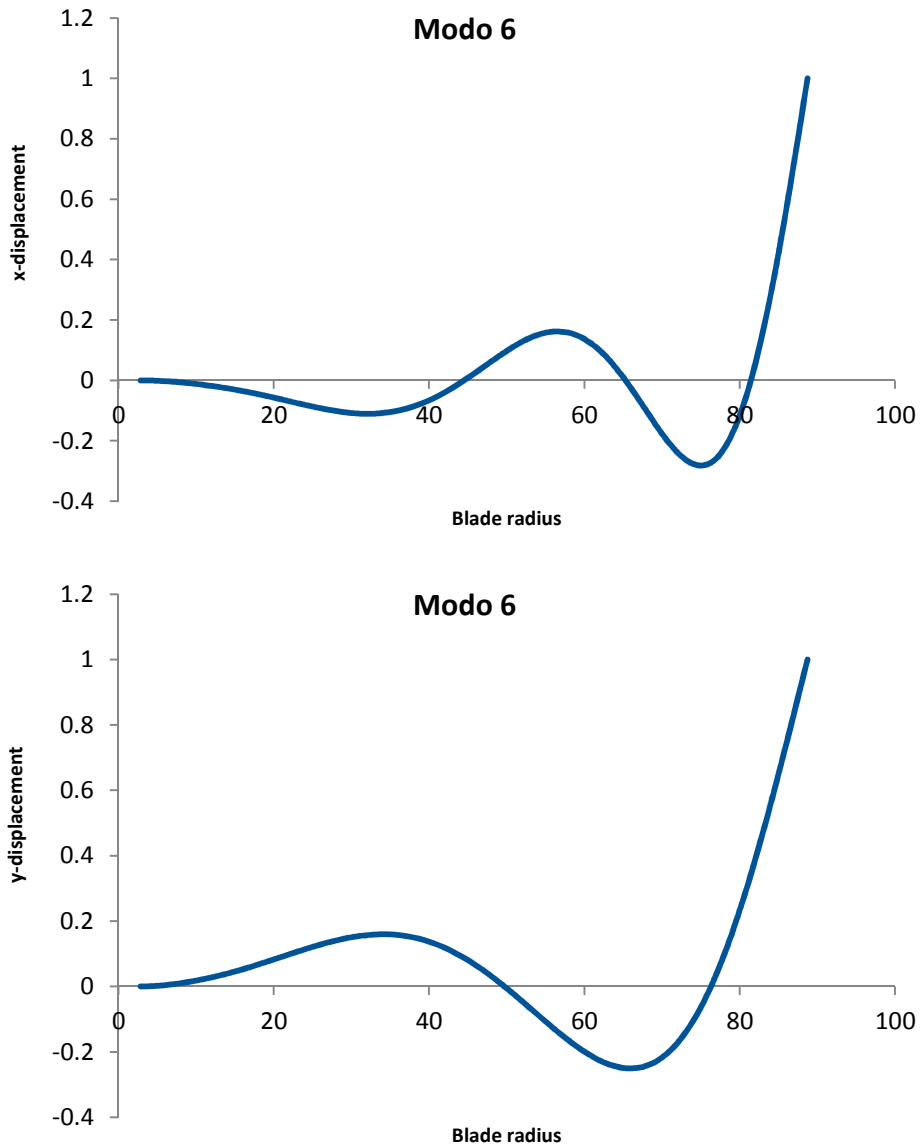


Figure 31. Mode shape for mode number 6

Table 8. *x* and *y* displacement for mode number 6

Blade radius (m)	x [m]	y [m]	Blade radius (m)	x [m]	y [m]
2.8311	0.00E+00	0.00E+00	46.9929	4.38E-02	4.95E-02
3.3211	-1.51E-04	2.24E-04	47.71	5.69E-02	3.72E-02
4.3021	-7.54E-04	1.16E-03	47.8073	5.87E-02	3.55E-02
4.7896	-1.21E-03	1.87E-03	48.6178	7.33E-02	2.09E-02
5.7504	-2.41E-03	3.67E-03	49.424	8.75E-02	5.80E-03
6.6819	-3.92E-03	5.95E-03	51.0219	1.14E-01	-2.54E-02
7.5842	-5.68E-03	8.68E-03	51.8128	1.25E-01	-4.14E-02
8.5169	-7.85E-03	1.19E-02	52.029	1.28E-01	-4.58E-02
9.4913	-1.04E-02	1.58E-02	52.5977	1.36E-01	-5.74E-02
9.9942	-1.19E-02	1.80E-02	53.3764	1.45E-01	-7.34E-02
11.0321	-1.51E-02	2.29E-02	54.1485	1.52E-01	-8.93E-02
12.1126	-1.89E-02	2.85E-02	54.9136	1.57E-01	-1.05E-01
12.6689	-2.09E-02	3.15E-02	55.6714	1.61E-01	-1.20E-01

Blade radius (m)	x [m]	y [m]	Blade radius (m)	x [m]	y [m]
13.8135	-2.55E-02	3.83E-02	56.4216	1.62E-01	-1.35E-01
14.4019	-2.80E-02	4.19E-02	57.898	1.58E-01	-1.63E-01
15.6103	-3.35E-02	4.99E-02	58.6236	1.53E-01	-1.76E-01
16.2303	-3.65E-02	5.43E-02	59.3405	1.46E-01	-1.89E-01
16.8606	-3.97E-02	5.88E-02	60.0484	1.36E-01	-2.00E-01
18.1521	-4.65E-02	6.84E-02	61.4365	1.11E-01	-2.19E-01
18.813	-5.02E-02	7.34E-02	62.1163	9.59E-02	-2.28E-01
19.4839	-5.40E-02	7.86E-02	62.393	8.92E-02	-2.31E-01
20.073	-5.75E-02	8.33E-02	62.7863	7.89E-02	-2.35E-01
20.1644	-5.80E-02	8.40E-02	63.4463	6.04E-02	-2.40E-01
21.554	-6.64E-02	9.49E-02	64.7362	1.96E-02	-2.48E-01
22.2627	-7.07E-02	1.00E-01	65.3657	-2.14E-03	-2.50E-01
22.9803	-7.50E-02	1.06E-01	65.847	-1.94E-02	-2.51E-01
23.7067	-7.93E-02	1.12E-01	65.9848	-2.45E-02	-2.51E-01
25.1844	-8.78E-02	1.22E-01	67.1914	-7.01E-02	-2.48E-01
25.9352	-9.19E-02	1.28E-01	67.7789	-9.27E-02	-2.44E-01
26.6937	-9.58E-02	1.33E-01	68.9218	-1.37E-01	-2.33E-01
27.4594	-9.93E-02	1.37E-01	69.4772	-1.57E-01	-2.26E-01
28.232	-1.03E-01	1.42E-01	70.5559	-1.96E-01	-2.07E-01
29.0112	-1.05E-01	1.46E-01	71.592	-2.28E-01	-1.83E-01
29.7967	-1.08E-01	1.50E-01	72.0941	-2.41E-01	-1.70E-01
30.437	-1.09E-01	1.52E-01	73.0667	-2.63E-01	-1.40E-01
30.588	-1.09E-01	1.53E-01	73.9977	-2.77E-01	-1.06E-01
31.3849	-1.10E-01	1.56E-01	74.8878	-2.82E-01	-6.90E-02
32.9933	-1.10E-01	1.59E-01	75.7376	-2.79E-01	-2.92E-02
33.028	-1.10E-01	1.59E-01	76.211	-2.74E-01	-5.27E-03
33.8042	-1.09E-01	1.60E-01	76.548	-2.68E-01	1.26E-02
34.6188	-1.07E-01	1.60E-01	77.3201	-2.50E-01	5.59E-02
35.4369	-1.03E-01	1.59E-01	78.4087	-2.09E-01	1.23E-01
36.258	-9.92E-02	1.57E-01	79.4171	-1.56E-01	1.91E-01
37.0815	-9.38E-02	1.54E-01	80.0467	-1.15E-01	2.36E-01
37.9072	-8.74E-02	1.51E-01	80.9305	-4.61E-02	3.02E-01
38.7344	-7.99E-02	1.46E-01	81.7449	2.78E-02	3.67E-01
39.5628	-7.13E-02	1.41E-01	82.7303	1.31E-01	4.48E-01
40.3918	-6.17E-02	1.34E-01	83.6098	2.34E-01	5.24E-01
41.2211	-5.11E-02	1.27E-01	84.3929	3.36E-01	5.94E-01
42.0501	-3.96E-02	1.18E-01	84.848	3.98E-01	6.35E-01
42.8784	-2.71E-02	1.09E-01	85.25	4.55E-01	6.72E-01
43.7055	-1.40E-02	9.87E-02	86.1217	5.83E-01	7.52E-01
44.5309	-1.26E-04	8.76E-02	87.0597	7.29E-01	8.41E-01
45.3543	1.42E-02	7.56E-02	87.8686	8.58E-01	9.17E-01
46.1751	2.89E-02	6.29E-02	88.744	1.00E+00	1.00E+00

Deflection analysis

For the simple load case deflection analysis it has been used the beam FE model explained in chapter 1.1. Loads in Table 6 from the document “Information on the Benchmark of blade structural models_ver2.pdf” [2] have been simply applied at one single node centred in the pitch axis of each load r-location. Output results from MSC. Nastran linear calculation are only obtained at the nodes defining each beam, which are centred in the pitch axis of each section. Hence, displacements at the various tip key points are not given.

Tip displacement of blade under **simple** load case

Table 9. *Tip displacement under simple case*

Key point No.	Coordinates			Displacement solution simple case		
	x [m]	y [m]	z [m]	x [m]	y [m]	z [m]
-	0.000	0.000	89.166	2.066106E+01	-3.250417E+00	0.0

Tip displacement of blade under **Reference** load case

As the simple load case has been provided in order to reduce the variability in simulation results and we use a FE bar model to obtain the displacements, we have calculated the displacements only for the simple load case.

Buckling analysis

NA

Extreme load carrying capacity analysis

This analysis has been performed with the software BASSF only at the five reference sections loaded under the Reference Load Case . Therefore failure arising at other r-locations different from the ones of the reference sections is not assessed.

Extreme load carrying capacity multiplication factor (static strength under **reference** case): 0.3405.

The worst failure index is found according to Hill failure criteria in RefSec_4 (R 54149 m) in a triax ply of the leading panel in the suction side.

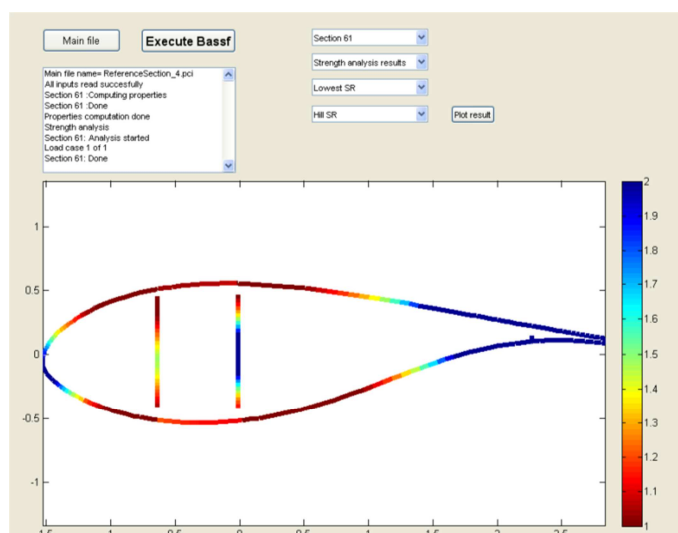


Figure 32. Output simulation results from BASSF

Table 10. *Failure indexes in RefSection_4 in the leading panel of the suction side*

Hill	Hoffman	Tsai-Wu	MaxStrain	Puck
0.3405	0.3570	0.3449	0.3660	NA*

* Puck criteria is only checked for Uniax plies.

2.2 Reference blade sections results

Mass properties of reference blade sections

Table 11. Mass properties of reference blade sections

Property		Sec_1	Sec_2	Sec_3	Sec_4	Sec_5
Z-position	(m)	2.800	26.694	37.907	54.149	71.592
Mass/Length	(kg/m)	1213.404	642.911	500.500	333.426	158.343
Mass Centre	x (m)	-0.0247	- 0.3283	- 0.2510	-0.1746	-0.1284
	y (m)	0.0071	0.0849	0.0404	0.0275	0.0191
Mass moment of inertia (ρI)	ρI_{xx} (kg-m)	4.0457E+003	515.0437	215.2488	57.9253	11.6029
	ρI_{yy} (kg-m)	3.8159E+003	1.7658E+003	983.1538	346.1245	71.5781
	ρI_{xy} (kg-m)	-20.8864	-240.3247	-106.6380	-18.6901	0.3603
Polar mass inertia (ρI_p)	ρI_p (kg-m)	7861.6301	2280.7963	1198.4026	404.0499	83.1810

Stiffness properties of reference blade sections

Table 12. Stiffness properties of reference blade sections

Property		Sec_1	Sec_2	Sec_3	Sec_4	Sec_5
Z-position	(m)	2.800	26.694	37.907	54.149	71.592
Axial Stiffness	EA (N)	1.8102E+010	9.5134E+009	7.6884E+009	5.3747E+009	2.5884E+009
Elastic Centre	x (m)	-0.0275	- 0.1672	- 0.0596	-0.0190	-0.0490
	y (m)	0.0077	0.0581	0.0146	0.0118	0.0175
Bending Stiffness	EI_{xx} (Nm ²)	6.29503E+010	9.12197E+009	3.89100E+009	1.09032E+009	2.22265E+008
	EI_{yy} (Nm ²)	6.26438E+010	2.39623E+010	1.29216E+010	4.54031E+009	9.55089E+008
	EI_{xy} (Nm ²)	-3.49946E+008	-3.33997E+009	-1.36243E+009	-2.30872E+008	7.43428E+006
Shear Centre	x (m)	-0.0362	- 0.4440	-0.3762	-0.2533	-0.1082
	y (m)	0.0130	-0.0689	-0.0145	-0.0465	-0.0465
Torsional Stiffness	GJ (Nm ²)	2.704E+010	1.694E+009	6.575E+008	1.856E+008	4.376E+007
Shear Stiffness	S_x (N)	-	-	-	-	-
	S_y (N)	-	-	-	-	-
Coupling stiffness, Other as needed...						

Extreme load carrying capacity analysis under simple load case

Displacements for reference blade sections under the simple load case application

Table 13. Displacement solution under simple load case for RefSection_2 (26.694m)

Key point No.	Key Point Coordinates			Displacement solution simple case		
	x [m]	y [m]	z [m]	x [m]	y [m]	z [m]
-	0.000	0.000	26.694	4.033450E-01	-1.688033E-01	0.0

Table 14. *Displacement solution under simple load case for RefSection_3 (37.907m)*

Key point No.	Key Point Coordinates			Displacement solution simple case		
	x [m]	y [m]	z [m]	x [m]	y [m]	z [m]
-	0.000	0.000	37.907	1.259370E+00	-4.399931E-01	0.0

Table 15. *Displacement solution under simple load case for RefSection_4 (54.149m)*

Key point No.	Key Point Coordinates			Displacement solution simple case		
	x [m]	y [m]	z [m]	x [m]	y [m]	z [m]
-	0.000	0.000	54.149	4.131765E+00	-1.106134E+00	0.0

Table 16. *Displacement solution under simple load case for RefSection_5 (71.592m)*

Key point No.	Key Point Coordinates			Displacement solution simple case		
	x [m]	y [m]	z [m]	x [m]	y [m]	z [m]
-	0.000	0.000	71.952	1.050504E+01	-2.114279E+00	0.0

Layer strains and/or stresses at key points of reference sections under simple load case

We assumed that the simple load case was provided only for the model using FEM and our FE bar model does not have the ability of analysing the strains and/or stresses at key points of reference sections, because of the beam theory used.

Extreme load carrying capacity analysis under reference load case

Displacements for reference blade sections under the reference load case application

As the simple load case has been provided in order to reduce the variability in simulation results and we use a FE bar model to obtain the displacements, only the displacements for the simple load case have been calculated.

Layer strains and/or stresses at key points of reference sections under reference load case

See excel template*

* Due to the Beam Euler - Bernoulli Theory in which is based the software BASSF, the strains in the direction towards the trailing edge (ϵ_y in GL2010 Fig 4.A.1 coordinate system; $-\epsilon_x$ in the global coordinate system of the present structural benchmark) are not calculated. It is assumed a plane strain state in which $\epsilon_x=0$ and σ_x according to it (in the global coordinate system of the present structural benchmark). The assumption of iso-deformation through the segment width and through the laminate thickness is followed so that all laminae within the laminate stack-up suffer the same axial strain (ϵ_z), in-plane shear strain (γ_{xz}) and “transverse” strain (ϵ_x). The stresses (σ_z , σ_x , τ_{xz} ; given in the global coordinate system of the present structural benchmark) in each type of lamina within the segment laminate are calculated based on the stiffness matrix [Q] of each lamina type.

CRES contribution on the Benchmark of blade structural models

D. I. Chortis & D. J. Lekou

Center for Renewable Energy Sources and Saving

SHORT DESCRIPTION OF STRUCTURAL ANALYSIS TOOL(S) USED

The structural analysis of the reference blade rotor was conducted in two steps and involved two structural analysis tools, respectively, which are briefly described in the next paragraphs.

I. THIN

“THIN” is an in-house developed code for the cross-sectional analysis of composite rotor blades. It consists of three sub-modules and it is capable of representing the mechanical properties of the full three-dimensional blade in the one-dimensional beam element [1-2]. In addition, it is able to perform a detailed strength assessment after stress resultants at each section have been introduced into the code. The analysis performed is based on the usual Euler-Bernoulli beam assumptions. “THIN” uses as an input the material properties and the lamination sequences of the cross-section segments, and therefore provides the effective properties of each laminate based on the assumptions of the Classical Lamination Theory (CLT). Its output capabilities further include the estimation of the geometric centres as well as the mass and stiffness parameters of the cross-sections. It is also capable of calculating the developed stresses both at the bottom and at the top layer of each element of the section (including the shear webs) by taking into account the provided internal resultant forces and moments, at each section.

II. EMRC/NISA II

The structural analysis of the benchmark blade on global level was further conducted by the commercial finite element package, EMRC/NISA II. Each cross-section was modeled by 107 KeyPoints, which divided the sections into segments with various material lay-up configurations, according to the detailed piece of information provided by DTU [3]. Thereafter, the rotor was discretized into 100 stations along its length, each one entailing a different geometry shape [3]. The blade model was built by 3-D laminated 8-node composite shell elements, each one having six degrees of freedom per node (three displacements and three rotations) and consisting of a number of layers of perfectly bonded orthotropic materials. The blade structure is supported on three shear webs, two of which run along the total blade length, whereas the third one begins at $R_{webC}=21.801\text{m}$ up to the blade’s tip ($R_{tip}=89.166\text{m}$).

The capabilities of the 3-D shell element include the prediction of the static, modal and buckling response of the blade, which is assumed to be clamped at its root. The element also provides the nodal displacements of the blade as well as the developed stresses and strains fields of the whole structure. In addition, it is able to predict the response of the rotor blade against failure and to provide its buckling mode shapes.

Due to modeling issues at the tip of the rotor blade, the primary analysis, neglected the modeling of the blade’s tip, starting at station $R_{start}=88.302\text{m}$ and ending up at station, $R_{end}=89.166\text{m}$. In that case the whole structure consisted of 22276 layered shell elements and 63265 nodes in total. Based on that model, an updated version of the blade was further built, including the missing tip of the structure. Consequently, an updated full blade model was incorporated into FEA environment, which resulted in 23716 shell elements and 67345 nodes, respectively.

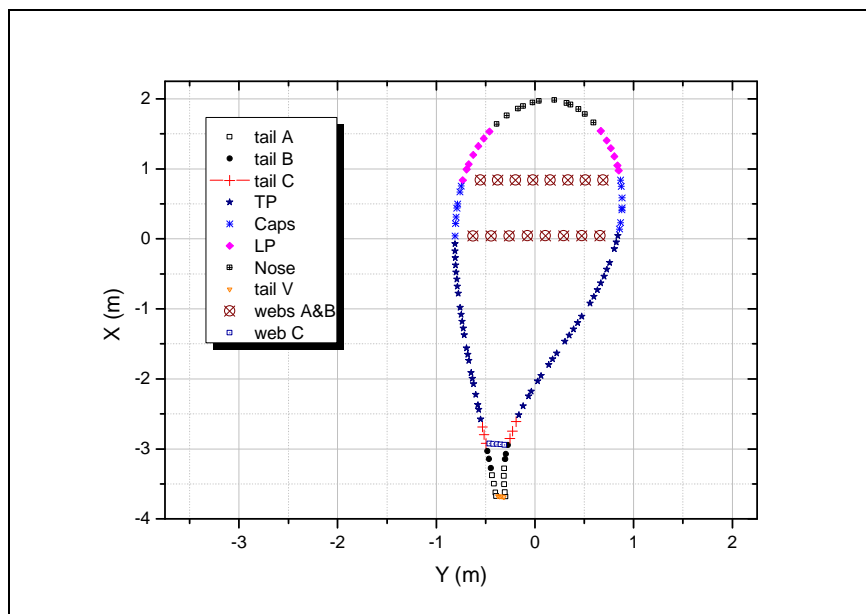
1.1. For the analysis for the extraction of blade properties

The blade properties on sectional level were predicted by “THIN” structural analysis tool, which requires as input the technical elastic properties of each material used in the blade analysis. In detail these are: the material density, Young’s modulus in the two main directions of the orthotropic lamina, the in-plane Poisson ratio and the respective in-plane shear modulus. In addition, the strength design properties per material should also be

included in the input data set in order to investigate the blade's response against failure. Up to this stage, the solver calculates the homogenized multilayer construction effective properties, namely the total thickness of the laminate, the mass density and the elasticity and shear modulus on the primary laminate axis (considered to correspond with the blade axis) [1-2].

The next step refers to the incorporation of the cross-section geometry data, which gives out the geometric centers as well as the stiffness and mass properties of the cross-section. The code, estimates the section's mass centre, the elastic and shear centres, as well as the sectional properties, with respect to the elastic centre of the section. It also provides the line mass, ρA , the mass inertia in the flap and edge directions, ρI_{xx} and ρI_{yy} respectively, and the cross-mass inertia, ρI_{xy} , with respect to the mass-weighted centre of the section. Regarding the stiffness parameters, the code calculates the axial stiffness, EA , the bending stiffness in the flap and edge directions, EI_{xx} and EI_{yy} , respectively, the cross-bending stiffness, EI_{xy} , and torsional stiffness, GJ , with respect to the section's elastic centre, taking as input the effective laminate properties described above. Based on the strength design properties and the provided internal resultant forces and moments values (input from aeroelastic codes), "THIN" modules may predict the stresses σ_{xx} , σ_{yy} and σ_{xy} per layer for all segments laminations of the cross-section. In addition it calculates the failure criterion values per ply and per laminate.

A typical example of the 3rd reference section at $R_3=37.907\text{m}$ is shown in Graph 1. The cross-section consists of three shear webs, which form four cells. In order to model the "reference sections" of the present report, each section is discretized into 136 elements and 133 nodes, based on the coordinates provided by DTU (107 KeyPoints) [3]. Each segment (including the shear webs) is characterized by a specific lamination sequence and material set of properties at each station along the blade's length.



Graph 1. Nodes and segments of the 3rd reference section incorporated in "THIN" code environment

1.2. For the natural frequencies (modal) analysis

The eigenvalue analysis of the model is performed using a conventional subspace iteration technique in the EMRC/NISA II FEM package. Two cases were investigated, depending on the existence or not of blade's tip ($R_{start}=88.302m$ - $R_{end}=89.166m$).

Missing Blade's Tip. The blade is supposed to start at $R_{root}=2.800m$, where the blade's nodes are fully clamped and ends up at $R_{tip}=88.302m$. In order to obtain more accurate results, the missing last section at the blade's tip is substituted in the FEM program by an appropriate mass element of $m_{el}=16.15kg$ according to the mass density values (kg/m) provided by DTU [3].

Full Blade Model. The wind turbine model is fully clamped at $R_{root}=2.800m$, and reaches its real length at $R_{real_tip}=89.166m$

Modal analyses for both of the blade models were carried out, which predicted the six first natural frequencies and the respective mode shapes of the structure in the flapwise and edgewise directions and it is further described in section 2.1 of the present report. For the sake of completeness, the 7th natural frequency, which corresponds to the 1st torsional mode, is also presented.

1.3. For the extreme load carrying capacity analysis (static analysis)

The static analysis of the blade was conducted both for the reference and the simple load cases using **EMRC/NISA II** FEM package, in order to calculate the displacements and predict the stresses and strains field developed on the rotor blade. Additional results regarding the failure of the reference cross-sections using "**THIN**" structural analysis tool were also carried out. It should be highlighted that both the failure and the buckling analyses were done by taking into account only the reference load case scenario, which assumed a smooth distribution of the applied loads along the blade's length.

Failure criterion used

The investigation of blade's response against failure was carried out based on the Tsai-Wu criterion, which was introduced into the model by implementing the strength design properties provided in Ref. [4], under section 2.3. Additionally, the interaction coefficient F_{12} was also introduced into the properties of the blade's materials and is given by the following relation:

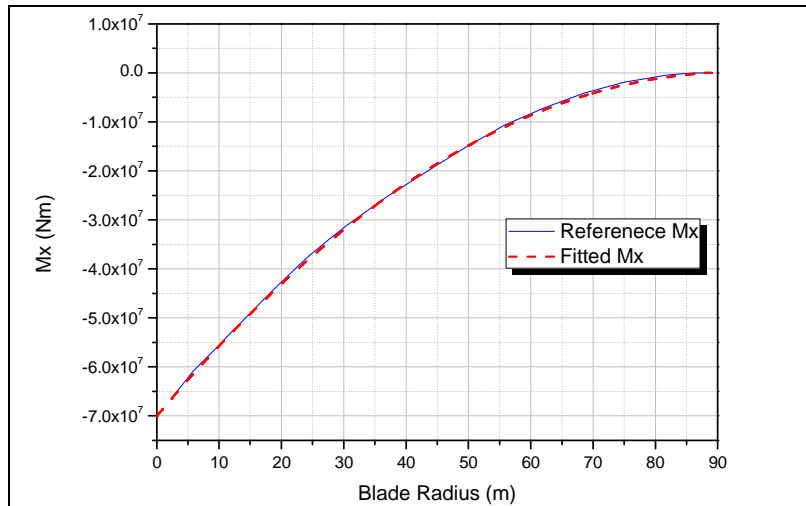
$$F_{12} = \frac{-1}{\sqrt{X_T X_C Y_T Y_C}} \quad (1)$$

The Tsai-Wu failure criterion was incorporated in both NISA II and "THIN" structural analysis tools for the structural analysis of the whole blade and the 5 reference cross-sections, respectively.

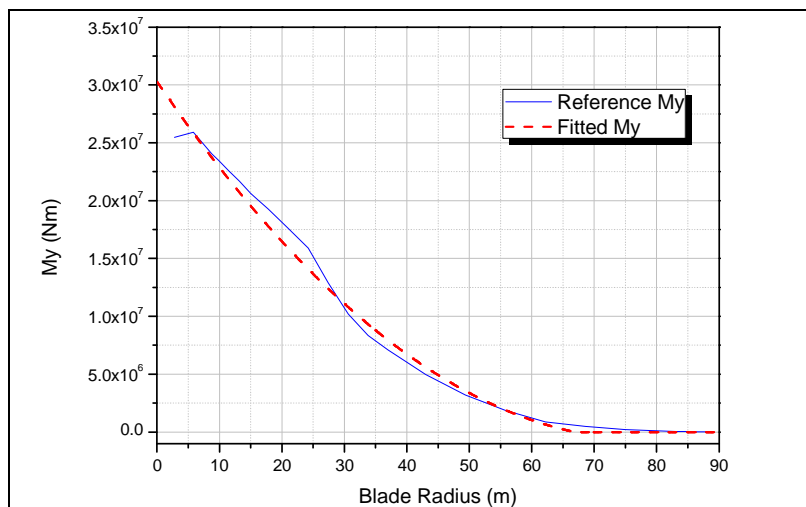
Modelling of the reference load case

The reference load case proposed by [4] was incorporated both in "**THIN**" and **EMRC/NISA II** structural analysis tools towards the calculation of the displacements, the strains and stresses, as well as the failure criterion values on each ply of the rotor blade elements. The provided sectional stress resultants data were transformed into concentrated loads in the flapwise and edgewise directions, F_y and F_x , respectively, through the use of 2nd order polynomial fitting equations. Following the proposed forces application method in the "simple load case" [4], the flapwise concentrated force per

section was divided by four so that it can be applied on the four nodes (KeyPoints 5, 7, 11, 13) between the two caps and the shear webs A & B. Accordingly, the edgewise concentrated force per section was divided by three, so that it can be applied on nodes (KeyPoints 8, 9, 10) defining the leading edge of each section. The in-house code used for the calculation of the concentrated loads also provided the post-fitting flapwise and edgewise moments values, which are shown in the Graphs 2 and 3, respectively, in comparison with the reference data.



Graph 2. Reference vs. fitted resultant flapwise moment values



Graph 3. Reference vs. fitted resultant edgewise moment values

1.4. For the buckling analysis

The buckling analysis of the rotor blade was based on the reference load case. Two simulation cases were carried out, depending of the way of applying the safety factor of **2.042** suggested by Ref. [4]:

Table A. Buckling simulation cases

	Material Properties $E_{xx}, E_{yy}, E_{zz}, G_{xy}, G_{xz}, G_{yz}$	Reference Load Case Flapwise & Edgewise Loads
CASE A	Multiplication factor: $(2.042)^{-1}$	Normal
CASE B	Normal	Multiplication factor: 2.042

In CASE A, material properties values provided by DTU [2] were decreased by a factor of $1/2.042=0.4897$, while the primary calculated reference load data were incorporated into the model.

On the other hand, in CASE B, the primary material properties were introduced into the model, while all concentrated loads were increased by a multiplication factor of **2.042**.

1.5. For the variable load carrying capacity analysis (fatigue analysis)

This section is going to be discussed in a future report

Failure criterion used

N/A

DATA OUTPUT

2.1 Global blade properties

The global blade properties were estimated by modelling the blade structure in the **EMRC/NISA II** FEM package. In detail:

Missing Blade's Tip

- Overall mass of blade: **42365.6 kg**
- Location of centre of gravity of blade: **x: -0.157 (m), y: 0.035 (m), z: 28.806 (m)**

Full Blade Model

- Overall mass of blade: **42362.7 kg**
- Location of centre of gravity of blade: **x: -0.157 (m), y: 0.035 (m), z: 28.802 (m)**

Natural frequencies analysis

The first seven natural frequencies of the blade with and without blade's tip are presented in Table 1.

Table 1. *Natural frequencies of the blade*

Mode (#)	Missing Blade's Tip		Full Blade Model	
	Frequency (Hz)	Damping ratio (%)	Frequency (Hz)	Damping ratio (%)
1	0.639	n/a	0.640	n/a
2	0.959	n/a	0.959	n/a
3	1.847	n/a	1.849	n/a
4	2.860	n/a	2.863	n/a
5	3.758	n/a	3.764	n/a
6	5.816	n/a	5.823	n/a
7	6.005	n/a	6.011	n/a

It is clearly seen that the results between the two modeling cases are identical. The difference of 2.9kg in the blade's total mass does not affect the position of centre of gravity, as well as the eigenfrequency values and the eigenmodes order of the rotor.

Modes 1, 3 and 5 correspond to the first three bending eigenfrequencies along the flapwise direction whereas modes 2, 4 and 6 refer to the first three bending eigenfrequencies along the edgewise direction of the structure. Accordingly, Figs. 1–6 illustrate the respective six mode shapes of the rotor. Red color corresponds to the deflected blade whereas cyan corresponds to the undeformed blade shape. Figures 1–6 outline the existence of coupling between the flapwise and the edgewise modes shapes of the blade, which is mainly attributed to the geometry of the structure's cross-sections. Finally, Fig. 7 presents the 1st torsional mode of the blade. The torsion of the cross-sections is better illustrated at the part of the blade near its tip.

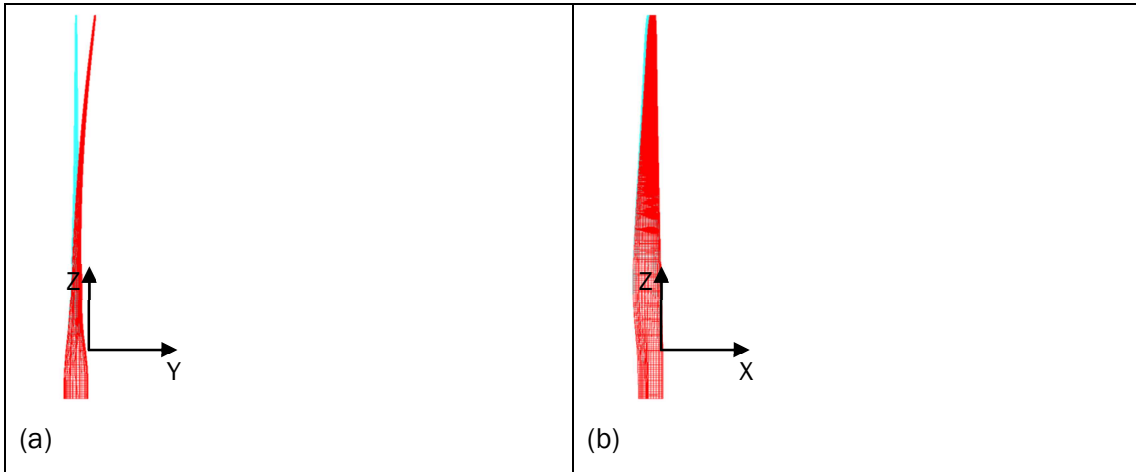


Figure 33. Mode shape for mode number 1: (a) Flapwise; (b) Edgewise

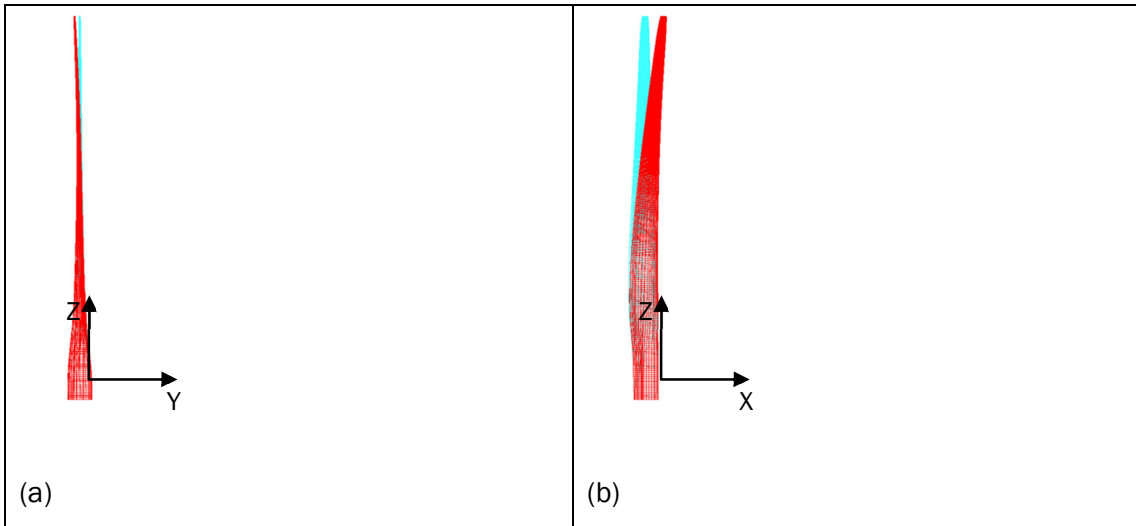


Figure 34. Mode shape for mode number 2: (a) Flapwise; (b) Edgewise

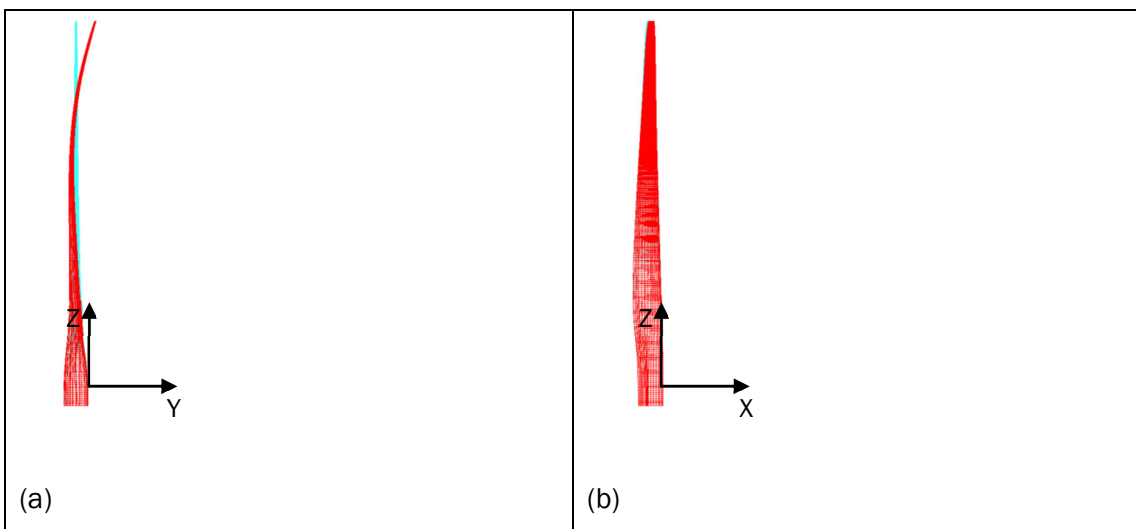


Figure 35. Mode shape for mode number 3: (a) Flapwise; (b) Edgewise

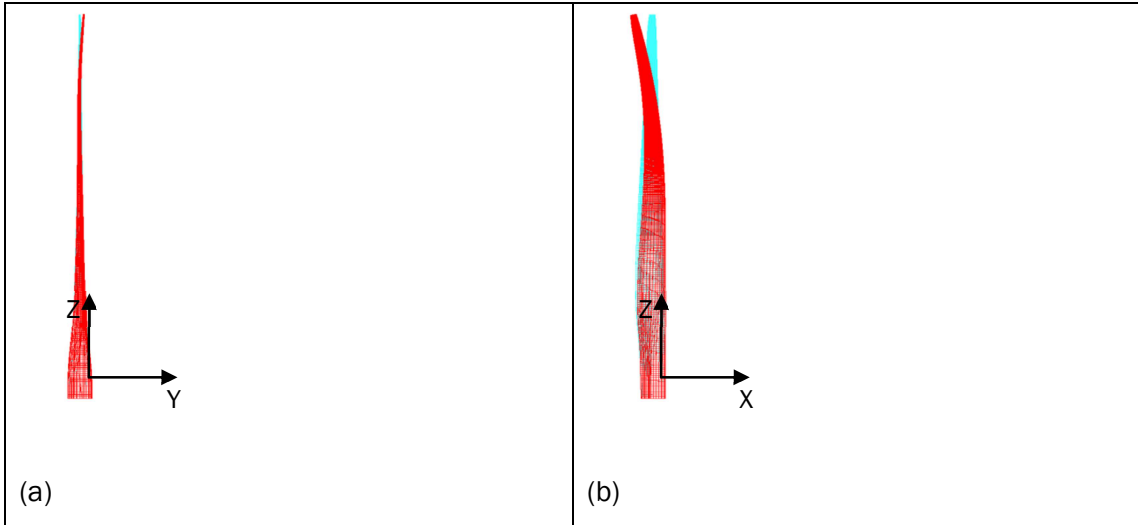


Figure 36. Mode shape for mode number 4: (a) Flapwise; (b) Edgewise

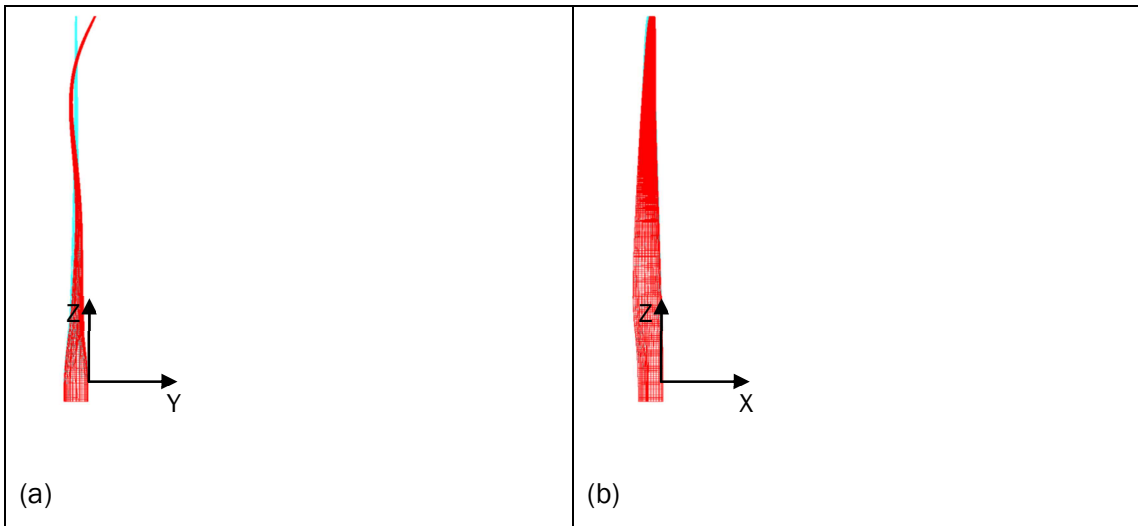


Figure 37. Mode shape for mode number 5: (a) Flapwise; (b) Edgewise

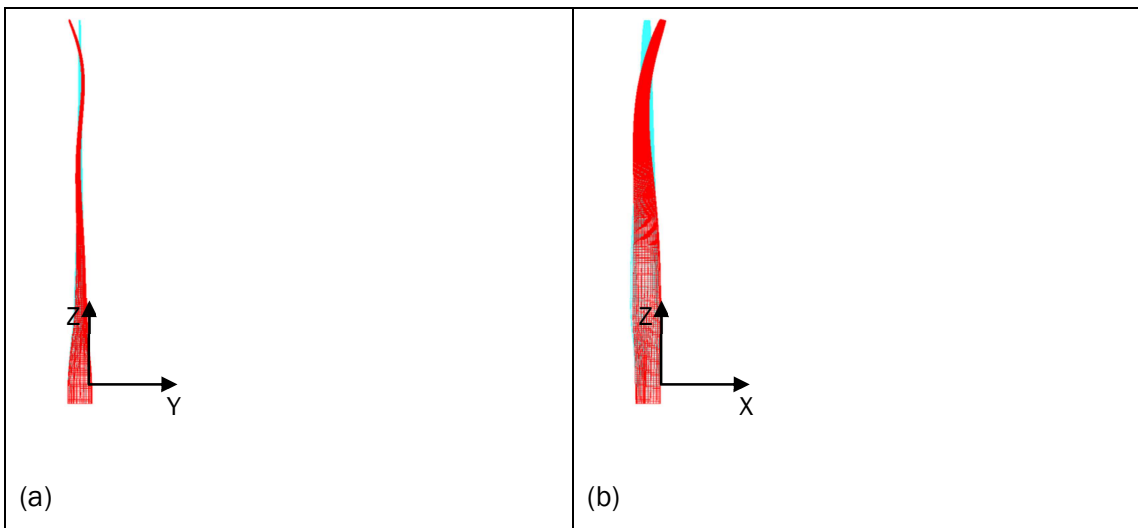


Figure 38. Mode shape for mode number 6: (a) Flapwise; (b) Edgewise

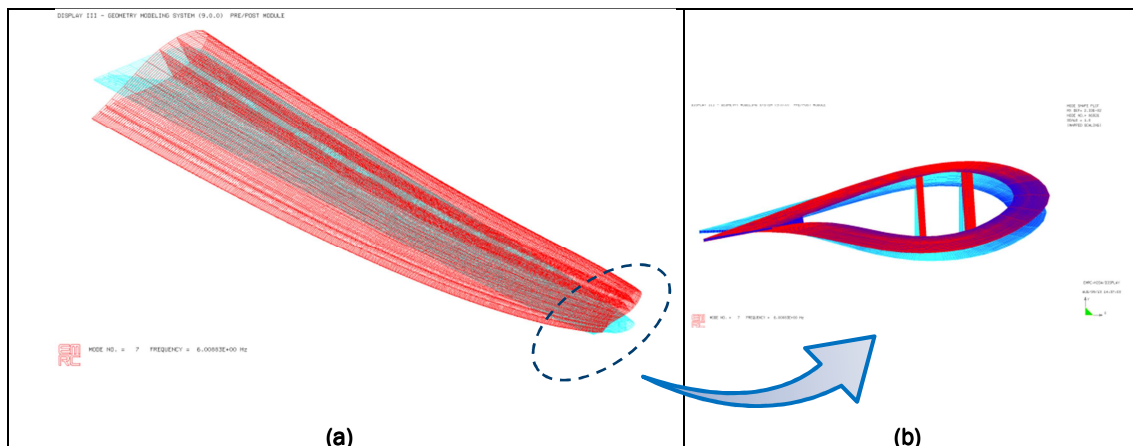


Figure 39. 1st Torsional mode shape of the rotor blade: (a) Tip area; (b) Torsion of tip cross-sections

Deflection analysis

Tip displacement and torsion of blade under **simple** load case

Due to the fact that in **NISA II** environment, the blade is modeled with and without the blade's tip, Tables 2 & 3 include the respective KeyPoint coordinates at R_{tip} , which are shown in grey color, and the respective values for the full blade model in blue color. In the latter case the coordinates of the key points coincide with the proposed values.

Table 2. *Tip displacement under simple case*

Key point No.	Coordinates			Displacement solution simple case		
	x [m]	y [m]	z [m]	x [m]	y [m]	z [m]
1	-0.389	-0.025	89.166	3.187	17.861	0.087
	-0.807	-0.052	88.302			
Full Blade	-0.389	-0.025	89.166	3.242	18.323	0.046
5	-0.004	-0.068	89.166	3.186	17.852	0.085
	-0.025	-0.140	88.302			
Full Blade	-0.004	-0.068	89.166	3.241	18.318	0.045
9	0.210	0.013	89.166	3.188	17.846	-0.033
	0.435	0.025	88.302			
Full Blade	0.210	0.013	89.166	3.242	18.316	-0.012
13	-0.004	0.074	89.166	3.189	17.852	-0.072
	-0.025	0.152	88.302			
Full Blade	-0.004	0.074	89.166	3.243	18.318	-0.032

Tip displacement and torsion of blade under **Reference** load case

Table 3. *Tip displacement under Reference case*

Key point No.	Coordinates			Displacement solution simple case		
	x [m]	y [m]	z [m]	x [m]	y [m]	z [m]
1	-0.389	-0.025	89.166	2.298	18.757	0.076
	-0.807	-0.052	88.302			
Full Blade	-0.389	-0.025	89.166	2.330	19.341	0.043
5	-0.004	-0.068	89.166	2.297	18.759	0.107
	-0.025	-0.140	88.302			
Full Blade	-0.004	-0.068	89.166	2.330	19.338	0.057
9	0.210	0.013	89.166	2.299	18.743	-0.022
	0.435	0.025	88.302			
Full Blade	0.210	0.013	89.166	2.330	19.335	-0.005
13	-0.004	0.074	89.166	2.299	18.759	-0.091
	-0.025	0.152	88.302			
Full Blade	-0.004	0.074	89.166	2.331	19.338	-0.039

Buckling analysis

Buckling load factor over **reference** load case: **0.66 (1st mode shape)**

Buckling analysis of the blade, which was carried out by implementing either CASE A or CASE B input data, provided almost the same load factor value and identical respective mode shapes. Figure 8 presents the 1st buckling mode, where the failure occurs at the area of $R \approx 85\text{m}$ from the blade's root. The buckling dominates the Trailing Panels (TP) on the suction side of the cross-section, which is attributed to the fact that, this area undergoes high concentrated loads, applied at the 4 nodes between the CAPS and the 2 shear webs of the section. This is better illustrated in Fig. 9, where the 3rd buckling mode shape is presented. It is obvious that the buckling occurs around the nodes where the flapwise force is applied, with greater impact on the two main shear webs at the blade's tip. For the sake of competence, the 7th and the 9th buckling mode shapes are also shown in Figs. 10a and b, respectively. The buckling described by the 7th mode occurs at $R \approx 79\text{m}$, whereas the 9th mode buckling at $R \approx 75\text{m}$ from the blade's root. Similarly to the 1st mode, the Trailing Panels (TP) on the suction side are mostly affected by the buckling loading.

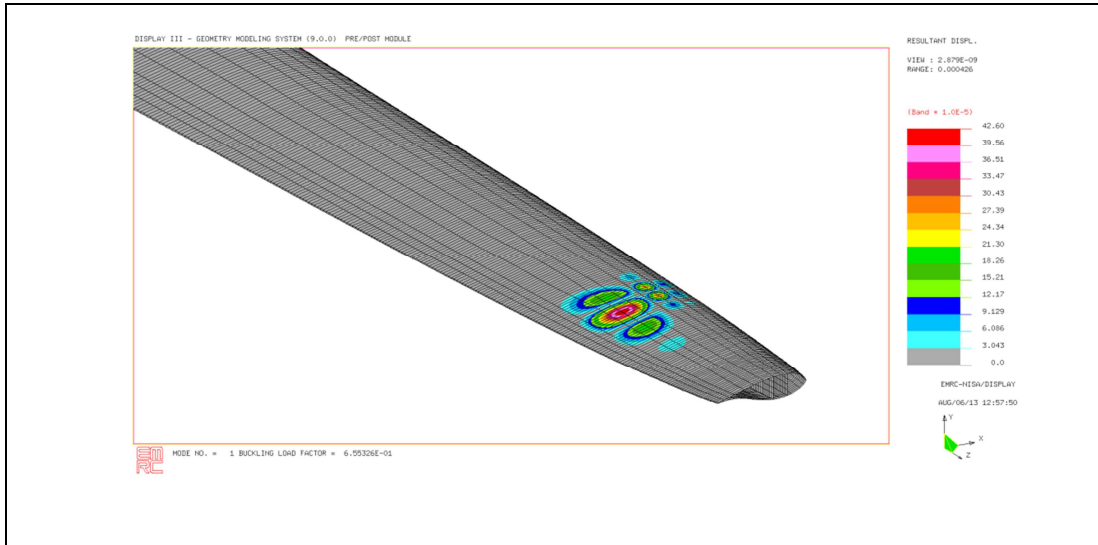


Figure 40. 1st Buckling mode shape

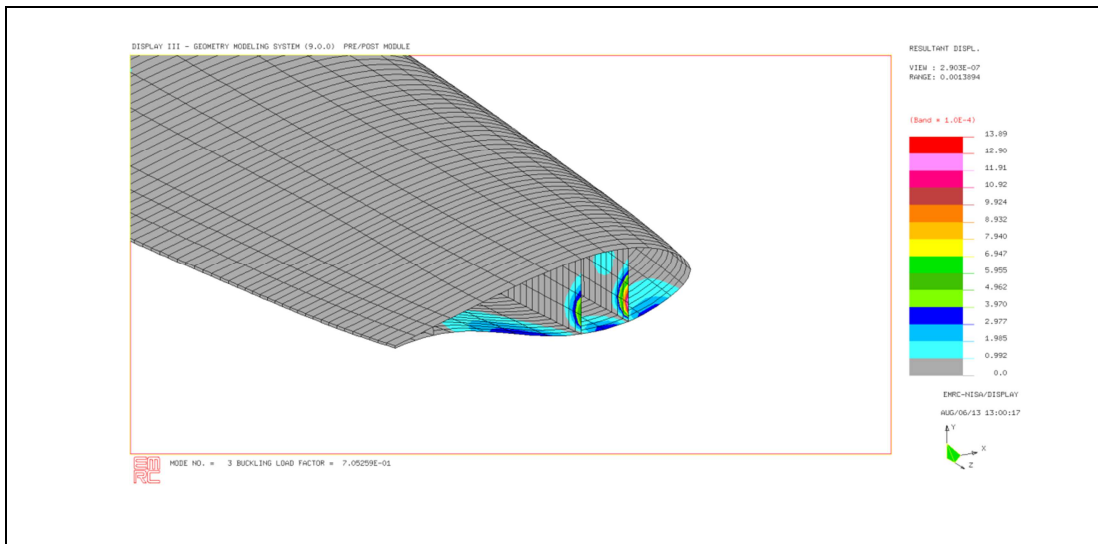


Figure 41. 3rd Buckling mode shape

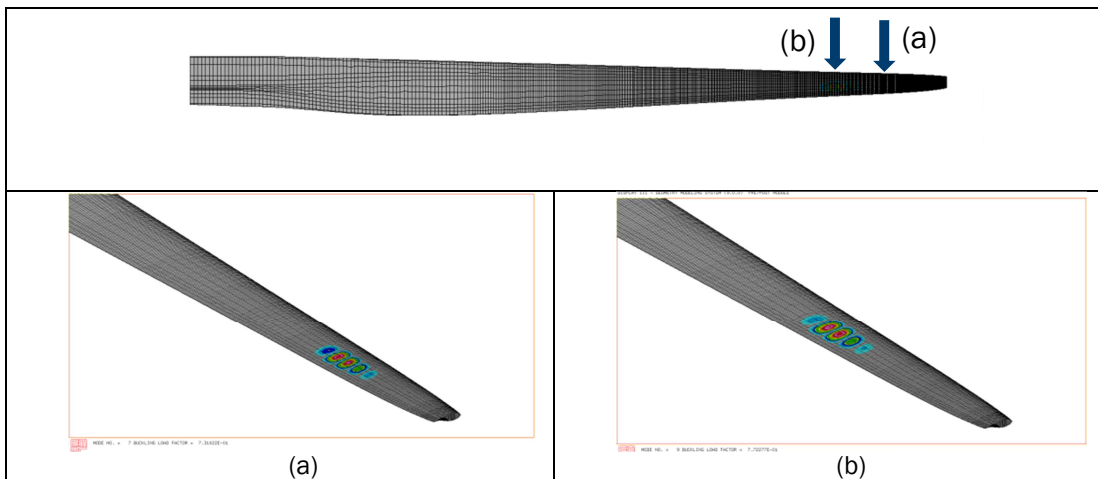


Figure 42. Higher buckling modes. (a) 7th mode shape; (b) 9th mode shape

Extreme load carrying capacity analysis

Extreme load carrying capacity multiplication factor (static strength under **reference** case): **0.520**

The application of the concentrated loads on the blade model nodes, according to the reference load case scenario, provided interesting results regarding the failure of the structure. The analysis consisted of two parts, the first of which was conducted by using the **NISA II** FEM package corresponding to the whole blade structure, whereas the second part was carried out by **"THIN"** code and included results regarding the five reference cross-sections of the current report.

1st PART

The primary analysis gave out a Tsai-Wu failure criterion value of **87.06**, which was located at the tip of blade, where the concentrated load along the flapwise direction takes its highest value (Fig. 11)

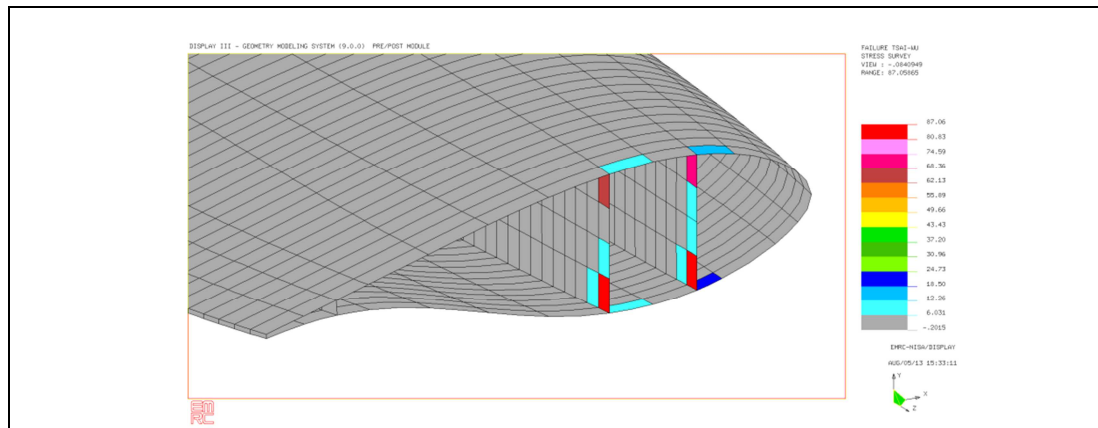


Figure 43. Highest Tsai-Wu criterion values at the blade's tip

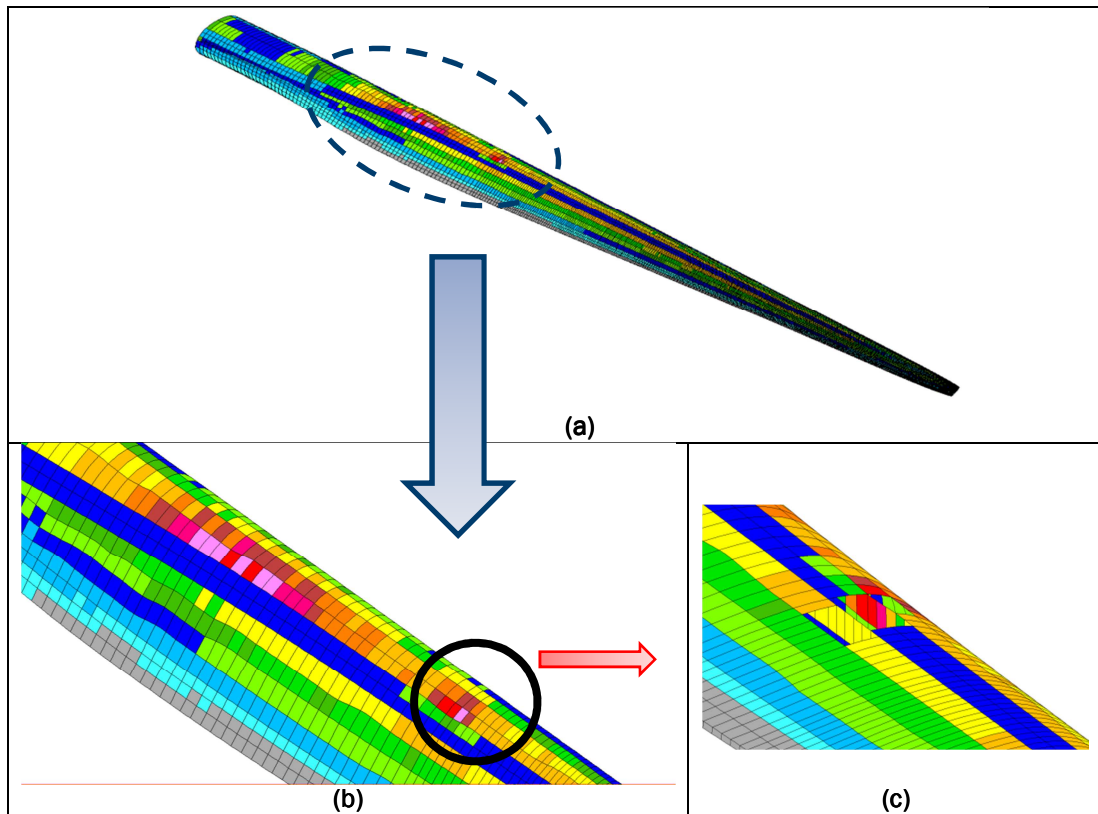


Figure 44. Tsai-Wu criterion values after the erasing of blade's tip elements

After erasing the elements corresponding to the last two discretised sections ($R=88.2158\text{m}$ to $R=88.3020\text{m}$) the Tsai-Wu failure criterion value of the whole structure decreased at 3.036 (Fig. 12). This value corresponds to the elements in the blade area shown in Fig. 12b and more specifically to the shear web A element attached to the suction side of the section (Fig. 12c). To better illustrate this type of failure, some elements of the LP suction side were removed in order to reveal the shear web A elements. Figure 13 better outlines the failure of shear web A at the same blade radius of $R=34.775\text{m}$ from the root. A possible reason for this type of failure could be the observed decrease of the distance between the two shear webs at this specific blade station.

A more careful look at Fig. 12b reveals that an extensive failure takes place in this specific area of the rotor blade. The elements that subject to failure are marked with red and magenta colors having a Tsai-Wu failure criterion value is up to 2.85. It should be outlined that the failure occurs at the suction side of the structure including elements mostly belonging to the Leading Panels (LP) sandwich segments of the respective sections.

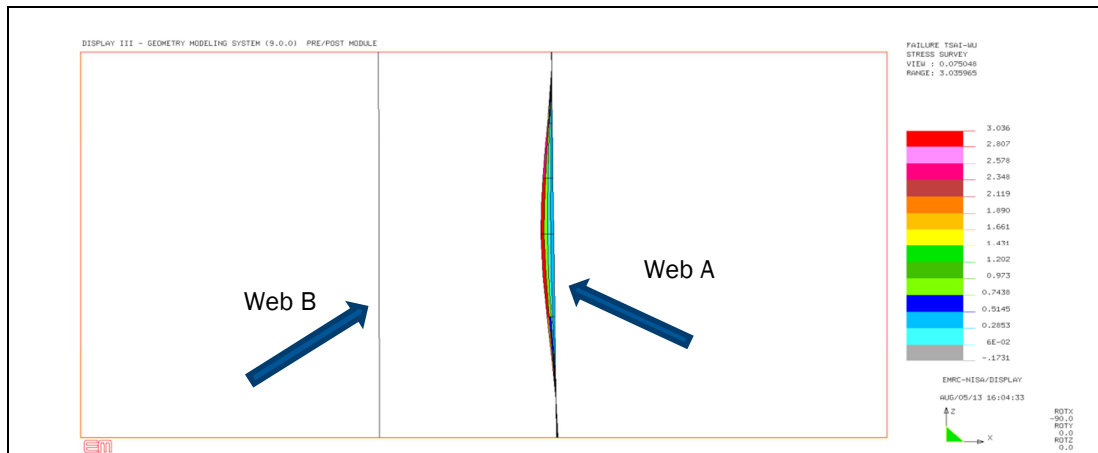


Figure 45. Failure of shear web A elements

The reduction the concentrated loads in the flapwise and edgewise directions by a factor of **0.52**, provided updated Tsai-Wu criterion values below the failure threshold. Nevertheless, the most sensitive area of the blade proved to be the same as in the reference load case (Fig. 12b) and for sake of completeness is also provided in Fig. 14.

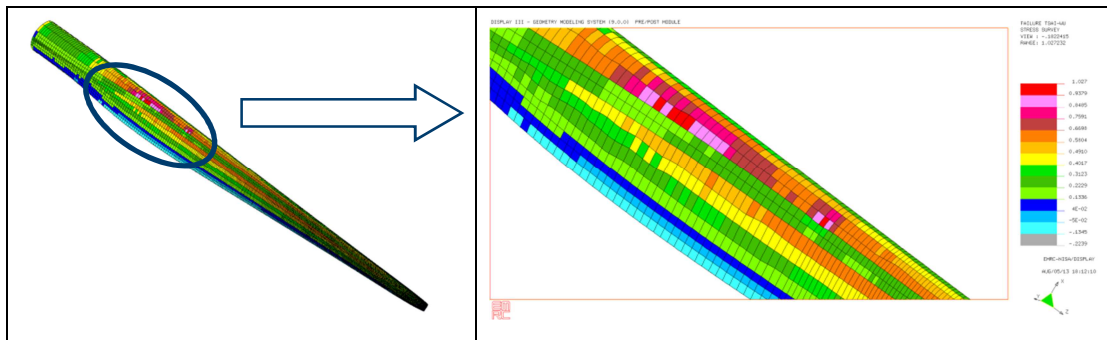
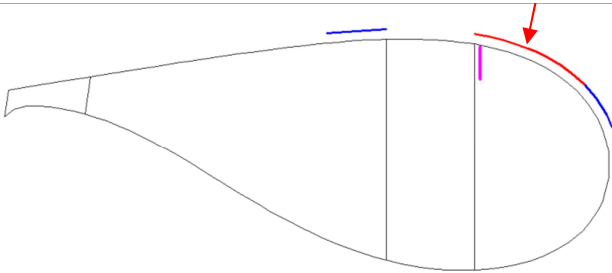
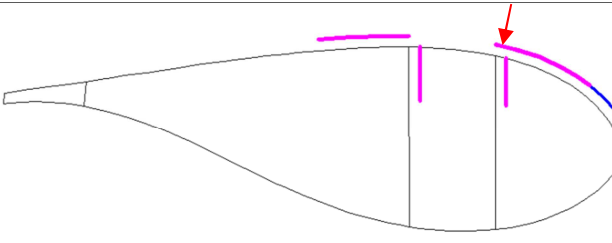
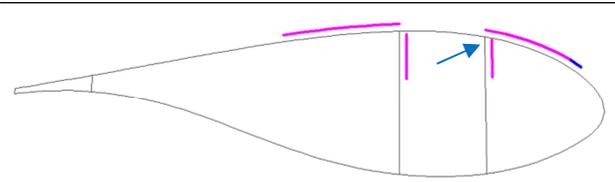
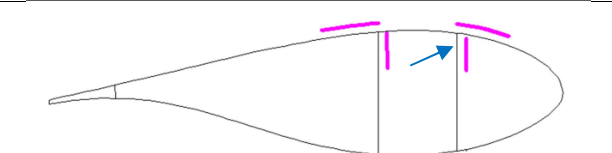


Figure 46. Updated Tsai-Wu criterion values below the failure threshold

2nd PART

The failure analysis included also results for the five reference cross-sections using the in-house code **"THIN"**. Table B presents the specific areas of each reference cross-section where failure was predicted. The code provides the safety factor value (R) per layer / per element of the cross-section and failure is supposed to take place for safety factor values below 1. Table B further includes the minimum element safety factor value, which usually corresponds to the Balsa ply either in the Leading Panel segment (indicated by a red arrow) or Shear Web A (blue arrow) on the suction side of the cross-section.

Table B. Failure of reference cross-section using “THIN” code

<p>REFERENCE SECTION 1</p>	<p style="text-align: center;"><u>NO FAILURE OCCURS</u></p> <p>The minimum safety factor is presented in LP segment of the suction side in the BALSA ply.</p>	<p>MINIMUM SAFETY FACTOR 1.154</p>
<p>REFERENCE SECTION 2</p>		<p>MINIMUM SAFETY FACTOR 0.653</p>
<p>REFERENCE SECTION 3</p>		<p>MINIMUM SAFETY FACTOR 0.670</p>
<p>REFERENCE SECTION 4</p>		<p>MINIMUM SAFETY FACTOR 0.677</p>
<p>REFERENCE SECTION 5</p>		<p>MINIMUM SAFETY FACTOR 0.858</p>

Each color corresponds to different ply failures, which in detail are:

- **Blue: 5 layer laminates, where Balsa ply failures**
- **Red: 5 layer laminates where UNIAX and Balsa plies failure, and**
- **Magenta: 3 layer laminates of which Balsa ply undergoes failure.**

2.2 Reference blade sections results

The mass and stiffness properties of the reference blade sections were calculated using “THIN” structural analysis tool. The geometrical, mass and stiffness data are expressed with respect to the Global Coordinate System (GCC) of the structure, using the Steiner Theorem, which is given in Eq. (2).

$$I'_x = I_x + a^2 A \Rightarrow EI'_x = EI_x + a^2 EA \quad (2)$$

Where $I'_{x'}$ is the second inertia moment w.r.t the Global Coordinate System, I_x is the second inertia moment w.r.t the section elastic centre, a is the distance between the x' and x axes, respectively and A is the cross-section area covered by material. Where available, the mass moments of inertia as well as the bending stiffness values with respect to the cross-section elastic centre are also provided.

Mass properties of reference blade sections

Table 4. Mass properties of reference blade sections

Property		Sec_1	Sec_2	Sec_3	Sec_4	Sec_5
Z-position	(m)	2.800	26.694	37.907	54.149	71.592
Mass/Length	(kg/m)	1.210E+03	6.408E+02	5.126E+02	3.426E+02	1.640E+02
Mass Centre	x (m)	-0.003	-0.2981	-0.2553	-0.1653	-0.1133
	y (m)	0.001	0.0803	0.0412	0.0319	0.0194
Mass moment of inertia (ρI) w.r.t. Global CS	ρI_{xx} (kg·m)	4.140E+03	5.531E+02	2.431E+02	6.860E+01	1.391E+01
	ρI_{yy} (kg·m)	3.803E+03	1.694E+03	1.025E+03	3.664E+02	7.584E+01
	ρI_{xy} (kg·m)	-7.615E-01	-2.318E+02	-1.133E+02	-2.013E+01	1.268E-01
Mass moment of inertia (ρI) w.r.t. the Elastic Centre	ρI_{xx} (kg·m)	4.140E+03	5.513E+02	2.429E+02	6.846E+01	1.386E+01
	ρI_{yy} (kg·m)	3.80E+03	1.68E+03	1.02E+03	3.664E+02	7.567E+01
	ρI_{xy} (kg·m)	7.615E-01	2.318E+02	1.133E+02	2.013E+01	-1.268E-01
Polar mass inertia (ρI_p) w.r.t. Global CS	ρI_p (kg·m)	7.943E+03	2.247E+03	1.268E+03	4.350E+02	8.975E+01
Polar mass inertia (ρI_p) w.r.t. Elastic Centre	ρI_p (kg·m)	7.943E+03	2.231E+03	1.265E+03	4.349E+02	8.953E+01

Stiffness properties of reference blade sections

Table 5. Stiffness properties of reference blade sections

Property		Sec_1	Sec_2	Sec_3	Sec_4	Sec_5
Z-position	(m)	2.800	26.694	37.907	54.149	71.592
Axial Stiffness	EA (N)	1.809E+10	9.336E+09	7.78E+09	5.463E+09	2.659E+09
Elastic Centre	x (m)	-0.0035	-0.1482	-0.0729	-0.0111	-0.0318
	y (m)	0.0010	0.0535	0.0175	0.0200	0.0181
Bending Stiffness w.r.t Global CS	EI_{xx} (Nm ²)	6.441E+10	9.590E+09	4.340E+09	1.279E+09	2.642E+08
	EI_{yy} (Nm ²)	6.285E+10	2.202E+10	1.311E+10	4.679E+09	9.922E+08
	EI_{xy} (Nm ²)	-1.223E+07	-3.021E+09	-1.428E+09	-2.425E+08	4.958E+06
Bending Stiffness w.r.t the Elastic Centre	EI_{xx} (Nm ²)	6.441E+10	9.563E+09	4.338E+09	1.277E+09	2.633E+08
	EI_{yy} (Nm ²)	6.285E+10	2.181E+10	1.307E+10	4.678E+09	9.895E+08
	EI_{xy} (Nm ²)	1.223E+07	3.021E+09	1.428E+09	2.425E+08	-4.958E+06
Shear Centre	x (m)	-0.0025	0.4537	0.4095	0.3058	0.1787
	y (m)	0.0009	0.0653	-0.0078	0.0184	0.0219
Torsional Stiffness	GJ (Nm ²)	2.851E+10	2.047E+09	8.252E+08	2.487E+08	6.105E+07
Shear Stiffness	S_x (N)	-	-	-	-	-
	S_y (N)	-	-	-	-	-

Extreme load carrying capacity analysis under simple load case

Displacements for reference blade sections under the **simple** load case application

The calculation of KeyPoints displacement values, both for the simple and the reference case, was carried out taking into account the results of the cross-section closer to the z-

axis coordinate value of the respective reference sections. For the sake of completeness, these KeyPoints coordinates are shown in the following tables in grey color.

Table 6. Displacement solution under simple load case for RefSection_2 (26.694m)

Key point No.	Key Point Coordinates			Displacement solution simple case		
	x [m]	y [m]	z [m]	x [m]	y [m]	z [m]
1	-3.875	0.334	26.694	0.188	0.418	0.059
	-3.877	0.333	26.766			
5	0.022	-1.126	26.694	0.167	0.387	0.054
	0.024	-1.124	26.766			
9	2.293	-0.293	26.694	0.176	0.398	-0.029
	2.291	-0.292	26.766			
13	0.022	1.127	26.694	0.197	0.387	-0.053
	0.024	1.125	26.766			

Table 7. Displacement solution under simple load case for RefSection_3 (37.907m)

Key point No.	Key Point Coordinates			Displacement solution simple case		
	x [m]	y [m]	z [m]	x [m]	y [m]	z [m]
1	-3.683	0.297	37.907	0.482	1.234	0.088
	-3.683	0.297	37.922			
5	0.042	-0.841	37.907	0.471	1.221	0.087
	0.042	-0.841	37.922			
9	1.984	-0.185	37.907	0.477	1.200	-0.045
	1.984	-0.185	37.922			
13	0.042	0.810	37.907	0.486	1.221	-0.085
	0.042	0.810	37.922			

Table 8. Displacement solution under simple load case for RefSection_4 (54.149m)

Key point No.	Key Point Coordinates			Displacement solution simple case		
	x [m]	y [m]	z [m]	x [m]	y [m]	z [m]
1	-2.843	0.087	54.149	1.161	3.878	0.124
	-2.844	0.087	54.126			
5	0.008	-0.518	54.149	1.154	3.868	0.122
	0.008	-0.518	54.126			
9	1.530	-0.056	54.149	1.159	3.847	-0.061
	1.531	-0.056	54.126			
13	0.008	0.550	54.149	1.165	3.868	-0.124
	0.008	0.550	54.126			

Table 9. *Displacement solution under simple load case for RefSection_5 (71.592m)*

Key point No.	Key Point Coordinates			Displacement solution simple case		
	x [m]	y [m]	z [m]	x [m]	y [m]	z [m]
1	-1.894	-0.047	71.592	2.144	9.514	0.142
	-1.912	-0.046	71.579			
5	-0.029	-0.330	71.592	2.140	9.503	0.147
	-0.028	-0.333	71.579			
9	1.020	0.020	71.592	2.144	9.488	-0.064
	1.030	0.019	71.579			
13	-0.029	0.359	71.592	2.148	9.503	-0.143
	-0.028	0.363	71.579			

The next step dealt with the calculation of layer strains and stresses at the provided KeyPoints of the reference sections under the simple load case. These data are in detail presented in the attached excel file.

In order to better understand the results, the following considerations should be taken into account:

- The stress-strains calculations were carried out by NISA II FEM package. Additional respective stress results were also calculated by “THIN” code.
- In NISA II, the strains were predicted with respect to the centroid at the midsurface of each layer/per element, in material principal directions.
- In NISA II, the stresses were calculated at the specific KeyPoint coordinates at the midsurface of each layer/per element, in material principal directions.
- In NISA II, at KeyPoint 9, the nodal stresses were calculated for both the elements at the pressure and the suction side at the NOSE segments.
- In NISA II, at KeyPoint 12, the nodal stresses were calculated for both the elements consisting of the CAP segment on the suction side of the cross-section.
- In “THIN”, the nodal stresses were calculated at each layer/per element, at the KeyPoints of the reference cross-sections.

It should be noted that the above considerations are also valid for the reference load case, which is thoroughly described in the following section of the present report.

Extreme load carrying capacity analysis under reference load case

Displacements for reference blade sections under the **reference** load case application

Table 10. *Displacement solution under reference load case for RefSection_2 (26.694m)*

Key point No.	Key Point Coordinates			Displacement solution simple case		
	x [m]	y [m]	z [m]	x [m]	y [m]	z [m]
1	-3.875	0.334	26.694	0.135	0.415	0.042
	-3.877	0.333	26.766			
5	0.022	-1.126	26.694	0.117	0.385	0.054
	0.024	-1.124	26.766			
9	2.293	-0.293	26.694	0.127	0.397	-0.018
	2.291	-0.292	26.766			
13	0.022	1.127	26.694	0.146	0.385	-0.053
	0.024	1.125	26.766			

Table 11. *Displacement solution under reference load case for RefSection_3 (37.907m)*

Key point No.	Key Point Coordinates			Displacement solution simple case		
	x [m]	y [m]	z [m]	x [m]	y [m]	z [m]
1	-3.683	0.297	37.907	0.362	1.227	0.063
	-3.683	0.297	37.922			
5	0.042	-0.841	37.907	0.352	1.216	0.087
	0.042	-0.841	37.922			
9	1.984	-0.185	37.907	0.358	1.196	-0.030
	1.984	-0.185	37.922			
13	0.042	0.810	37.907	0.367	1.216	-0.083
	0.042	0.810	37.922			

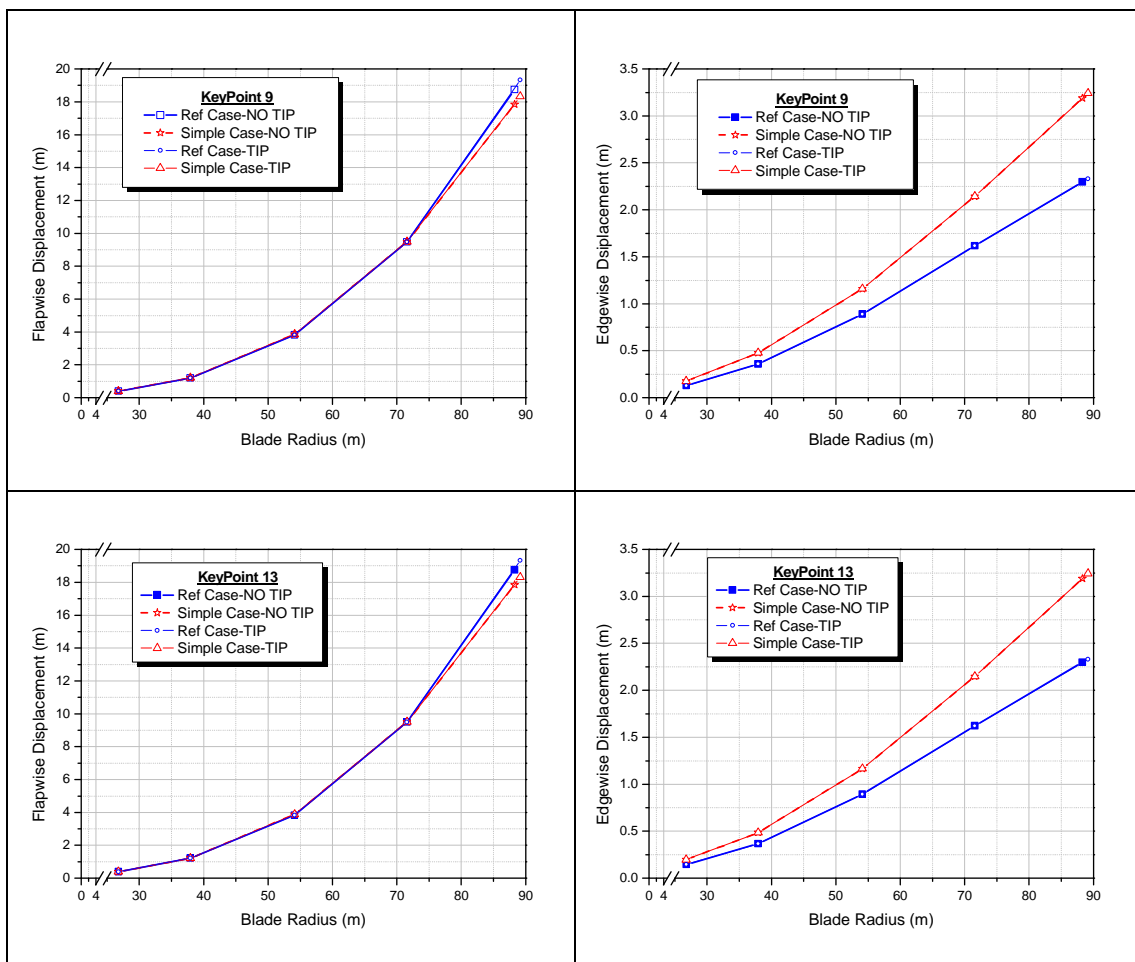
Table 12. *Displacement solution under reference load case for RefSection_4 (54.149m)*

Key point No.	Key Point Coordinates			Displacement solution simple case		
	x [m]	y [m]	z [m]	x [m]	y [m]	z [m]
1	-2.843	0.087	54.149	0.890	3.837	0.093
	-2.844	0.087	54.126			
5	0.008	-0.518	54.149	0.884	3.830	0.121
	0.008	-0.518	54.126			
9	1.530	-0.056	54.149	0.888	3.811	-0.043
	1.531	-0.056	54.126			
13	0.008	0.550	54.149	0.894	3.830	-0.122
	0.008	0.550	54.126			

Table 13. Displacement solution under reference load case for RefSection_5 (71.592m)

Key point No.	Key Point Coordinates			Displacement solution simple case		
	x [m]	y [m]	z [m]	x [m]	y [m]	z [m]
1	-1.894	-0.047	71.592	1.618	9.500	0.109
	-1.912	-0.046	71.579			
5	-0.029	-0.330	71.592	1.614	9.493	0.152
	-0.028	-0.333	71.579			
9	1.020	0.020	71.592	1.618	9.479	-0.045
	1.030	0.019	71.579			
13	-0.029	0.359	71.592	1.621	9.493	-0.147
	-0.028	0.363	71.579			

The following graphs present the displacements in edgewise and flapwise directions for KeyPoints 9 (Nose) and 13 (Upper CAP + Web B) at the reference sections 2, 3, 4, 5 as well as at the blade tip. The graphs include the values for the cases modelling with and without the blade tip.



Graph 4. Flapwise and edgewise displacement values at KeyPoints 9 and 13 at the four reference sections and at the tip of blade

References

- [1] Philippidis TP, Vasilopoulos AP, Katopis KG, Voutsinas SG, 1996, "THIN/PROBEAM: A software for fatigue design and analysis of composite rotor blades", *Wind Engineering*, Vol. 20 (50), pp. 349-362.
- [2] Lekou DJ, Philippidis TP, 2009, "PRE- and POST-THIN: A tool for the probabilistic design and analysis of composite rotor blade strength", *Wind Energy*, Vol. 12, pp. 676-691.
- [3] Bak C, Zahle F, Bitsche R, Kim T, Yde A, Henriksen LC, Andersen PB, Natarajan A, Hansen MH, 2013, "Design and performance of a 10 MW wind turbine", submitted to *J. Wind Energy*.
- [4] Lekou DJ, "Information on the Benchmark of blade structural models", *InnWind.EU Report*, July 2013.

TECHNICAL UNIVERSITY OF DENMARK (DTU).

Department of Wind Energy

Authors:

Christian Pavese
Peter Berring
Kim Branner

cpav@dtu.dk
pber@dtu.dk
kibr@dtu.dk

Contents

FINITE ELEMENT MODEL OF THE REFERENCE WIND TURBINE BLADE	81
Software	81
Modeling details and mesh.....	82
Model 1, high mesh density.....	82
Model 2, coarse mesh.....	82
DATA OUTPUT.....	84
Global blade properties.....	84
Natural frequencies analysis	84
Deflection analysis	85
Non – linear buckling analysis.....	86
REFERENCE BLADE SECTIONS RESULTS.....	89
EXTREME LOAD CARRYING CAPACITY ANALYSIS UNDER SIMPLE LOAD CASE.....	89
APPENDIX A – TSAI-WU FAILURE INDEX.....	95

FINITE ELEMENT MODEL OF THE REFERENCE WIND TURBINE BLADE

1.1 Software

The blade was modeled using the commercial finite element package MSC. Patran (version 2012.2). Based on input data available for the benchmark, the model was generated by utilizing Risø-DTU's in-house software Blade Modeling Tool (BMT). MSC.Marc was applied as the solver in all analysis.

As 20-noded layered continuum elements were used to model the blade structure, a volume representation of the geometry was required. This geometry was generated using BMT together with MSC Patran. All 101 cross-sections from the input data were applied in the modeling scheme, which describes the outer geometry of the blade. The curves defining these cross-sections were offset according to the layup definition in order to represent the thickness of the laminates. Finally, the individual cross-sections were connected by spline curves and interpolation surfaces to obtain a volume representation of the blade. This approach results in solids with varies in thickness between cross sections, which differs slightly from the input data, as these are constant between cross sections.

The process described in the previous paragraph was handled automatically by BMT, which utilizes 60 regions/solids to assign the different properties. Variations in thickness between regions results in tapered solids, which requires some assumptions of how to interpret the input data, as these do not include this level of information.

It is noted that for some cross sections there is an overlap of materials for the part of the blade called tail b. To avoid this overlapping the core thickness in the layup for tail b has been modified. The skins thicknesses are unchanged and therefore effect on the global response is assumed minor.

A custom-made script was used to model the small shear web (web C) in the trailing edge of the blade. This is modeled with 8-noded layered shell elements applying a thick shell formulation.

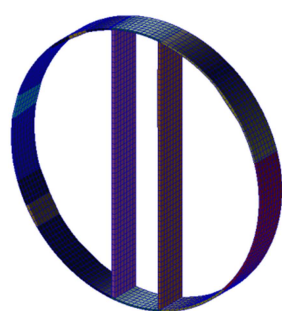


Figure 1, Root segment

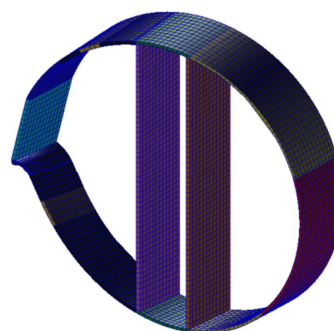


Figure 2, Inner segment

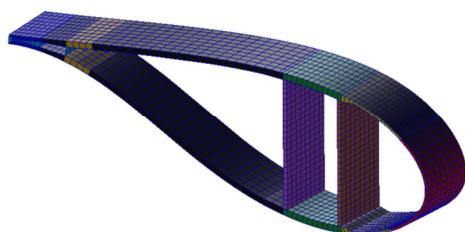


Figure 3, Middle segment

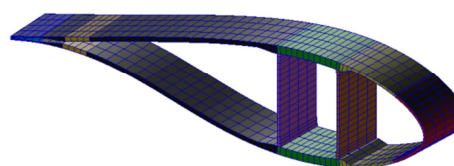


Figure 4, outer segment

1.2 Modeling details and mesh

The composite layup was modeled with 15-25 plies though the thickness via BMT and composite properties were assigned to layered 20-noded continuum elements.

The loads were applied via MPC-element (Multi Point Constrains) of the type RBE 3, which is a linear interpolation element which doesn't constrain the cross section. The master node was located in the center of load carrying box and connected to the nodes associated to the two caps.

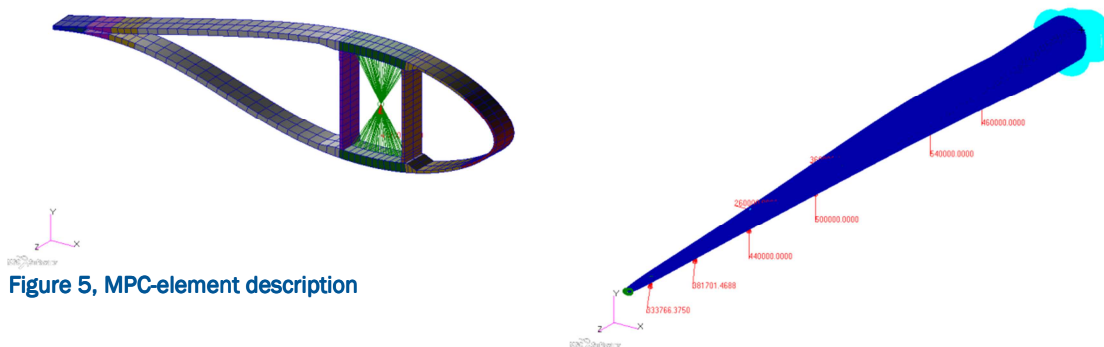


Figure 5, MPC-element description

For the studies performed in this benchmark two models were applied. The only difference between the models is the mesh density, as some types of analysis are not supported by parallelization and therefore a coarse mesh is required for these analyses.

1.2.1 Model 1, high mesh density

The model is densely meshed and it has approximately 200.000 layered 20-noded continuum elements.

Due to the size of the model and the geometric non-linear solving algorithm the analyses were done through a computer cluster. In this particular case, 36 CPUs were used.

The model is used for computing the following responses:

- Tip displacement and twist angle
- Load carrying capacity computed based on Tsai -Wu
- Strains and Stresses for the simple load case (via non-linear analysis)

The displacements reported in these studies were computed via non-linear geometric analysis. In the non-linear analysis the loads are applied with respect to the global coordinate system. This will result in a non-linear load history as the load points move closer to root as the blade deforms. Moreover the displacements at 5% load were determined and scaled linearly to the full load. The results from this latter analysis were reported and they should facilitate the comparison with the results from the other benchmarking partners performing linear analysis.

1.2.2 Model 2, coarse mesh

The model is meshed with approximately 85000 layered 20-noded continuum elements.

The model is used for computing the following responses:

- Natural Frequencies (Modal analysis)
- Non-linear Buckling analyses

The modal analyses were performed applying the Lanczos method in MSC.Marc.

Non-linear Buckling analyses, the geometric nonlinear effects, which a wind turbine blade is subjected to under extreme loading, are included in this analysis. The following eigenvalue problem was solved by applying the Lanczos method in MSC.Marc.

$$(\mathbf{K} + \lambda \cdot \Delta \mathbf{K}_G(\Delta u, u, \Delta \sigma)) \cdot \Phi = 0 \quad P_{\text{buckling}} = P_{\text{start}} + \lambda \cdot \Delta P$$

Equation 1, eigenvalue problem for buckling analysis

\mathbf{K} is the material stiffness matrix, λ is the eigenvalue and Φ is the eigenvector. The geometric stiffness matrix $\Delta \mathbf{K}_G$ is assumed to be a linear function of the load increment ΔP and is based on the stress and displacement state change at the start of the last increment. P_{start} is the load

applied at the start of the increment prior to the buckling analyses and λ is the value obtained by the power sweep method. For λ equal to unity the critical buckling load is obtained

DATA OUTPUT

Presented below are the results from the two numerical models applied in these studies. Only the simplified load case was used to compute the results.

1.3 Global blade properties

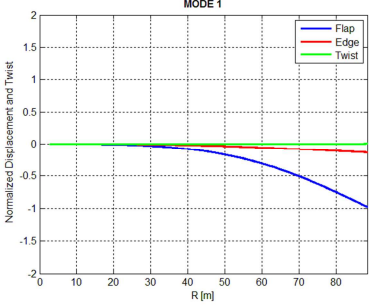
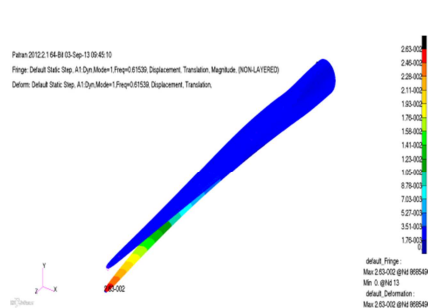
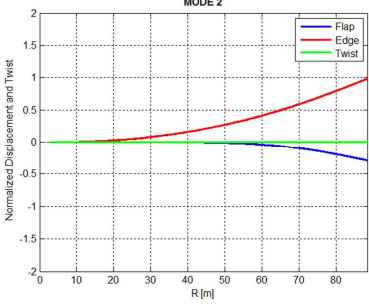
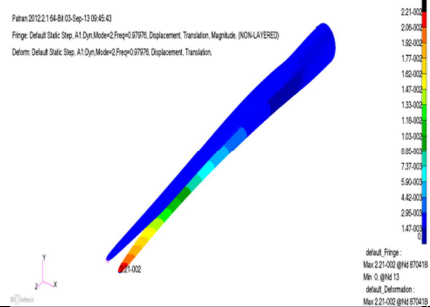
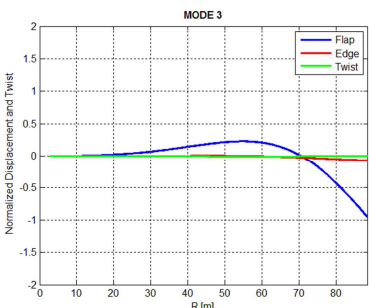
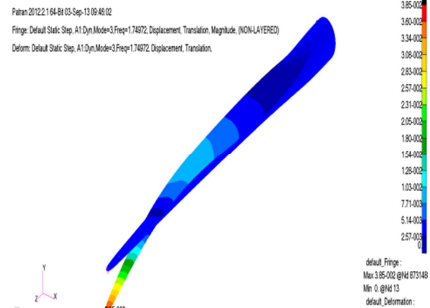
Overall mass of blade: 42894 kg.

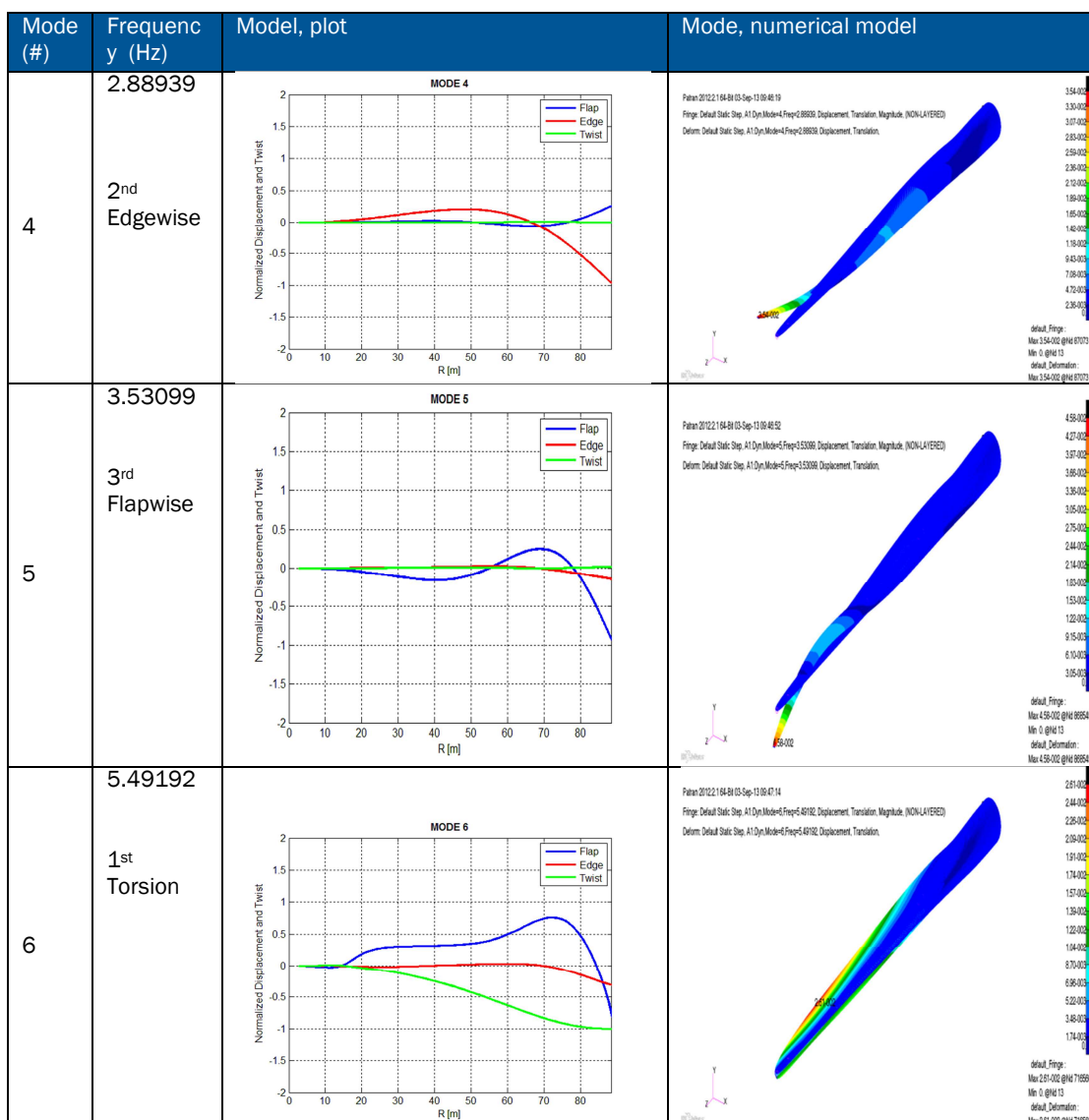
Location of centre of gravity of blade: x: -0.167 (m), y: 0.047 (m), z: 28.153 (m)

1.4 Natural frequencies analysis

Natural frequencies and modes shapes of the blade are determined as:

Table 1. *Natural frequencies of the blade*

Mode (#)	Frequenc y (Hz)	Model, plot	Mode, numerical model
1	0.61539 1 st Flapwise		
2	0.97976 1 st Edgewise		
3	1.74972 2 nd Flapwise		



1.5 Deflection analysis

Tip displacement and torsion of the blade subjected to the **simple load case** are presented below. The displacements in red are the results of the non-linear analysis. The displacements in black are the linearly scaled ones, as described earlier.

Table 2. *Tip displacement under simple case*

Key point No.	Coordinates			Displacement solution simple case					
	x [m]	y [m]	z [m]	x [m]	y [m]	z [m]	x [m]	y [m]	z [m]
1	-0.389	-0.025	89.166	3.417	3.341	20.906	18.885	-0.166	-3.829
5	-0.004	-0.068	89.166	3.417	3.340	20.903	18.873	-0.178	-3.837
9	0.210	0.013	89.166	3.417	3.340	20.900	18.851	-0.242	-3.891
13	-0.004	0.074	89.166	3.418	3.341	20.902	18.850	-0.267	-3.914

1.6

1.7 Non - linear buckling analysis

Buckling load factors for the blade subjected to the **simple load case** are presented below. The buckling factor does not include a partial safety factor.

The modeling scheme chosen in these studies offers an extra load carrying capacity towards buckling compared to a strategy implemented for a shell model utilizing the input data in this benchmark. As the thickness of the caps and sandwich panels differ it was chosen to model this as illustrated in figure 6. This stiffens the caps towards out-of-plan displacements, as the neighboring sandwich panels connections to the caps results in a very rotational stiff connection. It also observed in the presented buckling modes that the buckles in the cap are accompanied by corresponding buckles in the neighboring sandwich panels.

It is therefore assumed that the buckling factor for the model would be higher than the factor computed by the shell model.

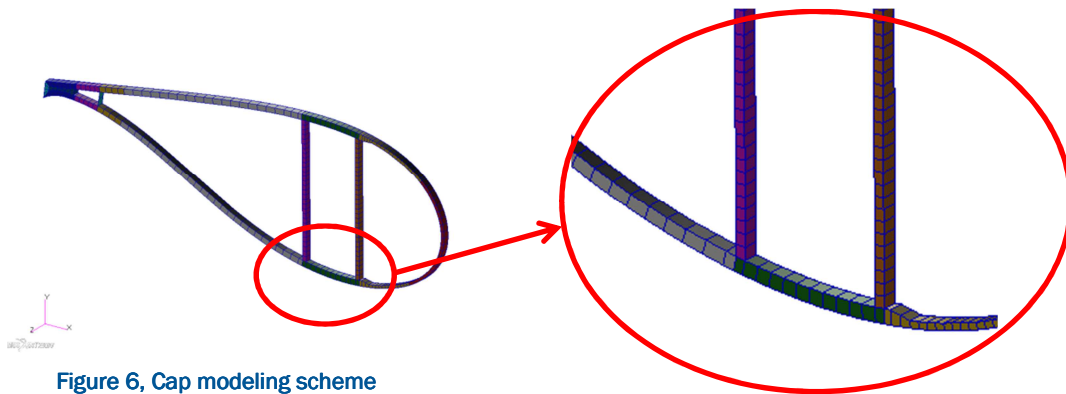
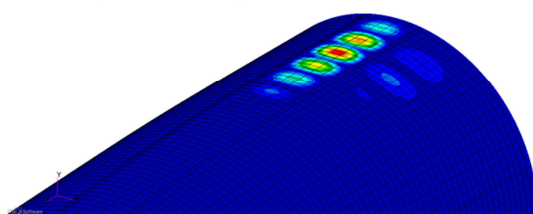
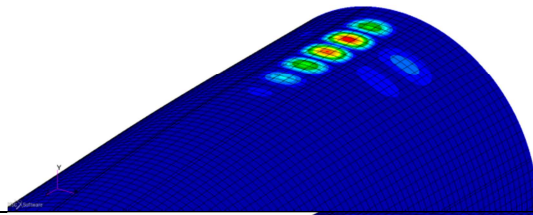
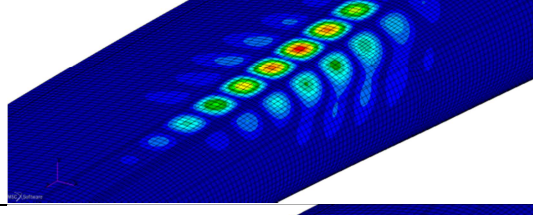
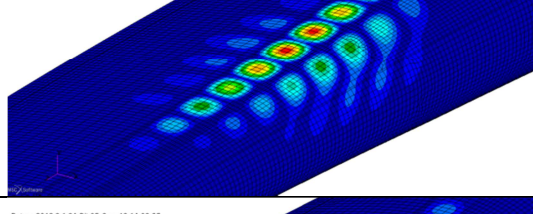
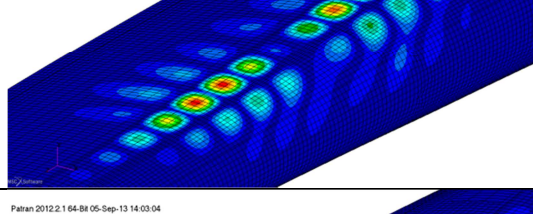
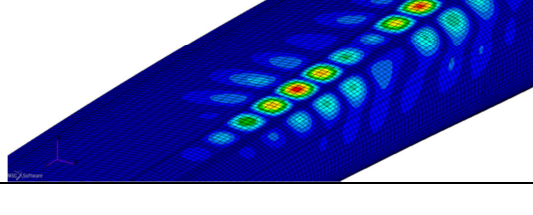
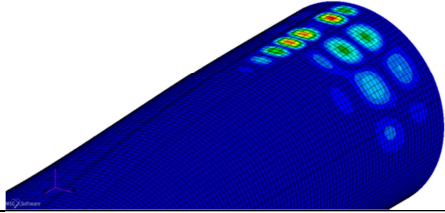
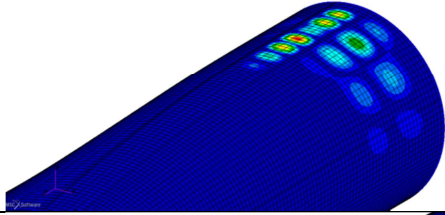
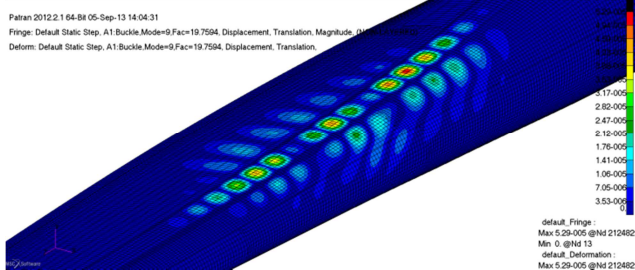
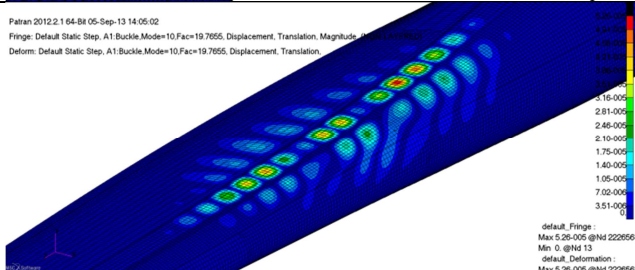


Figure 6, Cap modeling scheme

Table 3. *Buckling analysis under simple case*

Mode (#)	Buckling factor	Buckling mode	description/comments
1	2.698	<p>Patran 2012.2.1 04-08 05-Sep-13 13:59:29 Fringe: Default Static Step, A1:Buckle Mode=1:Fac=16.9775, Displacement, Translation, Magnitude, (NON-LAYERED) Deform: Default Static Step, A1:Buckle Mode=1:Fac=16.9775, Displacement, Translation.</p>  <p>Location : Root, Caps</p>	<p>1.56-000 1.45-004 1.35-004 1.25-004 1.14-004 1.04-004 9.34-003 8.31-003 7.27-003 6.23-003 5.19-003 4.15-003 3.11-003 2.08-003 1.04-003</p> <p>default, Fringe : Max: 1.55-004 @Nid 12269 Min: 0. @Nid 13 default, Deformation : Max: 1.55-004 @Nid 12269</p>
2	2.705	<p>Patran 2012.2.1 04-08 05-Sep-13 14:00:10 Fringe: Default Static Step, A1:Buckle Mode=2:Fac=17.0461, Displacement, Translation, Magnitude, (NON-LAYERED) Deform: Default Static Step, A1:Buckle Mode=2:Fac=17.0461, Displacement, Translation.</p>  <p>Location : Root, Caps</p>	<p>1.55-004 1.45-004 1.35-004 1.24-004 1.14-004 1.04-004 9.32-003 8.28-003 7.25-003 6.21-003 5.18-003 4.14-003 3.11-003 2.07-003 1.04-003</p> <p>default, Fringe : Max: 1.55-004 @Nid 12263 Min: 0. @Nid 13 default, Deformation : Max: 1.55-004 @Nid 12263</p>
3	2.798	<p>Patran 2012.2.1 04-08 05-Sep-13 14:01:42 Fringe: Default Static Step, A1:Buckle Mode=3:Fac=17.9822, Displacement, Translation, Magnitude, (NON-LAYERED) Deform: Default Static Step, A1:Buckle Mode=3:Fac=17.9822, Displacement, Translation.</p>  <p>Location : ~20-25 m, Caps/Leading Panel</p>	<p>5.03-000 4.91-000 4.79-000 4.67-000 4.55-000 4.43-000 4.31-000 4.19-000 4.07-000 3.95-000 3.83-000 3.71-000 3.59-000 3.47-000 3.35-000 3.23-000 3.11-000 2.99-000 2.87-000 2.75-000 2.63-000 2.51-000 2.39-000 2.27-000 2.15-000 2.03-000 1.91-000 1.79-000 1.67-000 1.55-000 1.43-000 1.31-000 1.19-000 1.07-000 0.95-000 0.83-000 0.71-000 0.59-000 0.47-000</p> <p>default, Fringe : Max: 6.41-005 @Nid 254497 Min: 0. @Nid 13 default, Deformation : Max: 6.41-005 @Nid 254497</p>
4	2.798	<p>Patran 2012.2.1 04-08 05-Sep-13 14:02:10 Fringe: Default Static Step, A1:Buckle Mode=4:Fac=17.9835, Displacement, Translation, Magnitude, (NON-LAYERED) Deform: Default Static Step, A1:Buckle Mode=4:Fac=17.9835, Displacement, Translation.</p>  <p>Location : ~20-25 m, Caps/Leading - Trailing Panel</p>	<p>5.03-000 4.91-000 4.79-000 4.67-000 4.55-000 4.43-000 4.31-000 4.19-000 4.07-000 3.95-000 3.83-000 3.71-000 3.59-000 3.47-000 3.35-000 3.23-000 3.11-000 2.99-000 2.87-000 2.75-000 2.63-000 2.51-000 2.39-000 2.27-000 2.15-000 2.03-000 1.91-000 1.79-000 1.67-000 1.55-000 1.43-000 1.31-000 1.19-000 1.07-000 0.95-000 0.83-000 0.71-000 0.59-000 0.47-000</p> <p>default, Fringe : Max: 6.25-005 @Nid 254501 Min: 0. @Nid 13 default, Deformation : Max: 6.25-005 @Nid 254501</p>
5	2.881	<p>Patran 2012.2.1 04-08 05-Sep-13 14:02:35 Fringe: Default Static Step, A1:Buckle Mode=5:Fac=18.8117, Displacement, Translation, Magnitude, (NON-LAYERED) Deform: Default Static Step, A1:Buckle Mode=5:Fac=18.8117, Displacement, Translation.</p>  <p>Location : ~20-25 m, Caps/Leading - Trailing Panel</p>	<p>5.03-000 4.91-000 4.79-000 4.67-000 4.55-000 4.43-000 4.31-000 4.19-000 4.07-000 3.95-000 3.83-000 3.71-000 3.59-000 3.47-000 3.35-000 3.23-000 3.11-000 2.99-000 2.87-000 2.75-000 2.63-000 2.51-000 2.39-000 2.27-000 2.14-000 1.78-000 1.43-000 1.07-000 7.14-000 3.57-000</p> <p>default, Fringe : Max: 5.35-005 @Nid 302324 Min: 0. @Nid 13 default, Deformation : Max: 5.35-005 @Nid 302324</p>
6	2.881	<p>Patran 2012.2.1 04-08 05-Sep-13 14:03:04 Fringe: Default Static Step, A1:Buckle Mode=6:Fac=18.8160, Displacement, Translation, Magnitude, (NON-LAYERED) Deform: Default Static Step, A1:Buckle Mode=6:Fac=18.8160, Displacement, Translation.</p>  <p>Location : ~20-25 m, Caps/Leading - Trailing Panel</p>	<p>5.03-000 4.91-000 4.79-000 4.67-000 4.55-000 4.43-000 4.31-000 4.19-000 4.07-000 3.95-000 3.83-000 3.71-000 3.59-000 3.47-000 3.35-000 3.23-000 3.11-000 2.99-000 2.87-000 2.75-000 2.63-000 2.51-000 2.39-000 2.27-000 1.88-000 1.50-000 1.13-000 7.51-000 3.78-000</p> <p>default, Fringe : Max: 5.04-005 @Nid 292971 Min: 0. @Nid 13 default, Deformation : Max: 5.04-005 @Nid 292971</p>

Mode (#)	Buckling factor	Buckling mode	description/comments
7	2.907	<p>Patran 2012.2.1 64-Bit 05-Sep-13 14:03:32 Fringe: Default Static Step, A1:Buckle Mode=7.Fac=19.0736, Displacement, Translation, Magnitude, (NON-LAYERED) Deform: Default Static Step, A1:Buckle Mode=7.Fac=19.0736, Displacement, Translation.</p>  <p>1.30-004 1.21-004 1.13-004 1.04-004 9.53-005 8.96-005 7.73-005 6.93-005 6.06-005 5.20-005 4.33-005 3.46-005 2.60-005 1.73-004 8.66-006</p> <p>default, Fringe : Max 1.30-004 @Nd 12265 Min 0. @Nd 13 default, Deformation : Max 1.30-004 @Nd 12265</p>	Location : Root, Caps/Leading Panel
8	2.919	<p>Patran 2012.2.1 64-Bit 05-Sep-13 14:04:12 Fringe: Default Static Step, A1:Buckle Mode=8.Fac=19.1864, Displacement, Translation, Magnitude, (NON-LAYERED) Deform: Default Static Step, A1:Buckle Mode=8.Fac=19.1864, Displacement, Translation.</p>  <p>1.34-004 1.25-004 1.16-004 1.07-004 9.80-005 8.91-005 8.02-005 7.13-005 6.24-005 5.35-005 4.46-005 3.57-005 2.67-005 1.78-005 8.91-006</p> <p>default, Fringe : Max 1.34-004 @Nd 22996 Min 0. @Nd 13 default, Deformation : Max 1.34-004 @Nd 22996</p>	Location : Root, Caps/Leading Panel
9	2.976	<p>Patran 2012.2.1 64-Bit 05-Sep-13 14:04:31 Fringe: Default Static Step, A1:Buckle Mode=9.Fac=19.7594, Displacement, Translation, Magnitude, (NON-LAYERED) Deform: Default Static Step, A1:Buckle Mode=9.Fac=19.7594, Displacement, Translation.</p>  <p>1.34-004 1.25-004 1.16-004 1.07-004 9.80-005 8.91-005 8.02-005 7.13-005 6.24-005 5.35-005 4.46-005 3.57-005 2.67-005 1.78-005 8.91-006</p> <p>default, Fringe : Max 5.29-005 @Nd 212482 Min 0. @Nd 13 default, Deformation : Max 5.29-005 @Nd 212482</p>	Location : ~19-26 m, Caps/Leading - Trailing Panel
10	2.977	<p>Patran 2012.2.1 64-Bit 05-Sep-13 14:05:02 Fringe: Default Static Step, A1:Buckle Mode=10.Fac=19.7655, Displacement, Translation, Magnitude, (NON-LAYERED) Deform: Default Static Step, A1:Buckle Mode=10.Fac=19.7655, Displacement, Translation.</p>  <p>1.34-004 1.25-004 1.16-004 1.07-004 9.80-005 8.91-005 8.02-005 7.13-005 6.24-005 5.35-005 4.46-005 3.57-005 2.67-005 1.78-005 8.91-006</p> <p>default, Fringe : Max 5.29-005 @Nd 222856 Min 0. @Nd 13 default, Deformation : Max 5.29-005 @Nd 222856</p>	Location : ~19-26 m, Caps/Leading - Trailing Panel

REFERENCE BLADE SECTIONS RESULTS

The Mass properties of reference blade sections are reported below. Mass moments of inertia are evaluated at the center of gravity. Chosen blade slices are picked as close as possible to the reference blade sections.

Table 1. *Mass properties of reference blade sections*

Property		Sec_1	Sec_2	Sec_3	Sec_4	Sec_5
Z-location	(m)	2.800	26.694	37.907	54.149	71.952
Mass/Length	(kg/m)	1.2324E+02	6.397E+02	5.058E+02	3.284E+02	1.546E+02
Mass Centre	x (m)	0.007	-0.311	-0.254	-0.142	-0.108
	y (m)	0.027	0.087	0.043	0.035	0.019
Mass moment of inertia (ρI)	ρI_{xx} (kg·m)	4.177E+03	0.516E+03	2.197E+02	5.877E+01	1.164E+01
	ρI_{yy} (kg·m)	3.815E+03	1.644E+03	9.678E+02	3.228E+02	6.775E+01
	ρI_{xy} (kg·m)	-0.772	2.329E+02	1.088E+02	1.732E+01	-1.372E-01
Polar mass inertia (ρI_p)	ρI_p (kg·m)	7.992E+03	2.160E+03	1.188E+03	3.816E+02	7.939E+01

EXTREME LOAD CARRYING CAPACITY ANALYSIS UNDER SIMPLE LOAD CASE

Some part of the cross section is not considered when the extreme load carrying capacity is determined, as these parts are subjected to singularities. The simplified cross section is presented below.

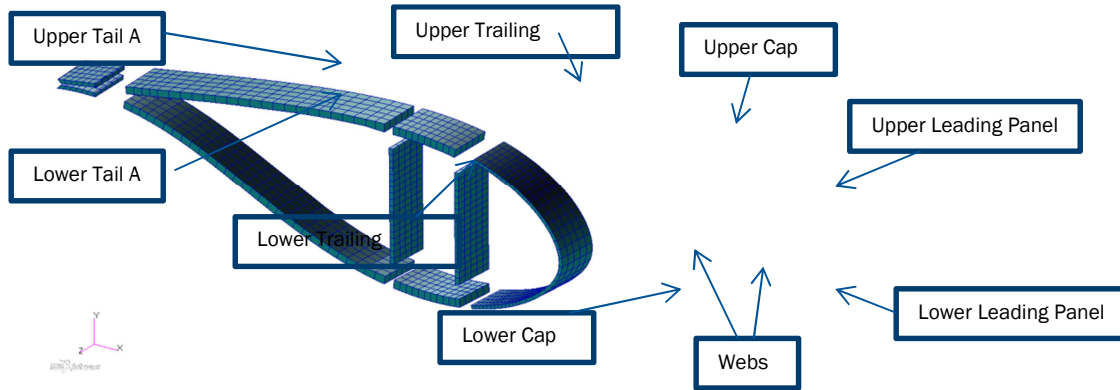
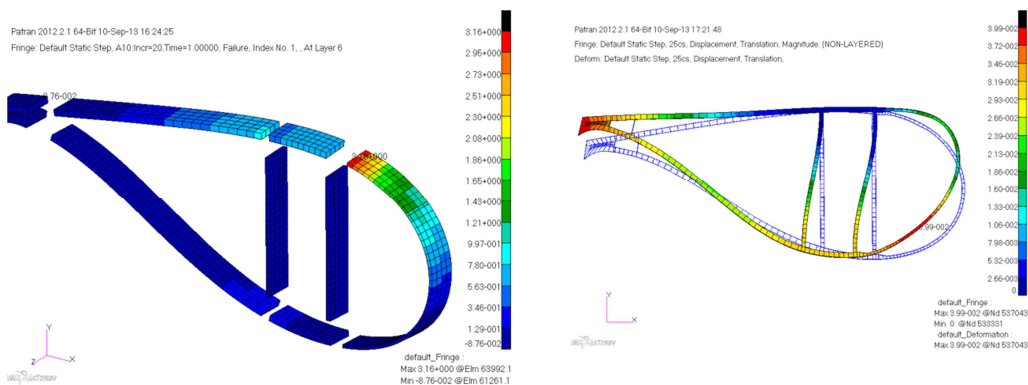


Figure 7, Simplified cross section to avoid parts subjected to singularities

The extreme load carrying capacity is computed as approximately 50% of the applied load via the material failure criterion Tsai-Wu. Failure occurs at radial position 25.4 meter at the upper part of the leading edge. The failure is mainly a result of in-plan shear stress in the upper part of the leading edge and the ply with the highest failure index is the uniaxial material on the inner side. At 100% load the failure index is equal to 3.15.

If a maximum stress failure criterion is applied, the extreme load carrying capacity is computed as approximately 82% of the applied load.

The inner TRIAX material at the upper part of the leading panel has a failure index equal to 1.85, which is also mainly due to in-plan shear stress. The shear stress in this part of the blade is assumed to be result of highly distorted profile, which is illustrated below via a rigid body transformation with a scale factor of 10.



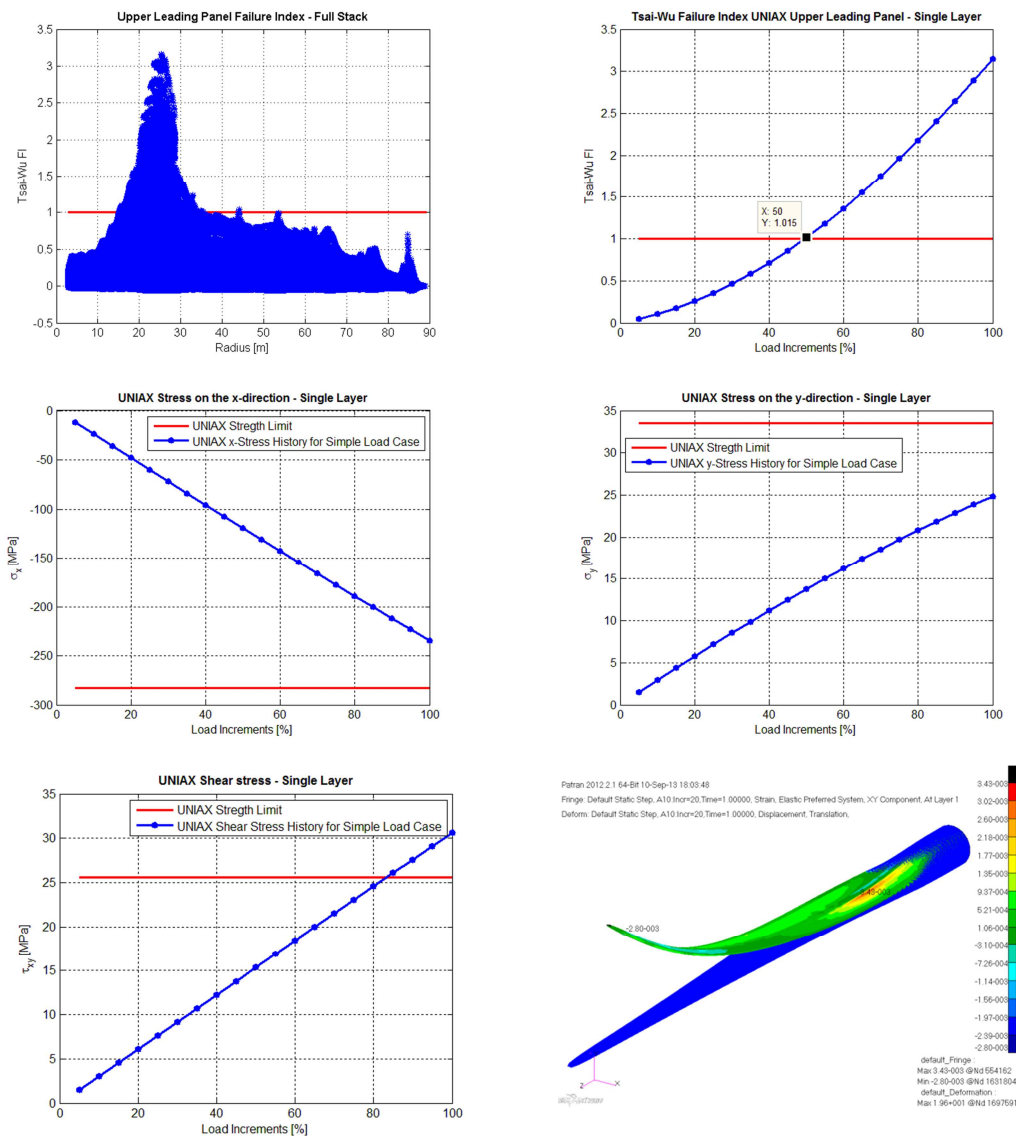


Figure 7, Summary of the failure occurred at 50% of the simple load case. Failure is located at radial position 25.4 m, leading panel. Failure of the layer (UNIAX material on the inner side) with highest index is reported

A failure index, slightly higher than 1 (1.06), is also determined for the upper trailing sandwich panel at radial position 28.3 meter. Failure is computed as 95% of the applied loads via the Tsai-Wu material failure criterion.

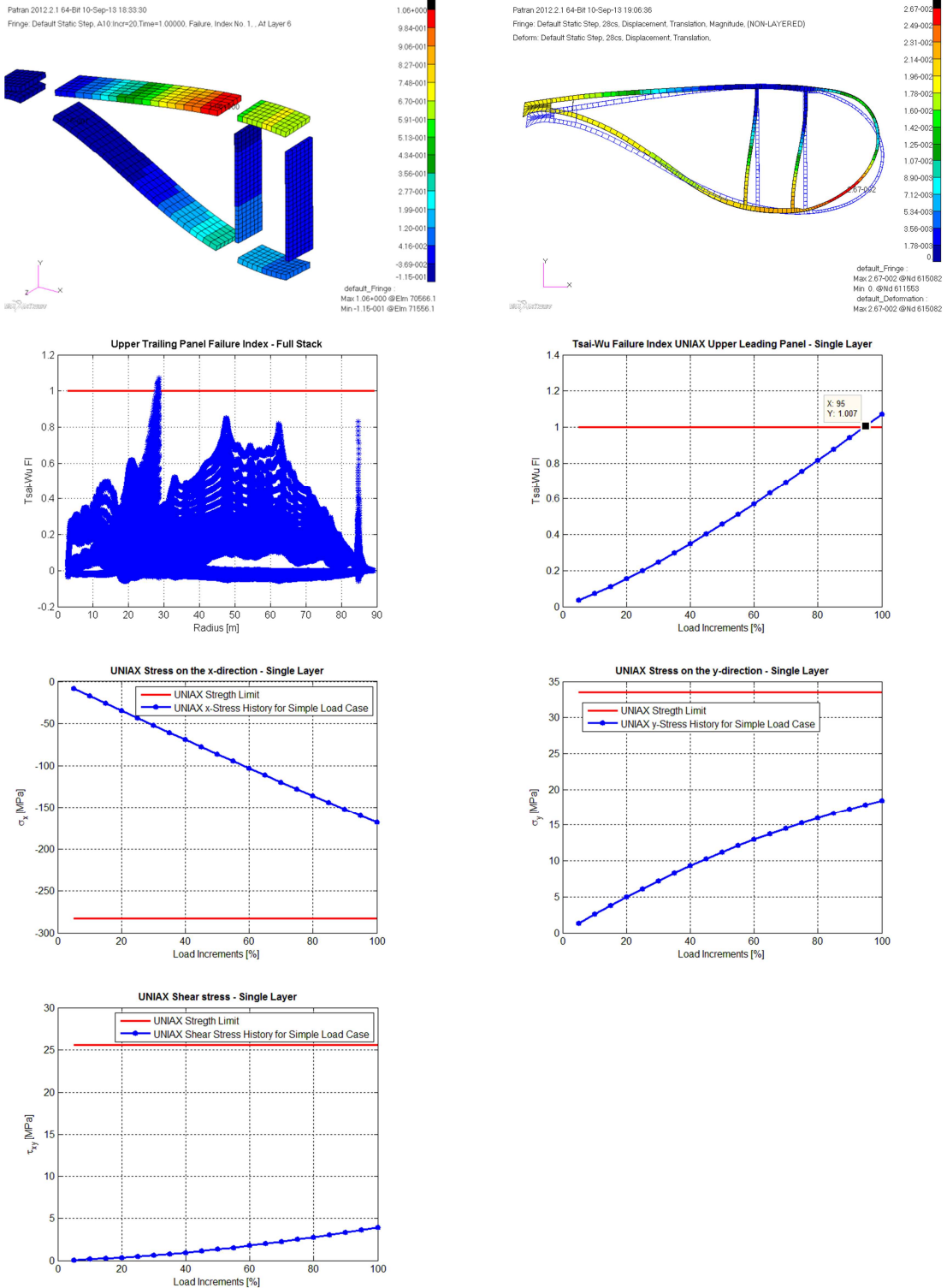


Figure 8, Summary of the failure occurred at 95% of the simple load case. Failure is located at radial position 28.3 m, trailing panel. Failure of the layer (UNIAX material on the inner side) with highest index is reported

A summary of the failure indices for the full stack of plies along the entire blade is reported in APPENDIX A.

1.8 Displacements for reference blade sections under the simple load case application

Presented below are the linear and non-linear displacements computed under the simple load case. Results from non-linear analysis are reported in red. The displacements in black are the linearly scaled ones, as described earlier.

Table 2. *Displacement solution under simple load case for RefSection_2 (26.694m)*

Key point No.	Key Point Coordinates			Displacement solution simple case					
	x [m]	y [m]	z [m]	x [m]	y [m]	z [m]	x [m]	y [m]	z [m]
1	-3.875	0.334	26.694	0.185	0.181	0.426	0.414	0.061	0.051
5	0.022	-1.126	26.694	0.161	0.160	0.383	0.378	0.057	0.050
9	2.293	-0.293	26.694	0.171	0.167	0.396	0.379	-0.028	-0.033
13	0.022	1.127	26.694	0.196	0.189	0.384	0.375	-0.056	-0.059

Table 3. *Displacement solution under simple load case for RefSection_3 (37.907m)*

Key point No.	Key Point Coordinates			Displacement solution simple case					
	x [m]	y [m]	z [m]	x [m]	y [m]	z [m]	x [m]	y [m]	z [m]
1	-3.683	0.297	37.907	0.490	0.478	1.307	1.282	0.088	0.041
5	0.042	-0.841	37.907	0.476	0.461	1.286	1.250	0.093	0.047
9	1.984	-0.185	37.907	0.484	0.468	1.257	1.204	-0.046	-0.084
13	0.042	0.810	37.907	0.496	0.482	1.285	1.240	-0.093	-0.132

Table 4. *Displacement solution under simple load case for RefSection_4 (54.149m)*

Key point No.	Key Point Coordinates			Displacement solution simple case					
	x [m]	y [m]	z [m]	x [m]	y [m]	z [m]	x [m]	y [m]	z [m]
1	-2.843	0.087	54.149	1.203	1.176	4.255	4.116	0.114	-0.200
5	0.008	-0.518	54.149	1.194	1.161	4.241	4.069	0.121	-0.188
9	1.530	-0.056	54.149	1.200	1.167	4.212	3.999	-0.080	-0.369
13	0.008	0.550	54.149	1.208	1.180	4.239	4.036	-0.156	-0.449

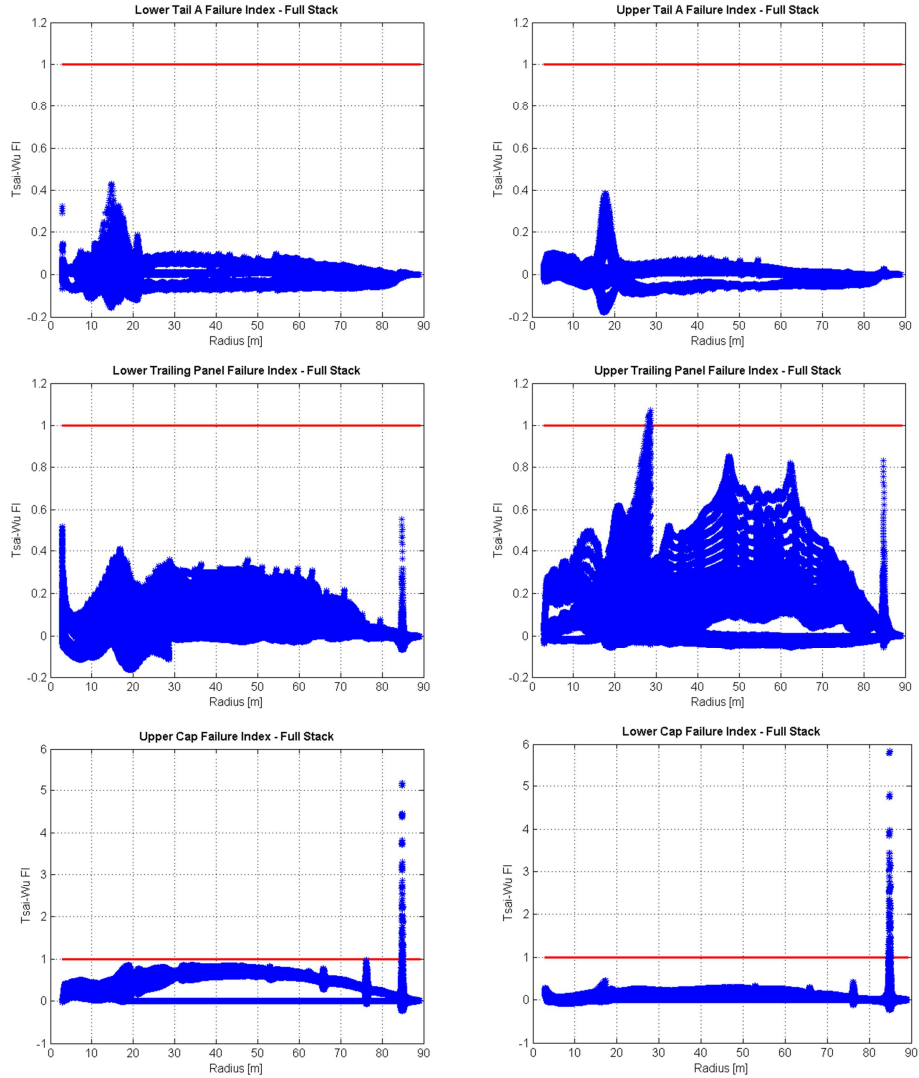
Table 5. *Displacement solution under simple load case for RefSection_5 (71.952m)*

Key point No.	Key Point Coordinates			Displacement solution simple case					
	x [m]	y [m]	z [m]	x [m]	y [m]	z [m]	x [m]	y [m]	z [m]
1	-1.894	-0.047	71.952	2.277	2.229	10.917	10.229	0.071	-1.331
5	-0.029	-0.330	71.952	2.273	2.220	10.907	10.189	0.088	-1.306
9	1.020	0.020	71.952	2.277	2.224	10.888	10.107	-0.150	-1.510
13	-0.029	0.359	71.952	2.281	2.231	10.903	10.119	-0.247	-1.607

Layer strains and/or stresses at key points of reference sections under simple load case are reported in the attached excel sheet.

APPENDIX A – TSAI-WU FAILURE INDEX

In the following appendix, it is reported a summary of the Tsai-Wu failure indices evaluated for every single region along the blade full length.



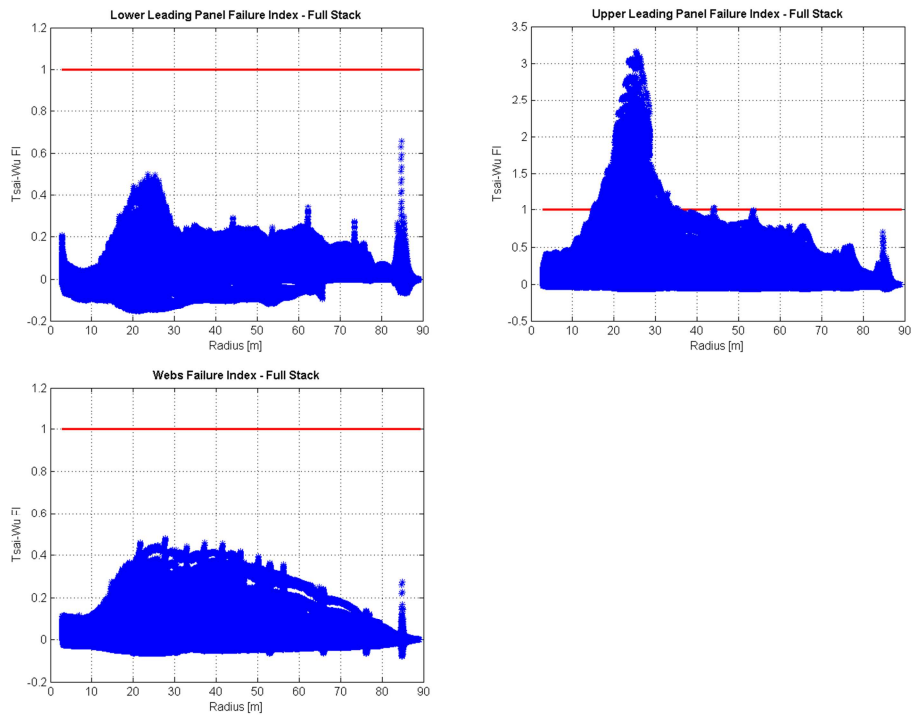


Figure 9, Summary of the Tsai-Wu failure indices for all the layers of the entire blade

Comments: the peaks observed for some of the regions are a result of the load application scheme and therefore they are not considered as material failure.

PoliMI contribution on the Benchmark of blade structural models

C L. Bottasso, A. Croce, F. Gualdoni

Politecnico di Milano

Department of Aerospace Science and Technology

SHORT DESCRIPTION OF STRUCTURAL ANALYSIS TOOL(S) USED

The 3D finite element model is developed in MSC Nastran 2011 format. The mesh procedure is obtained by Hypermesh, the properties definition is performed by Matlab functions. Elements are placed in mid thickness position while local lamination sequence is defined by PCOMP card. Orthotropic materials are set by MAT8 card, while isotropic material are modelled by MAT1. Further data are reported in following table.

Table 1. **FEM constitutive elements**

Entity	Number
GRID (nodes)	135149
CTRIA3 (triangular plate element)	852
CQUAD4 (quadrilateral plate element)	136242
RBE3 (interpolation constraint element)	36

The RBE3 elements are used to applied loads for reference load case. The loads distribution is discretized and applied to 36 nodes along blade span. The RBE3 allows to distribute the applied loads to elements defining the spar caps on suction and pressure side.

If the simple load case is considered, the loads are applied directly to the nodes of FE model. The forces are applied to the nodes nearest to the ones defined in benchmark document.

The applied constraint involve the displacements of the nodes at the blade root in direction x, y and z, while the rotations are free. This constrain set is applied for all considered analysis.

1.1. For the analysis for the extraction of blade properties

Sectional models are defined using either 2D finite element meshes modelling the stack sequence of plies or using equivalent panels. In this case the the latter approach has been used. From the sectional models, fully-populated stiffness matrices are computed using the code **ANBA** (**A**nisotropic **B**eam **A**nalysis), based on the anisotropic beam theory of Ref. [1]. From this sectional analysis code a six by six stiffness matrices and the mass matrix are obtained.

1.2. For the natural frequencies (modal) analysis

The modal analysis is performed by 3D FE model by MSC Nastran 2011. The model is constraint as reported in model description, the analysis is performed in vacuum and in a fixed position.

1.3. For the extreme load carrying capacity analysis (static analysis)

Linear static analysis is performed by MSC Nastran 2011. Both reference and simple load case are considered. Safety margins are computed with Matlab and Microsoft Excel.

1.4. Failure criterion used

The failure criteria is based on the definition of a safety margin. This safety margin compares the loading state in a specific point (for both stress and strain) with the allowable values defined for the material of the ply. A safety margin lower than zero means that the failure criteria is not satisfied.

1.5. Modelling of the reference load case

The reference load case is discretized and applied stepwise to the structure by RBE3 elements. Forces and moments are moved from elastic axis to pitch axis. Forces and torsional moment are discretized stepwise depending on the output distribution and applied to the structure. Bending moments are applied only to correct bending distribution due to shear forces distributions to obtain locally the imposed external bending moment distribution. The output are retrieved at the centroid of the elements near the key points position considering the current blade geometry.

1.6. For the buckling analysis

Linear buckling analysis is performed by MSC Nastran 2011. Reference and simple load case are considered. Examining the buckling results the reader should remember that the Web C elements is not include in the model. Five eigenvalues are computed, buckling appears in trailing edge panels at suction side.

1.7. For the variable load carrying capacity analysis (fatigue analysis)

N/A

1.8. Failure criterion used

N/A

DATA OUTPUT

2.1. Global blade properties

Overall mass of blade: 42262.44 kg

Location of centre of gravity of blade: x: -0.0859 (m), y: 0.0339 (m), z: 26.6211 (m)

2.2. Natural frequencies analysis

Natural frequencies of the blade and (if available) structural damping of the blade:

Table 2. *Natural frequencies of the blade*

Mode (#)	Frequency (Hz)	Damping ratio (%)
1	0.6123	N/A
2	0.9124	N/A
3	1.7426	N/A
4	2.7692	N/A
5	3.5516	N/A
6	5.6687	N/A

2.3. Deflection analysis

Tip displacement and torsion of blade under **simple** load case

Table 3. *Tip displacement under simple case*

Key point No.	Coordinates			Displacement solution simple case		
	x [m]	y [m]	z [m]	x [m]	y [m]	z [m]
*	0	0	89.166	2.6713	19.3777	0.0112

* The tip displacement is measured placing a node at blade tip (GRID ID: 1000000). The node is linked to nearest nodes by RBE3 element

Tip displacement and torsion of blade under **Reference** load case

Table 4. *Tip displacement under Reference case*

Key point No.	Coordinates			Displacement solution reference case		
	x [m]	y [m]	z [m]	x [m]	y [m]	z [m]
*	0	0	89.166	2.6743	19.6090	0.0154

* The tip displacement is measured placing a node at blade tip (GRID ID: 1000000). The node is linked to nearest nodes by RBE3 element

2.4. Buckling analysis

Buckling load factor over **reference** load case: 0.5291

Buckling appears in trailing edge panels at suction side between 59.5m and 80.7m from the blade root. Since in this NASTRAN FE model the third shear web is not (yet) modelled, the buckling may be over-estimated.

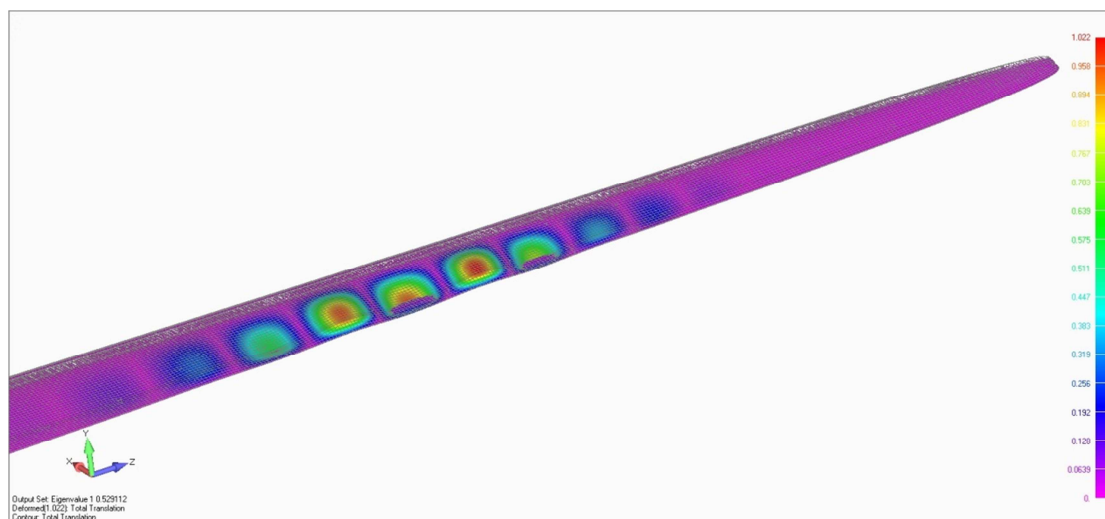


Figure 1: Buckling mode shape - Reference load case

Buckling load factor over **simple** load case: 0.5691

Buckling appears in trailing edge panels at suction side between 57.4m and 78.2m from the blade root.

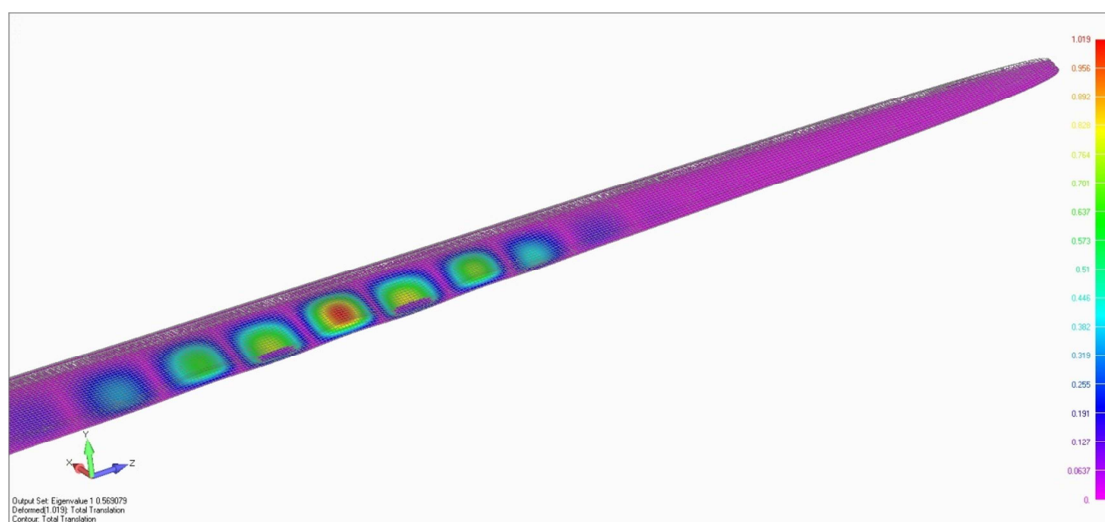


Figure 47. Buckling mode shape - Simple load case

2.5. Extreme load carrying capacity analysis

Extreme load carrying capacity multiplication factor (static strength under **reference** case): 0.648.

Extreme load carrying capacity multiplication factor (static strength under **simple** case): 0.682.

These values are estimated from the safety margin in each ply of the five the reference sections.

The safety margin is computed as:

$$SM = 1 - \frac{ActualLoad * SafetyFactor}{FailureLoad}$$

These values are computed in each key points of the reference sections both for stresses and

strains. The failure criteria based on this safety margin compare the loading state in the point (both stress and strain) with the allowable values defined for the material of the ply. A safety margin lower than zero means that the failure criteria is not satisfied.

Under the reference load, the second section (Z-position =26.694m) presents a negative SM in the key points 7 and 8 in the suction side leading panel both in the uniax and in the triax plies in the transversal strains.

This extreme load analysis has been performed only on the structural plies, i.e. the core (and the external paint which is automatically included by the design tool Cp-Max, see ref. [2]) was not included in the analysis.

In the next table is reported the SM for these key points.

The safety margins for each key point in every plies may be seen in the attached file "StrainsStressesDescription_PoliMi_29082013.xlsx" file, sheet "SafetyMargin4Report".

Table 5. Simple Load Case: Safety margin details

Sec_2									
Z-position [m]	26,69			Strain %			Stress [MPa]		
Key point	Lamination Sequence	n_ply_ext	Layer Name	Longitudi	Transvers	Shear	Longitudi	Transvers	Shear
7	Leading panels	1	Triax	0,394	0,981	0,409	0,282	0,386	0,410
		16	Triax	0,395	0,990	0,410	0,288	0,416	0,411
		31	Triax	0,396	0,947	0,412	0,294	0,447	0,412
		32	Uniax	0,275	0,931	0,364	0,263	0,817	0,365
		33	Uniax	0,275	0,928	0,364	0,264	0,818	0,365
		34	Uniax	0,275	0,924	0,365	0,264	0,820	0,365
		35-41	Balsa						
		42	Uniax	0,298	-0,311	0,394	0,323	0,173	0,395
		43	Uniax	0,298	-0,315	0,394	0,323	0,169	0,395
		44	Uniax	0,298	-0,318	0,394	0,323	0,165	0,395
		45	Triax	0,415	-0,066	0,440	0,449	0,698	0,440
		60	Triax	0,416	-0,109	0,441	0,456	0,646	0,441
		75	Triax	0,416	-0,151	0,442	0,462	0,594	0,442
		8	Leading panels	1	Triax	0,487	0,035	0,711	0,521
16	Triax			0,488	0,064	0,711	0,518	0,733	0,711
31	Triax			0,488	0,094	0,711	0,515	0,767	0,712
32	Uniax			0,386	-0,122	0,688	0,407	0,302	0,689
33	Uniax			0,386	-0,119	0,688	0,407	0,305	0,689
34	Uniax			0,386	-0,117	0,688	0,407	0,307	0,689
35-41	Balsa								
42	Uniax			0,403	0,735	0,697	0,400	0,933	0,697
43	Uniax			0,403	0,738	0,697	0,400	0,932	0,697
44	Uniax			0,403	0,740	0,697	0,400	0,931	0,697
45	Triax			0,503	0,792	0,720	0,441	0,661	0,720
60	Triax			0,504	0,822	0,720	0,438	0,641	0,720
75	Triax			0,504	0,851	0,720	0,435	0,621	0,721

Table 6. Reference Load Case: Safety margin details

Sec_2									
Z-position [m]	26,69			Strain %			Stress [MPa]		
Key point	Lamination Sequence	n_ply_ext	Layer Name	Longitudi	Transvers	Shear	Longitudi	Transvers	Shear
7	Leading panels	1	Triax	0,399	0,941	0,314	0,278	0,343	0,315
		16	Triax	0,400	0,968	0,314	0,285	0,376	0,315
		31	Triax	0,401	0,996	0,314	0,292	0,410	0,315
		32	Uniax	0,281	0,998	0,259	0,267	0,789	0,260
		33	Uniax	0,281	1,000	0,259	0,267	0,790	0,260
		34	Uniax	0,281	0,997	0,259	0,267	0,792	0,260
		35-41	Balsa						
		42	Uniax	0,303	-0,344	0,255	0,330	0,134	0,256
		43	Uniax	0,303	-0,348	0,255	0,330	0,130	0,256
		44	Uniax	0,304	-0,352	0,255	0,330	0,126	0,256
		45	Triax	0,420	-0,094	0,311	0,459	0,657	0,311
		60	Triax	0,420	-0,140	0,311	0,465	0,601	0,311
		75	Triax	0,421	-0,186	0,310	0,472	0,545	0,311
		8	Leading panels	1	Triax	0,491	0,021	0,658	0,528
16	Triax			0,491	0,052	0,659	0,524	0,711	0,659
31	Triax			0,492	0,082	0,660	0,521	0,747	0,660
32	Uniax			0,390	-0,135	0,633	0,412	0,285	0,633
33	Uniax			0,391	-0,133	0,633	0,412	0,287	0,633
34	Uniax			0,391	-0,130	0,633	0,412	0,290	0,633
35-41	Balsa								
42	Uniax			0,407	0,766	0,657	0,403	0,922	0,658
43	Uniax			0,407	0,769	0,657	0,403	0,921	0,658
44	Uniax			0,407	0,771	0,657	0,403	0,920	0,658
45	Triax			0,506	0,818	0,683	0,441	0,646	0,683
60	Triax			0,507	0,849	0,684	0,438	0,625	0,684
75	Triax			0,507	0,880	0,685	0,435	0,604	0,685

2.6. Reference blade sections results

The following table shows the mass properties of reference blade sections. These properties are defined wrt a reference system whose axes are parallel to the principal axes of inertia and are centred in the pitch axis as showed in the figure [3].

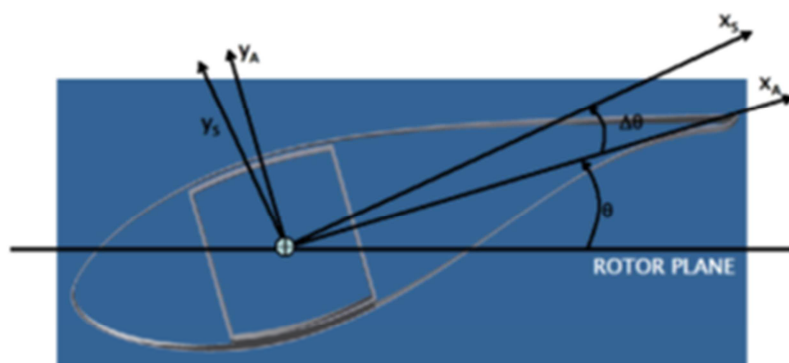


Figure 3. Reference system for blade section results

Table 7. Mass properties of reference blade sections

Property		Sec_1	Sec_2	Sec_3	Sec_4	Sec_5
Z-position	(m)	2.800	26.694	37.907	54.149	71.592
Mass/Length	(kg/m)	1101.83	659.82	523.58	350.82	169.28
Mass Centre	x (m)	-0,0001	-0,3713	-0,3562	-0,2683	-0,2031
	y (m)	0,0005	0,0436	0,0177	0,0324	0,0258
Mass moment of inertia (I)	ρI_{xx} (kg·m)	3610.64	450.81	197.10	58.13	12.11
	ρI_{yy} (kg·m)	3610.46	1062.93	616.74	230.11	52.30
	ρI_{xy} (kg·m)					
Polar mass inertia (ρI_p)	ρI_p (kg·m)	7221.09	1513.74	813.84	288.24	64.40

The following table shows the stiffness properties of reference blade sections. These properties are defined wrt a reference system whose axes are parallel to the principal axes of inertia and are centred in the pitch axis as showed in figure [3]. The angle between the chord axis (the aerodynamic x-axis) and the principal x-axis of inertia $\Delta\Theta$ are also reported in the next table.

Table 8. *Stiffness properties of reference blade sections*

Property		Sec_1	Sec_2	Sec_3	Sec_4	Sec_5
Z-position	(m)	2.800	26.694	37.907	54.149	71.592
Axial Stiffness	EA (N)	1,7169E+10	9,7363E+09	7,8524E+09	5,5107E+09	2,6871E+09
Elastic Centre	x (m)	-0,0001	-0,3638	0,0148	-0,2392	-0,1832
	y (m)	0,0005	0,0408	0,0148	0,0310	0,0252
Bending Stiffness	EI_{xx} (Nm ²)	6,1326E+10	8,5330E+09	3,7824E+09	1,1247E+09	2,3032E+08
	EI_{yy} (Nm ²)	6,1329E+10	1,6932E+10	9,5180E+09	3,4877E+09	7,6090E+08
	EI_{xy} (Nm ²)					
Shear Centre	x (m)	-0,0001	0,0893	0,0362	0,0078	-0,0197
	y (m)	0,0005	0,0865	0,0639	0,0641	0,0437
Torsional Stiffness	GJ (Nm ²)	2,7754E+10	2,1217E+09	8,3513E+08	2,5364E+08	6,1231E+07
Shear Stiffness	S_x (N)	1.9430e+009	5.3687e+008	3.8620e+008	2.2465e+008	1.1732e+008
	S_y (N)	1.9431e+009	7.7744e+008	5.1195e+008	3.5816e+008	2.0450e+008
Angle between chord axis and principal x-axis of inertia	$\Delta\theta$ (deg)	79.21	-1.90	-0.33	1.26	2.26

A complete description of the blade properties are reported in the attached file "ReferenceBladeSection_29082013_PoliMI.xlsx"

2.7. Extreme load carrying capacity analysis under simple load case

The following tables show the displacements for reference blade sections under the simple load case application.

** The key-points No. are for reference case only. The real points considered here are the FE model nodes closest to the key-points defined for the benchmark. Hence, the key-point coordinates in the first columns of the tables may be different from the key-point coordinates defined in the “Information on the Benchmark of blade structural models_ver2.pdf” document.

Table 9. *Displacement solution under simple load case for RefSection_2 (26.694m)*

Key point No. **	Key Point Coordinates			Displacement solution simple case		
	x [m]	y [m]	z [m]	x [m]	y [m]	z [m]
1	-3,84E+00	6,09E-01	26.694	1,79E-01	4,22E-01	4,00E-02
13	-1,19E-01	-1,04E+00	26.694	1,62E-01	4,02E-01	5,38E-02
9	2,29E+00	-2,99E-01	26.694	1,71E-01	4,04E-01	-2,36E-02
5	1,80E-01	1,09E+00	26.694	1,84E-01	3,92E-01	-5,27E-02

Table 10. *Displacement solution under simple load case for RefSection_3 (37.907m)*

Key point No. **	Key Point Coordinates			Displacement solution simple case		
	x [m]	y [m]	z [m]	x [m]	y [m]	z [m]
1	-3,67E+00	3,93E-01	37.907	4,37E-01	1,24E+00	6,54E-02
13	-6,84E-02	-7,75E-01	37.907	4,29E-01	1,23E+00	8,62E-02
9	1,98E+00	-1,01E-01	37.907	4,35E-01	1,21E+00	-4,29E-02
5	1,52E-01	7,69E-01	37.907	4,41E-01	1,23E+00	-8,23E-02

Table 11. *Displacement solution under simple load case for RefSection_4 (54.149m)*

Key point No. **	Key Point Coordinates			Displacement solution simple case		
	x [m]	y [m]	z [m]	x [m]	y [m]	z [m]
1	-2,84E+00	1,34E-01	54.149	1,03E+00	3,98E+00	9,39E-02
13	-6,30E-02	-4,76E-01	54.149	1,02E+00	3,97E+00	1,22E-01
9	1,53E+00	-7,35E-02	54.149	1,02E+00	3,95E+00	-4,22E-02
5	8,42E-02	5,21E-01	54.149	1,03E+00	3,97E+00	-1,24E-01

Table 12. *Displacement solution under simple load case for RefSection_5 (71.592m)*

Key point No. **	Key Point Coordinates			Displacement solution simple case		
	x [m]	y [m]	z [m]	x [m]	y [m]	z [m]
1	-1,91E+00	-3,87E-02	71.952	1,84E+00	1,00E+01	1,19E-01
13	-7,56E-02	-3,09E-01	71.952	1,83E+00	9,94E+00	1,51E-01
9	1,02E+00	-6,54E-03	71.952	1,84E+00	9,94E+00	-3,69E-02
5	2,32E-02	3,45E-01	71.952	1,84E+00	9,96E+00	-1,47E-01

Layer strains and/or stresses at key points of reference sections under simple load case: see attached “StrainsStressesDescription_PoliMi_29082013.xlsx” file, Sheet “StressStrain4ReportSimple”.

2.8. Extreme load carrying capacity analysis under reference load case

The following tables show the displacements for reference blade sections under the reference load case application.

** The key-points No. are for reference case only. The real points considered here are the FE model nodes closest to the key-points defined for the benchmark. Hence, the key-point coordinates in the first columns of the tables may be different from the key-point coordinates defined in the “Information on the Benchmark of blade structural models_ver2.pdf” document.

Table 13. *Displacement solution under reference load case for RefSection_2 (26.694m)*

Key point No. **	Key Point Coordinates			Displacement solution reference case		
	x [m]	y [m]	z [m]	x [m]	y [m]	z [m]
1	-3,84E+00	6,09E-01	26.694	1,80E-01	4,26E-01	4,35E-02
13	-1,19E-01	-1,04E+00	26.694	1,63E-01	4,04E-01	5,62E-02
9	2,29E+00	-2,99E-01	26.694	1,71E-01	4,04E-01	-2,36E-02
5	1,80E-01	1,09E+00	26.694	1,86E-01	3,94E-01	-5,13E-02

Table 14. *Displacement solution under reference load case for RefSection_3 (37.907m)*

Key point No. **	Key Point Coordinates			Displacement solution reference case		
	x [m]	y [m]	z [m]	x [m]	y [m]	z [m]
1	-3,67E+00	3,93E-01	37.907	4,46E-01	1,26E+00	6,95E-02
13	-6,84E-02	-7,75E-01	37.907	4,37E-01	1,24E+00	8,93E-02
9	1,98E+00	-1,01E-01	37.907	4,43E-01	1,22E+00	-4,13E-02
5	1,52E-01	7,69E-01	37.907	4,50E-01	1,24E+00	-8,02E-02

Table 15. *Displacement solution under reference load case for RefSection_4 (54.149m)*

Key point No. **	Key Point Coordinates			Displacement solution reference case		
	x [m]	y [m]	z [m]	x [m]	y [m]	z [m]
1	-2,84E+00	1,34E-01	54.149	1,04E+00	4,01E+00	9,83E-02
13	-6,30E-02	-4,76E-01	54.149	1,04E+00	4,00E+00	1,27E-01
9	1,53E+00	-7,35E-02	54.149	1,04E+00	3,97E+00	-3,92E-02
5	8,42E-02	5,21E-01	54.149	1,05E+00	4,00E+00	-1,21E-01

Table 16. *Displacement solution under reference load case for RefSection_5 (71.592m)*

Key point No. **	Key Point Coordinates			Displacement solution reference case		
	x [m]	y [m]	z [m]	x [m]	y [m]	z [m]
1	-1,91E+00	-3,87E-02	71.952	1,86E+00	1,01E+01	1,22E-01
13	-7,56E-02	-3,09E-01	71.952	1,85E+00	1,00E+01	1,56E-01
9	1,02E+00	-6,54E-03	71.952	1,85E+00	9,99E+00	-3,26E-02
5	2,32E-02	3,45E-01	71.952	1,86E+00	1,00E+01	-1,44E-01

Layer strains and/or stresses at key points of reference sections under reference load case: see attached “StrainsStressesDescription_PoliMi_29082013.xlsx” file, Sheet “StressStrain4ReportReference”.

REFERENCES

- [1] Giavotto V., Borri M., Mantegazza P., Ghiringhelli G.L., “Anisotropic beam theory and applications”. *Computers & Structures*, 16:403–413, (1983).
- [2] Bottasso C.L., Campagnolo F., Croce A., “Multi-Disciplinary Constrained Optimization of Wind Turbines”, *Multibody System Dynamics*, 27-1, pp. 21-53, (2012)

UPAT-CORE team contribution on the Benchmark of blade structural models

Theodore P. Philippidis, Iordanis T. Masmanidis, George A. Roukis

University of Patras, Department of Mechanical Engineering & Aeronautics

Applied Mechanics Laboratory-CORE team.

P.O. Box 1401, Panepistimioupolis Rion, 265 04 Patras, Greece

SHORT DESCRIPTION OF STRUCTURAL ANALYSIS TOOL(S) USED

For the Benchmark calculations UPAT CORE-team used the commercial FE program ANSYS and the in-house developed code PROBUST, a refined and enhanced with buckling analysis capabilities version of code THIN [1]-[2]. The latter, was used specifically for the extraction of blade sectional characteristics and ply stresses for the reference load case. The blade has also been modelled in ANSYS to calculate the ply stresses/strains for the simple load case and ply strains for the reference load case. Failure, buckling and modal analyses as well as nodal displacement output of the reference blade for the various load cases were performed using ANSYS solvers.

The FE model in ANSYS is based on a Reissner-Mindlin shell formulation consisting of 311,800 elements. The element type used is a 4-node multilayer *shell181*. It is noted that the adhesive paste has not been modelled. Blade geometry, lamination plans, material properties and loads were all based on the benchmark input provided in [3]-[4] and various input files provided by the coordinators. Concerning composite materials, multi-directional (MD) fabrics, i.e. stitched bi-directional [± 45] and tri-axial [0/ ± 45], were modelled as homogeneous orthotropic materials. A more detailed and accurate ply-by-ply analysis is foreseen for the future.

Blade section models used along with PROBUST, consist of ca. 220 elements while MD fabrics were modelled as in FE models.

1.6. For the analysis for the extraction of blade properties

PROBUST was used to derive sectional characteristics.

1.7. For the natural frequencies (modal) analysis

The commercial code ANSYS was used to derive natural frequencies and respective mode shapes. The modal analysis of the reference blade was carried out via the subspace iteration method.

1.8. For the extreme load carrying capacity analysis (static analysis)

For the static analysis under ultimate loading both FE and PROBUST models were used.

Failure criterion used

Failure criteria for composites in each ply were calculated with ANSYS for both load cases although results are presented only for the reference load case. By *failure*, First Ply Failure (FPF) is meant; element failure occurs when a single layer fails first. Results are presented specifically by means of Tsai-Wu (Tsai-Hahn version) criteria. The inverse of the strength ratio (R-value) is used; its value should be ≤ 1 for safe states.

Modelling of the reference load case

The reference load case was implemented in the FE model as a nodal force set statically equivalent to the flap and edge moment distributions as well as the axial force distribution mentioned in Table 5 of [4]. These forces were applied in 95 stations of the reference blade; a typical output of the numerical tool is presented in Fig.1.3.1, where the flap moment distribution as derived by the applied concentrated forces is compared to the given reference one.

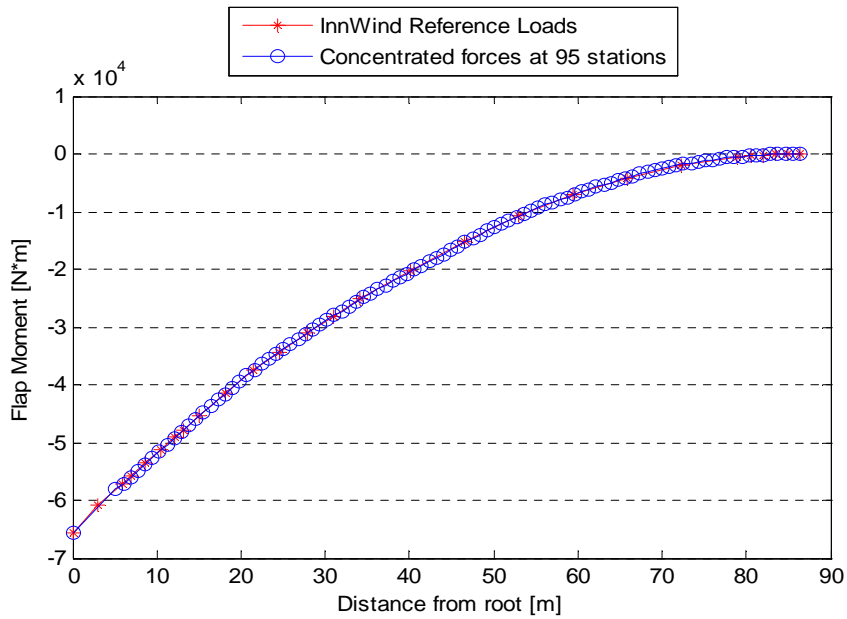


Figure 1.3.1 Modeling of reference Flap moment distribution.

1.9. For the buckling analysis

Linear buckling analysis (eigenvalues and respective mode shapes) was performed by means of the Block Lanczos method implemented in ANSYS commercial code.

1.10. For the variable load carrying capacity analysis (fatigue analysis)

N/A

Failure criterion used

N/A

DATA OUTPUT

2.1 Global blade properties

Overall mass of blade: 42379 kg

Location of centre of gravity of blade: x: -0.15766 (m), y: 0.034504 (m), z: 28.802 (m)

It is noted that the first section of the FE model is at 2.8m

Natural frequencies analysis

Natural frequencies of the blade and (if available) structural damping of the blade:

Table 1. *Natural frequencies of the blade*

Mode (#)	Frequency (Hz)	Damping ratio (%)
1	0.60949	-
2	0.94768	-
3	1.7486	-
4	2.8333	-
5	3.5714	-
6	5.5506	-

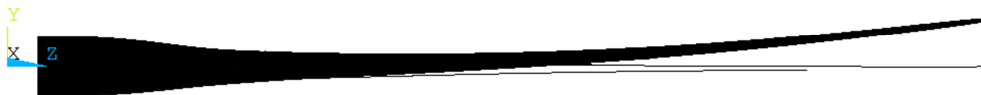


Figure 2.1.1 Mode shape for mode number 1



Figure 2.1.2 Mode shape for mode number 2



Figure 2.1.3 Mode shape for mode number 3



Figure 2.1.4 Mode shape for mode number 4



Figure 2.1.5 Mode shape for mode number 5



Figure 2.1.6 Mode shape for mode number 6

Deflection analysis

Tip displacement and torsion of blade under **simple** load case

Table 2. *Tip displacement under simple case*

Key point No.	Coordinates			Displacement solution simple case		
	x [m]	y [m]	z [m]	x [m]	y [m]	z [m]
1	-0.389	-0.025	89.166	3.4246	20.508	0.51205E-01
5	-0.004	-0.068	89.166	3.4240	20.504	0.51638E-01
9	0.210	0.013	89.166	3.4251	20.501	-0.13147E-01
13	-0.004	0.074	89.166	3.4258	20.504	-0.35282E-01

Tip displacement and torsion of blade under **Reference** load case

Table 3. *Tip displacement under Reference case*

Key point No.	Coordinates			Displacement solution reference case		
	x [m]	y [m]	z [m]	x [m]	y [m]	z [m]
1	-0.389	-0.025	89.166	3.3938	20.593	0.55517E-01
5	-0.004	-0.068	89.166	3.3933	20.589	0.57568E-01
9	0.210	0.013	89.166	3.3943	20.586	-0.87421E-02
13	-0.004	0.074	89.166	3.3951	20.589	-0.32587E-01

Buckling analysis

Buckling load factor over **reference** load case: 0.966549 (critical load factor)

The blade buckles at ca. 65m from the root in the spar cap area and shear webs.

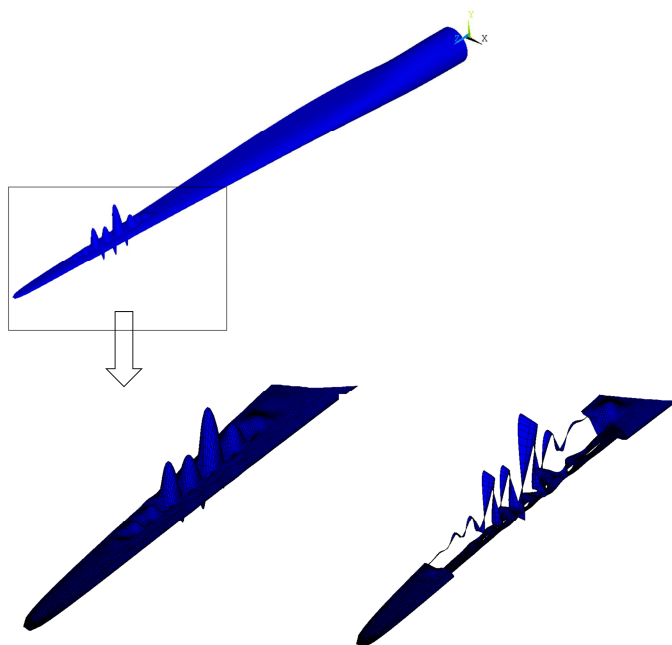


Figure 48.1.7 Buckling mode shape

Extreme load carrying capacity analysis

Extreme load carrying capacity multiplication factor (static strength under **reference** case): 0.544671

The blade fails under reference load case in the area of Leading Panels at 25.2 m. Failure occurs at the UNIAX layer of the Leading Panel lay-up. The failure criteria maximum value is 1.83597 hence the multiplication factor is 0.544671 (=1/1.83597).

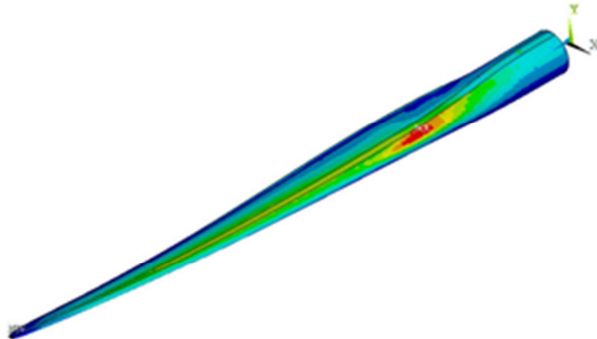


Figure 49.1.8 Failure pattern of reference blade under the reference load

2.2 Reference blade sections results

Mass properties of reference blade sections

Table 4. Mass properties of reference blade sections

Property		Sec_1	Sec_2	Sec_3	Sec_4	Sec_5
Z-position	(m)	2.800	26.694	37.907	54.149	71.592
Mass/Length	(kg/m)	1201	632.2	506.7	336.9	162
Mass Centre	x (m)	0.0032	-0.2872	-0.2593	0.1818	0.1257
	y (m)	0.001	0.0821	0.0441	0.0378	0.0197
Mass moment of inertia (ρI)	ρI_{xx} (kg·m)	4051	511.9	218.8	58.31	11.92
	ρI_{yy} (kg·m)	3716	1631	1004	363	74.55
	ρI_{xy} (kg·m)	1.184	-225.7	-111.1	18.63	-0.2219
Polar mass inertia (ρI_p)	ρI_p (kg·m)	7767	2142.9	1222.8	421.31	86.47

Stiffness properties of reference blade sections

Table 5. Stiffness properties of reference blade sections

Property		Sec_1	Sec_2	Sec_3	Sec_4	Sec_5
Z-position	(m)	2.800	26.694	37.907	54.149	71.592
Axial Stiffness	EA(N)	1.80E+10	9.23E+09	7.71E+09	5.37E+09	2.64E+09
Elastic Centre	x (m)	0.0035	-0.1343	-0.0779	0.0282	0.0463
	y (m)	0.001	0.0558	0.0209	0.02	0.0096
Bending Stiffness	EI_{xx} (Nm ²)	6.30E+10	8.89E+09	3.91E+09	1.09E+09	2.26E+08
	EI_{yy} (Nm ²)	6.14E+10	2.11E+10	1.29E+10	4.68E+09	9.87E+08
	EI_{xy} (Nm ²)	1.62E+07	-2.94E+09	-1.41E+09	2.22E+08	-6.36E+06
Shear Centre	x (m)	-0.00736868	0.609	0.496	-0.31995	-0.21294
	y (m)	-0.01049989	0.012	-0.005	0.001659	0.007251
Torsional Stiffness	GJ (Nm ²)	2.81E+10	1.90E+09	7.40E+08	2.25E+08	5.58E+07
Shear Stiffness	S_x (N)	-	-	-	-	-
	S_y (N)	-	-	-	-	-
Coupling stiffness, Other as needed...						

Extreme load carrying capacity analysis under simple load case

Displacements for reference blade sections under the simple load case application

Table 6. Displacement solution under simple load case for RefSection_2 (26.694m)

Key point No.	Key Point Coordinates			Displacement solution simple case		
	x [m]	y [m]	z [m]	x [m]	y [m]	z [m]
1	-3.875	0.334	26.694	0.19544	0.44118	0.61799E-01
5	0.022	-1.126	26.694	0.17304	0.39650	0.56677E-01
9	2.293	-0.293	26.694	0.18196	0.40864	-0.30308E-01
13	0.022	1.127	26.694	0.20587	0.39961	-0.65217E-01

Table 7. Displacement solution under simple load case for RefSection_3 (37.907m)

Key point No.	Key Point Coordinates			Displacement solution simple case		
	x [m]	y [m]	z [m]	x [m]	y [m]	z [m]
1	-3.683	0.297	37.907	0.50394	1.3129	0.91932E-01
5	0.042	-0.841	37.907	0.49116	1.2863	0.93752E-01
9	1.984	-0.185	37.907	0.49815	1.2644	-0.46780E-01
13	0.042	0.810	37.907	0.50874	1.2823	-0.10171

Table 8. Displacement solution under simple load case for RefSection_4 (54.149m)

Key point No.	Key Point Coordinates			Displacement solution simple case		
	x [m]	y [m]	z [m]	x [m]	y [m]	z [m]
1	-2.843	0.087	54.149	1.2199	4.2050	0.13158
5	0.008	-0.518	54.149	1.2122	4.1835	0.13494
9	1.530	-0.056	54.149	1.2178	4.1611	-0.67642E-01
13	0.008	0.550	54.149	1.2251	4.1796	-0.15229

Table 9. Displacement solution under simple load case for RefSection_5 (71.592m)

Key point No.	Key Point Coordinates			Displacement solution simple case		
	x [m]	y [m]	z [m]	x [m]	y [m]	z [m]
1	-1.894	-0.047	71.952	2.2869	10.702	0.15283
5	-0.029	-0.330	71.952	2.2825	10.684	0.16772
9	1.020	0.020	71.952	2.2874	10.667	-0.72717E-01
13	-0.029	0.359	71.952	2.2919	10.680	-0.18067

Layer strains and/or stresses at key points of reference sections under simple load case

[See excel template](#)

Extreme load carrying capacity analysis under reference load case

Displacements for reference blade sections under the reference load case application

Table 10. Displacement solution under reference load case for RefSection_2 (26.694m)

Key point No.	Key Point Coordinates			Displacement solution reference case		
	x [m]	y [m]	z [m]	x [m]	y [m]	z [m]
1	-3.875	0.334	26.694	0.19262	0.44617	0.64315E-01
5	0.022	-1.126	26.694	0.16879	0.39992	0.59082E-01
9	2.293	-0.293	26.694	0.17839	0.41087	-0.29264E-01
13	0.022	1.127	26.694	0.20292	0.40286	-0.63902E-01

Table 11. Displacement solution under reference load case for RefSection_3 (37.907m)

Key point No.	Key Point Coordinates			Displacement solution reference case		
	x [m]	y [m]	z [m]	x [m]	y [m]	z [m]
1	-3.683	0.297	37.907	0.50504	1.3241	0.94976E-01
5	0.042	-0.841	37.907	0.49186	1.2962	0.96719E-01
9	1.984	-0.185	37.907	0.49919	1.2712	-0.44364E-01
13	0.042	0.810	37.907	0.51011	1.2919	-0.99327E-01

Table 12. Displacement solution under reference load case for RefSection_4 (54.149m)

Key point No.	Key Point Coordinates			Displacement solution reference case		
	x [m]	y [m]	z [m]	x [m]	y [m]	z [m]
1	-2.843	0.087	54.149	1.2208	4.2187	0.13504
5	0.008	-0.518	54.149	1.2127	4.1950	0.13894
9	1.530	-0.056	54.149	1.2187	4.1708	-0.64025E-01
13	0.008	0.550	54.149	1.2265	4.1908	-0.14896

Table 13. Displacement solution under reference load case for RefSection_5 (71.592m)

Key point No.	Key Point Coordinates			Displacement solution reference case		
	x [m]	y [m]	z [m]	x [m]	y [m]	z [m]
1	-1.894	-0.047	71.952	2.2802	10.706	0.15530
5	-0.029	-0.330	71.952	2.2758	10.687	0.17163
9	1.020	0.020	71.952	2.2809	10.669	-0.67574E-01
13	-0.029	0.359	71.952	2.2856	10.683	-0.17601

Layer strains and/or stresses at key points of reference sections under reference load case

[See excel template](#)

2.3 References

- [1] Philippidis TP, Vassilopoulos AP, Katopis KG, Voutsinas SG, THIN/PROBEAM: Software for fatigue design and analysis of composite rotor blades, Wind Eng. 1996; 20, No. 5
- [2] Lekou DJ, Philippidis TP. PRE-and POST_THIN: A Tool for the Probabilistic Design and Analysis of Composite Rotor Blade Strength. Wind Energy 2009; 12: 676-91
- [3] D. J. Lekou, Information on the Benchmark of blade structural models, Innwind report, 17.07.2013
- [4] C. Bak, F. Zahle, R. Bitsche, T. Kim, A. Yde, L. C. Henriksen, A. Natarajan, M. Hansen, Description of the DTU 10 MW Reference Wind Turbine, DTU Wind Energy Report-I-0092, June 2013

WMC contribution on the Benchmark of blade structural models

Dr.ir. G.D. de Winkel, Dr. H. Dekker

Knowledge Centre WMC

Report: WMC-2013-083 (Rev. 4)

SHORT DESCRIPTION OF STRUCTURAL ANALYSIS TOOL(S) USED

1.1. For the analysis for the extraction of blade properties

Application: FOCUS6 version 6.2 Structural blade design, Module frbex_build_blade_database.

Using the FOCUS6 Blade Modeler, the blade geometry is defined at 100 stations along the blade. The model is based on the “open cross section” shapes. The trailing edge is closed with a web between the end-points of the profile shapes. Lines are defined along the blade using the “key point” definitions. These lines are used to define the ply-edges and shear webs. The thickness distribution of the plies is defined at 100 stations along the blade. At 527 stations along the blade cross section properties are calculated (at each side of a layup change, each geometry change and using a maximum element length at span wise direction of 0.25 m.). A dedicated script is written to convert the output properties in the FOCUS6 axis definition (based on the GL blade axis system), into the axis system and units as used with this project.

1.2. For the natural frequencies (modal) analysis

Application: FOCUS6 version 6.2 Structural blade design, Module frbex_eigen_frequencies.

Using the blade properties blade on the previous section a beam model with 200 elements is generated. The element type is a tapered Timoshenko-beam.

The first 12 coupled eigenfrequencies are extracted. The first six are reported. Besides the numerical output, pictures of the mode shapes are generated.

1.3. For the extreme load carrying capacity analysis (static analysis)

Applications:

FOCUS6 version 6.2 Structural blade design, Module frbex_finite_element_mesh_generator

Based on the blade model created with the FOCUS6 Blade Modeler, a finite element mesh is generated with 121788 4-node thick shell composite elements. At the blade root a default element size of 300 mm, at z=80 m a size of 70 mm, and at the very tip a size of 8 mm. The used element is compatible with MSC.Marc element type 75, extended with the option of allowing tapering of individual layers.

FOCUS6 version 6.2 WMC_FEM for Blade design, FEM solver

The program WMC_FEM for Blade design is a finite element code developed by WMC. It features four-node thick shell elements. The elements are constituted of composites of materials with isotropic and orthotropic properties. The kinematic and constitutive relations are linear. The displacement and force boundary conditions available also include body forces, such as gravity, and forces can be distributed using RBE3 elements. The linear finite element equations are solved using the Intel Math Kernel Library Sparse Matrix Solver. For post-processing, quantities like stress, strain and Pucks failure criterion values are available at material layer level. The results can be obtained in text format and in the Open Source vtk format, which can be used for visualisation.

Failure criterion used

The Puck criteria used in “WMC_FEM for Blade design” consider fibre fracture (FF) and inter-fibre fracture (IFF). The theoretical basis of these criteria can be found in [1] and [2]. This theory can also be found in the section on the two-dimensional stress states in section 4.5.2 in [3].

Definition of modes in output:

- mode 1 (FF_A): Fiber failure (FF) tension
- mode 2 (FF_B): Fiber failure (FF) compression
- mode 3 (IFF_A): Interfiber failure (IFF) tension
- mode 4 (IFF_B) : Interfiber failure (IFF) shear dominates compression
- mode 5 (IFF_C) : Interfiber failure (IFF) compression dominates shear

For the Puck calculations the BIAX and TRIAX materials has been converted into UD layers. The UD material properties are obtained from table 4.3 "Lamina 1" [5]. For the failure data for “Lamina 1, the properties of the UNIAX material was used. Symmetric layups are used to prevent introduction of additional tension/bending coupling in the laminates.

For BIAX the following stacking is used, see also table 4.4 of [5]:

Table 2 Stacking order BIAX

Material	Ply angle (deg)	Rel. thickness (%)
"Lamina 1"	-45	25%
"Lamina 1"	+45	25%
"Lamina 1"	+45	25%
"Lamina 1"	-45	25%

Table 3 Stacking order TRIAX

Material	Ply angle (deg)	Rel. thickness (%)
"Lamina 1"	0	15%
"Lamina 1"	-45	17.5%
"Lamina 1"	+45	17.5%
"Lamina 1"	+45	17.5%
"Lamina 1"	-45	17.5%
"Lamina 1"	0	15%

Modelling of the reference load case

FOCUS6 version 6.2 WMC_FEM for Blade design, Module LF Convert Internal

This tool automatically converts internal loads into an external load distribution at the same stations as the internal loads.

The loads are applied using RBE3 elements at the same blade stations as the internal load distribution. Since this is the default and automated method within FOCUS6, this

method is used to apply the loads on the finite element model, rather than applying single point loads on key points.

1.4. For the buckling analysis

Application: FOCUS62 Structural Blade Design, Finstrip module

Cross section based buckling analyses tool based on the finite strip method.

Application: MSC.MARC 2010

General purpose finite element application created by MSC.Software

1.5. For the variable load carrying capacity analysis (fatigue analysis)

Application: FOCUS62 Structural Blade Design, frbex_structural_analysis module

General cross section based structural analyses module of FOCUS6. On blade cross sections sensors can be defined where for each material in the layup fatigue analyses can be performed. On selected cross sections and locations on cross sections stress time series are created based on a load set. Using rainflow counting this stress time series markov matrices are created used an input for the fatigue damage and Fatigue Stress Factor calculations.

Failure criterion used

Goodman diagram based on GL 2012. The fatigue damage and the Fatigue Stress Factor can be used as design criterion.

DATA OUTPUT

2.1 Global blade properties

Overall mass of blade: 42649.375 kg

Location of centre of gravity of blade: x: -0.137 (m), y: 0.036 (m), distance from blade root L: 26.112 (m), distance from rotor centre z= 28.912 (m)

Note:

y-axis (pos.) = downwind

Natural frequencies analysis

Natural frequencies of the blade and (if available) structural damping of the blade:

Table 1. *Natural frequencies of the blade*

Mode (#)	Frequency (Hz)	Damping ratio (%)
1	0.616	n/a
2	0.974	n/a
3	1.798	n/a
4	2.975	n/a
5	3.774	n/a
6	6.170	n/a

Figures 1 -6 show the modal shapes for mode 1-6.

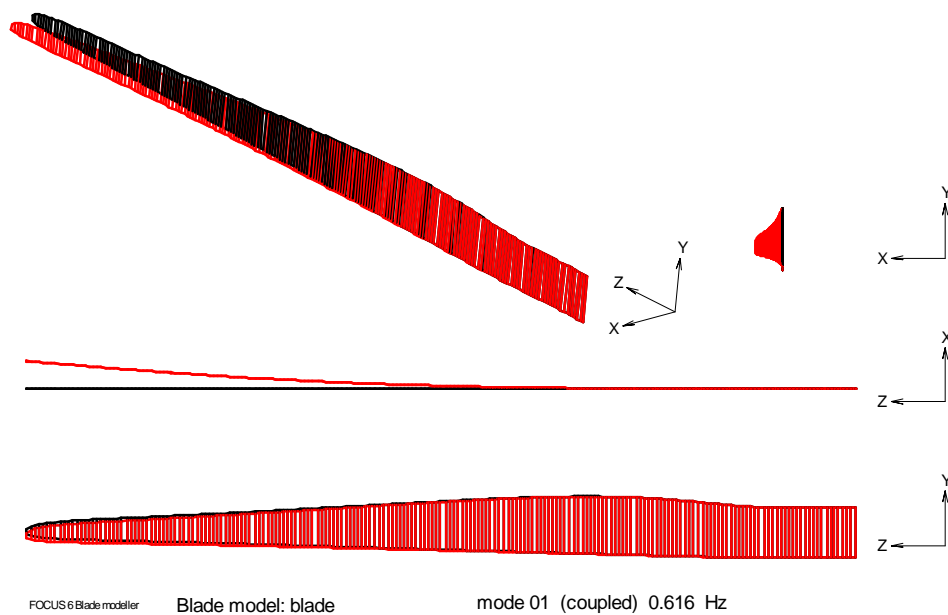


Figure 50 Mode shape for mode 1

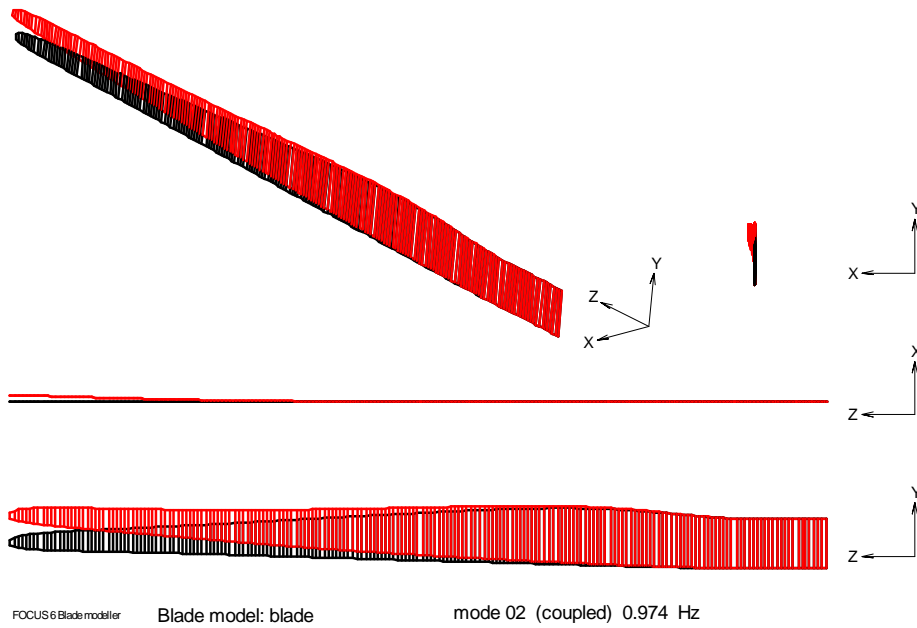


Figure 51 Mode shape for mode 2

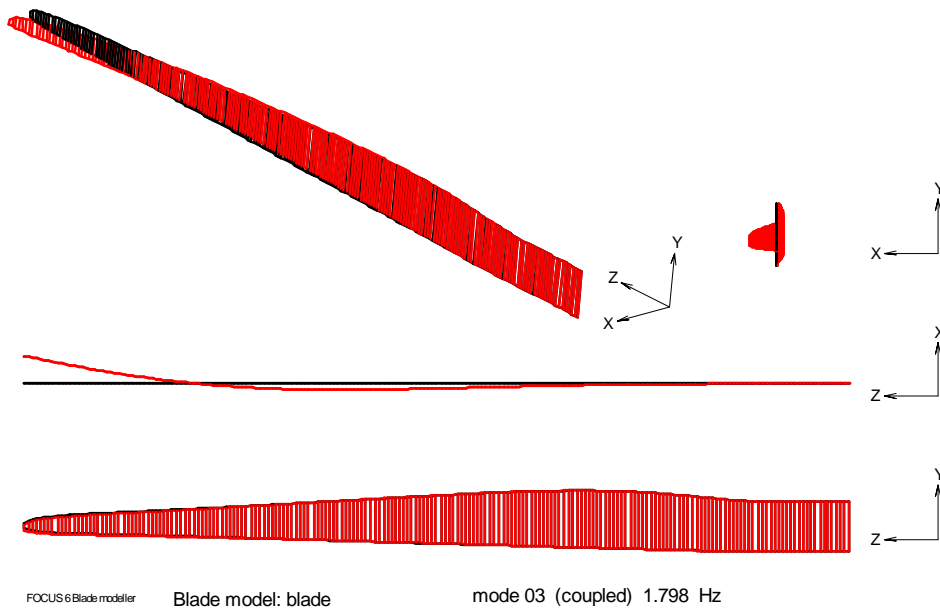


Figure 52 Mode shape for mode 3

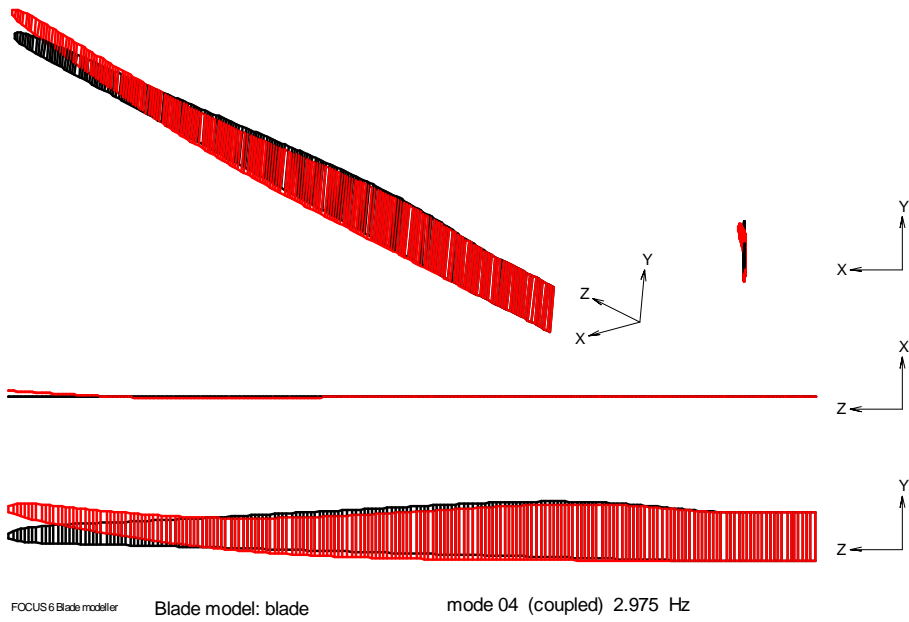


Figure 53 Mode shape for mode 4

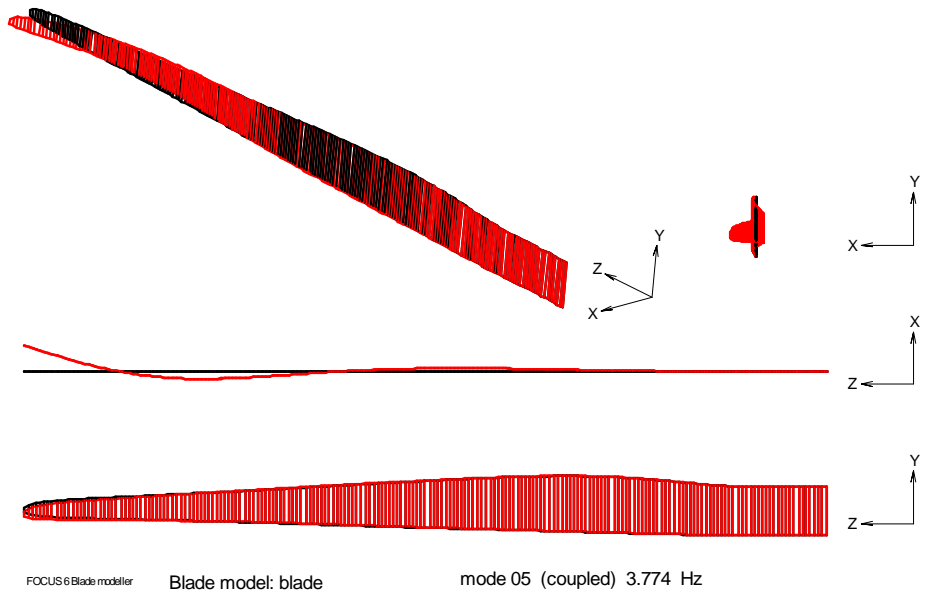


Figure 54 Mode shape for mode 5

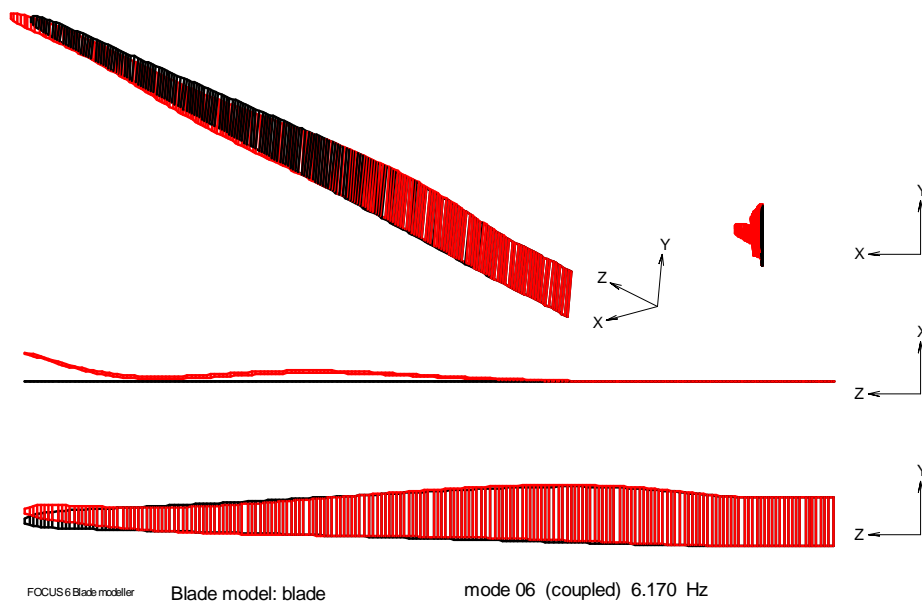


Figure 55 Mode shape for mode 6

Deflection analysis

Tip displacement and torsion of blade under **simple** load case

Table 2. *Tip displacement under simple case*

Key point No.	Coordinates			Displacement solution simple case		
	x [m]	y [m]	z [m]	x [m]	y [m]	z [m]
1	-0.389	-0.027	89.166	3.373	20.077	0.052
5	-0.013	-0.046	89.166	3.372	20.057	0.039
9	0.210	0.014	89.166	3.376	20.044	-0.011
13	-0.015	0.044	89.166	3.377	20.057	-0.014

Tip displacement and torsion of blade under **Reference** load case

Table 1. *Tip displacement under Reference case*

Key point No.	Coordinates			Displacement solution reference case		
	x [m]	y [m]	z [m]	x [m]	y [m]	z [m]
1	-0.389	-0.027	89.166	3.313	20.004	0.055
5	-0.013	-0.046	89.166	3.313	19.995	0.043
9	0.210	0.014	89.166	3.314	19.990	-0.007
13	-0.015	0.044	89.166	3.315	19.995	-0.011

Buckling analysis

Results obtained with FOCUS62 Structural Blade Design, Finstrip module

Results for cross section based buckling analyses:

Buckling load factor (without partial safety factor) over **reference** load case:

[CAP at blade root: 2.175 (at $z = 2.8$ m, half-wavelength= 0.551 m)]

CAP: 2.496 (at $z = 24.2$ m, half-wavelength=0.931 m)

Trailing edge panel: 2.905 (at $z = 68.6$ m, half-wavelength=1.158 m)

Buckling load factor (including a partial safety factor of 2.042) over **reference** load case:

CAP at blade root: 1.065 (at $z = 2.8$ m, half-wavelength= 0.551 m)]

CAP: 1.222 (at $z = 24.2$ m, half-wavelength=0.931 m)

Trailing edge panel: 1.423 (at $z = 68.6$ m, half-wavelength=1.158 m)

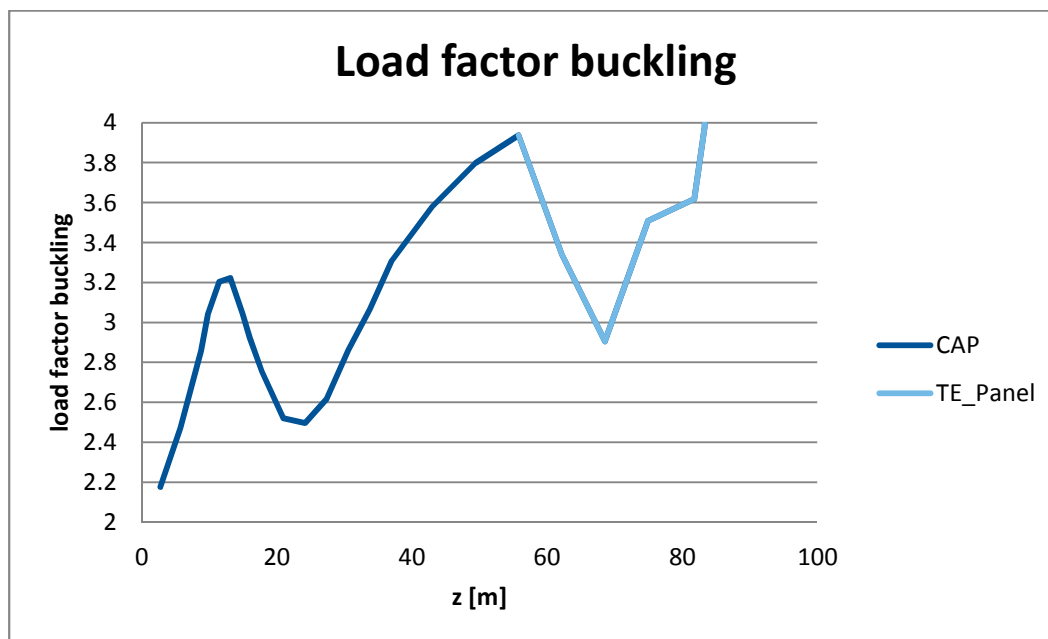


Figure 56 Buckling load factor (without partial safety factor) along the blade

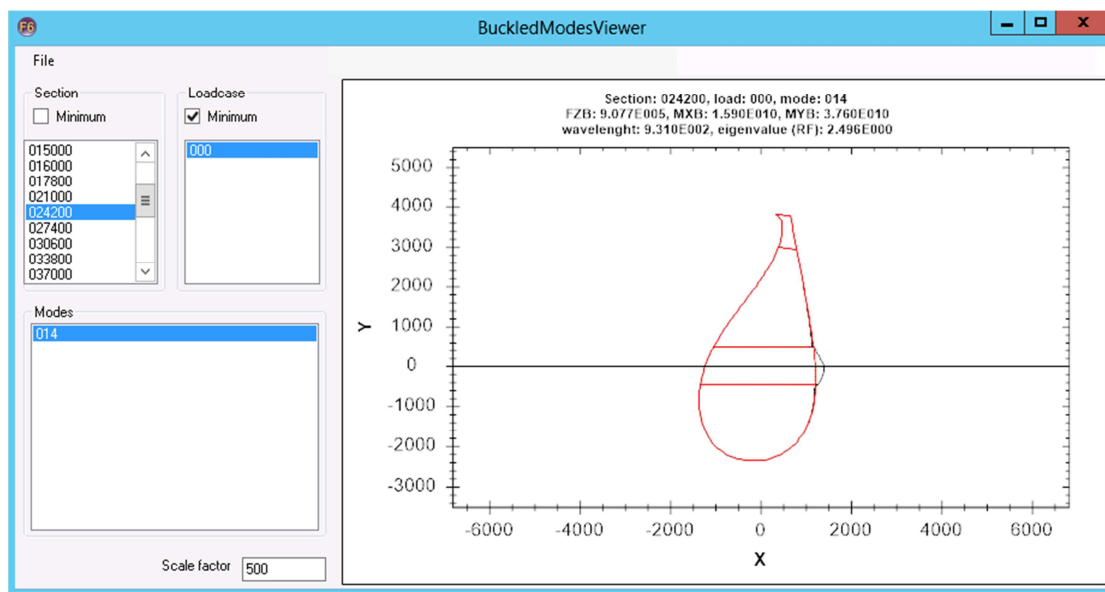


Figure 57 Buckling mode shape at z= 24.2 m

Although cross section based buckling analyses gives the lowest buckling load factor for design this value must be discarded, due to the boundary conditions at the blade root.

Taking into account the boundary conditions at the blade root the buckling load factor at the blade root is estimated 2.449 (including a partial safety factor of 2.042).

Results obtained with: MSC.MARC 2010

Additional buckling analysis is performed with MSC.MARC 2010 (Power sweep solution). using the same FE model as used for the extreme analyses

Buckling load factor (without partial safety factor) over reference load case: 3.085

Buckling load factor (including partial safety factor of 2.042) over reference load case: 1.511

The figure below shows the buckling mode:

buckling in the CAP at z=25.9 m (half wave length= 1.15 m)

In addition buckling of the trailing edge at z= 56 m.

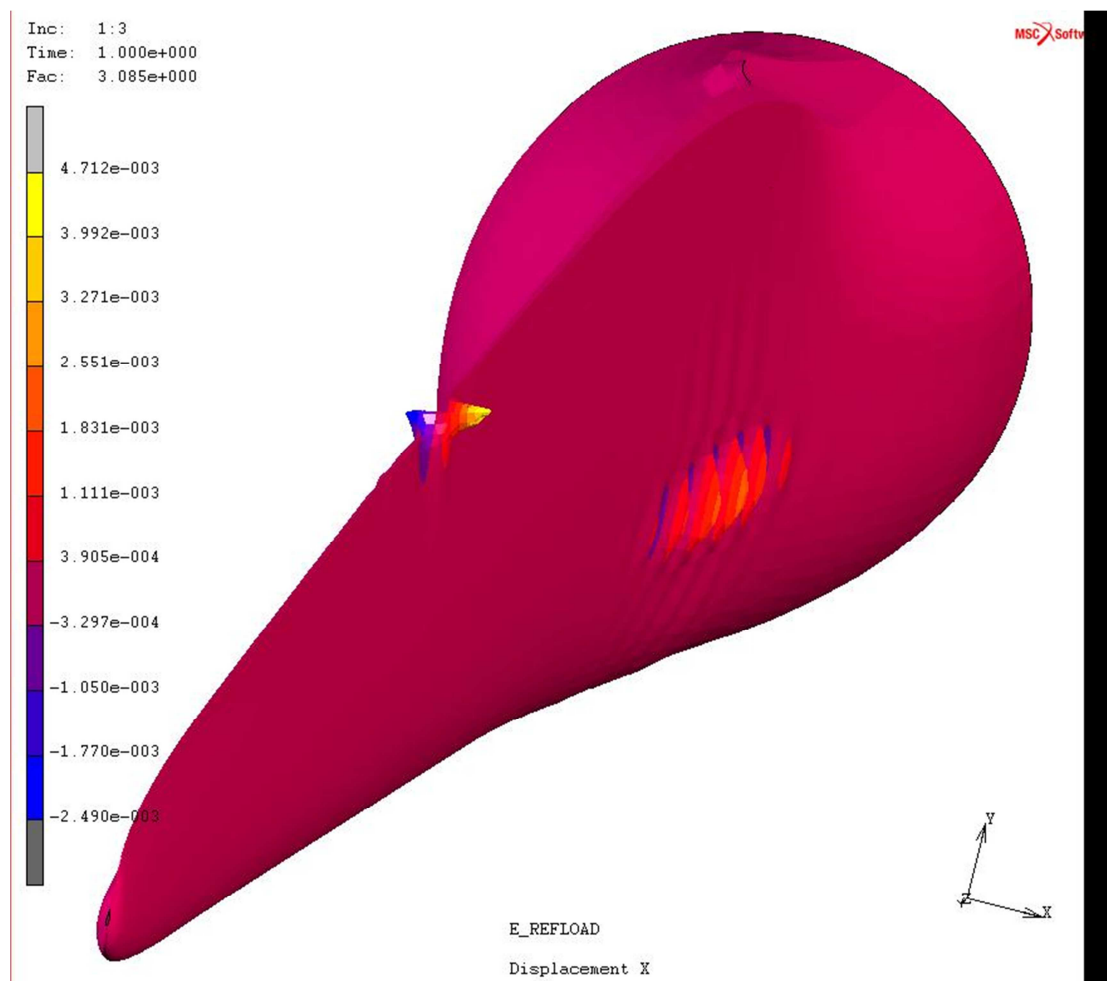


Figure 58 Buckling load factor MSC.MARC 2010

Extreme load carrying capacity analysis

Extreme load carrying capacity multiplication factor (static strength under **reference** case): 0.45

Extreme load carrying capacity multiplication factor breakdown per material:

UNIAX = 0.53 mode IFF_C at nose and trailing edge panels near the first part of spar caps (at about z 27 m)

TRIAx = 0.53 suction side of the blade, nose panel, IFF mode_B

BIAX = 0.50 shear webs at intersection with spar cap, IFF mode_A

BALSA = 0.45 mode compression failure: nose panel at suction side of the blade

See also the images in the Appendix: Extreme load analysis results.

2.2 Reference blade sections results

Mass properties of reference blade sections

Table 2. Mass properties of reference blade sections

Property		Sec_1	Sec_2	Sec_3	Sec_4	Sec_5
Z-position	(m)	2.8	26.694	37.907	54.149	71.592
Mass/Length	(kg/m)	1202.700	647.470	518.130	345.200	165.290
Mass Centre	x (m)	0	-0.271	-0.226	-0.143	-0.099
	y (m)	0.001	0.081	0.04	0.035	0.019
Mass moment of inertia (ρI)	ρI_{xx} (kg-m)	4.060E+03	5.236E+02	2.246E+02	6.182E+01	1.263E+01
	ρI_{yy} (kg-m)	3.730E+03	1.693E+03	1.013E+03	3.608E+02	7.506E+01
	ρI_{xy} (kg-m)	-4.838E+00	-2.254E+02	-1.106E+02	-1.747E+01	4.309E-01
Polar mass inertia (ρI_p)	ρI_p (kg-m)	7.789E+03	2.216E+03	1.237E+03	4.226E+02	8.769E+01

Stiffness properties of reference blade sections

Table 1. Stiffness properties of reference blade sections

Property		Sec_1	Sec_2	Sec_3	Sec_4	Sec_5
Z-position	(m)	2.800	26.694	37.907	54.149	71.592
Axial Stiffness	EA (N)	1.78E+10	9.29E+09	7.75E+09	5.39E+09	2.65E+09
Elastic Centre	x (m)	0.004	-0.142	-0.066	-0.010	-0.026
	y (m)	-0.0006	0.0560	0.0185	0.0260	0.0183
Bending Stiffness	$E I_{xx}$ (Nm ²)	6.26E+10	8.91E+09	3.93E+09	1.12E+09	2.34E+08
	$E I_{yy}$ (Nm ²)	6.08E+10	2.17E+10	1.30E+10	4.62E+09	9.86E+08
	$E I_{xy}$ (Nm ²)	2.07E+07	-2.92E+09	-1.41E+09	-2.14E+08	7.80E+06
Shear Centre	x (m)	0.027	0.582	0.514	0.391	0.230
	y (m)	-0.001	0.056	0.018	0.026	0.018
Torsional Stiffness	GJ (Nm ²)	2.63E+10	1.73E+09	6.91E+08	2.08E+08	5.28E+07
Shear Stiffness	S_x (N)	1.95E+09	7.03E+08	5.00E+08	3.43E+08	2.00E+08
	S_y (N)	2.57E+09	4.72E+08	3.28E+08	1.84E+08	9.95E+07

Extreme load carrying capacity analysis under simple load case

Displacements for reference blade sections under the simple load case application

Table 2. Displacement solution under simple load case for RefSection_2 (26.694m)

Key point No.	Key Point Coordinates			Displacement solution simple case		
	x [m]	y [m]	z [m]	x [m]	y [m]	z [m]
1	-3.875	0.332	26.694	0.200	0.446	0.062
5	0.009	-1.123	26.694	0.175	0.402	0.057
9	2.290	-0.306	26.694	0.188	0.408	-0.028
13	0.035	1.127	26.694	0.210	0.402	-0.056

Table 1. Displacement solution under simple load case for RefSection_3 (37.907m)

Key point No.	Key Point Coordinates			Displacement solution simple case		
	x [m]	y [m]	z [m]	x [m]	y [m]	z [m]
1	-3.686	0.295	37.907	0.508	1.322	0.093

Key point No.	Key Point Coordinates			Displacement solution simple case		
	x [m]	y [m]	z [m]	x [m]	y [m]	z [m]
5	0.043	-0.842	37.907	0.490	1.292	0.094
9	1.981	-0.183	37.907	0.500	1.261	-0.045
13	0.040	0.812	37.907	0.514	1.292	-0.090

Table 2. *Displacement solution under simple load case for RefSection_4 (54.149m)*

Key point No.	Key Point Coordinates			Displacement solution simple case		
	x [m]	y [m]	z [m]	x [m]	y [m]	z [m]
1	-2.844	0.088	54.149	1.220	4.215	0.131
5	0.014	-0.527	54.149	1.203	4.167	0.136
9	1.529	-0.047	54.149	1.215	4.127	-0.064
13	0.007	0.560	54.149	1.230	4.167	-0.136

Table 3. *Displacement solution under simple load case for RefSection_5 (71.592m)*

Key point No.	Key Point Coordinates			Displacement solution simple case		
	x [m]	y [m]	z [m]	x [m]	y [m]	z [m]
1	-1.895	-0.046	71.952	2.265	10.598	0.150
5	-0.025	-0.336	71.952	2.252	10.532	0.167
9	1.018	0.027	71.952	2.267	10.486	-0.068
13	-0.030	0.366	71.952	2.281	10.532	-0.160

Layer strains and/or stresses at key points of reference sections under simple load case
See excel file: WMC_structural_benchmark_strains_stresses_v1.xlsx

Extreme load carrying capacity analysis under reference load case

Displacements for reference blade sections under the reference load case application

Table 4. *Displacement solution under reference load case for RefSection_2 (26.694m)*

Key point No.	Key Point Coordinates			Displacement solution reference case		
	x [m]	y [m]	z [m]	x [m]	y [m]	z [m]
1	-3.875	0.332	26.694	0.201	0.435	0.066
5	0.009	-1.123	26.694	0.178	0.404	0.059
9	2.290	-0.306	26.694	0.189	0.412	-0.028
13	0.035	1.127	26.694	0.208	0.404	-0.055

Table 5. *Displacement solution under reference load case for RefSection_3 (37.907m)*

Key point No.	Key Point Coordinates			Displacement solution reference case		
	x [m]	y [m]	z [m]	x [m]	y [m]	z [m]
3	1	-3.686	0.295	37.907	0.508	1.310
3	5	0.043	-0.842	37.907	0.496	1.301
3	9	1.981	-0.183	37.907	0.502	1.280
3	13	0.040	0.812	37.907	0.511	1.301

Table 6. *Displacement solution under reference load case for RefSection_4 (54.149m)*

Key point No.	Key Point Coordinates			Displacement solution reference case		
	x [m]	y [m]	z [m]	x [m]	y [m]	z [m]
1	-2.844	0.088	54.149	1.215	4.197	0.133
5	0.014	-0.527	54.149	1.206	4.183	0.140
9	1.529	-0.047	54.149	1.212	4.161	-0.060
13	0.007	0.560	54.149	1.219	4.183	-0.134

Table 7. *Displacement solution under reference load case for RefSection_5 (71.592m)*

Key point No.	Key Point Coordinates			Displacement solution reference case		
	x [m]	y [m]	z [m]	x [m]	y [m]	z [m]
1	-1.895	-0.046	71.952	2.242	10.567	0.151
5	-0.025	-0.336	71.952	2.235	10.539	0.170
9	1.018	0.027	71.952	2.243	10.516	-0.062
13	-0.030	0.366	71.952	2.250	10.539	-0.155

Layer strains and/or stresses at key points of reference sections under reference load case

See excel file: WMC_structural_benchmark_strains_stresses_v1.xlsx

3 References

- [1] Failure analysis of FRP laminates by means of physically based phenomenological models, A. Puck and H. Schürmann, Composites Science and Technology 58 (1998) 1045–1067
- [2] Guidelines for the determination of the parameters in Puck's action plane strength criterion, A. Puck, J. Kopp and M. Knops, Composites Science and Technology 62 (2002) 371–378
- [3] Development of FRP components (fibre reinforced plastics) Analysis, VDI2014 Part 3, september 2006
- [4] DTU Wind Energy Report-I-0094, Christian Bak, Frederik Zahle, et al., DTU, 2013.

Appendix: Extreme load analysis results

Table 4 Puck results UNIAX

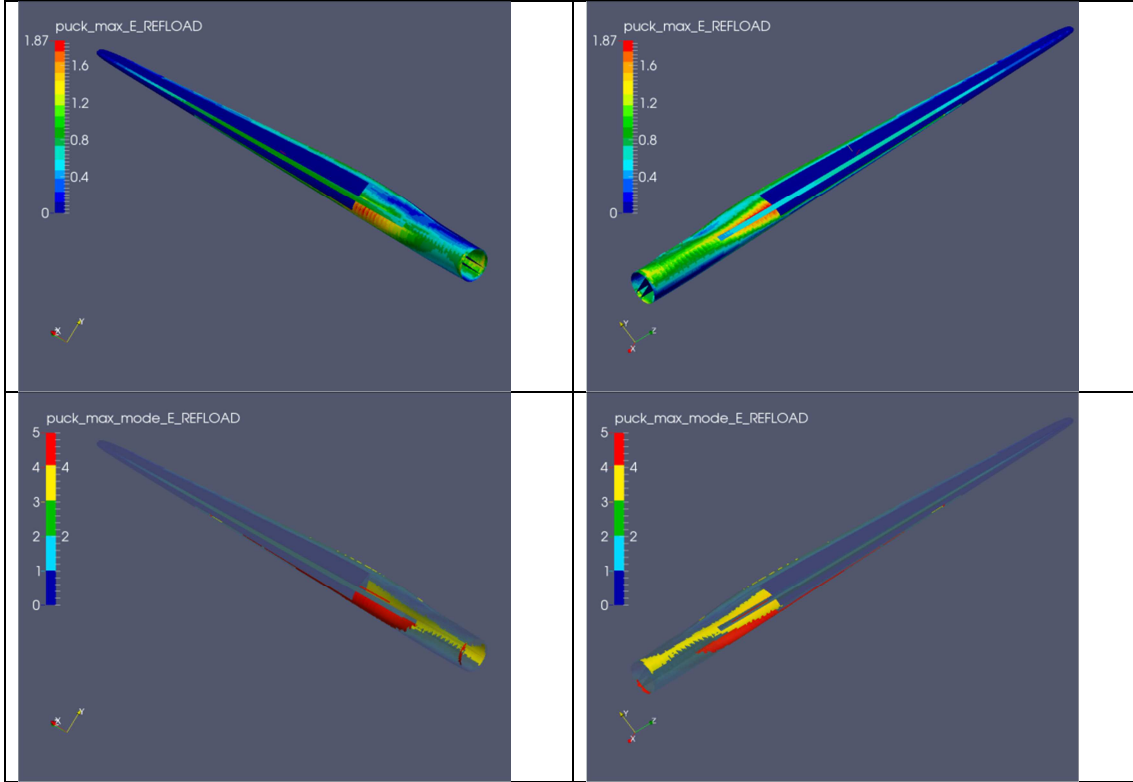


Table 5 Puck results TRIAX

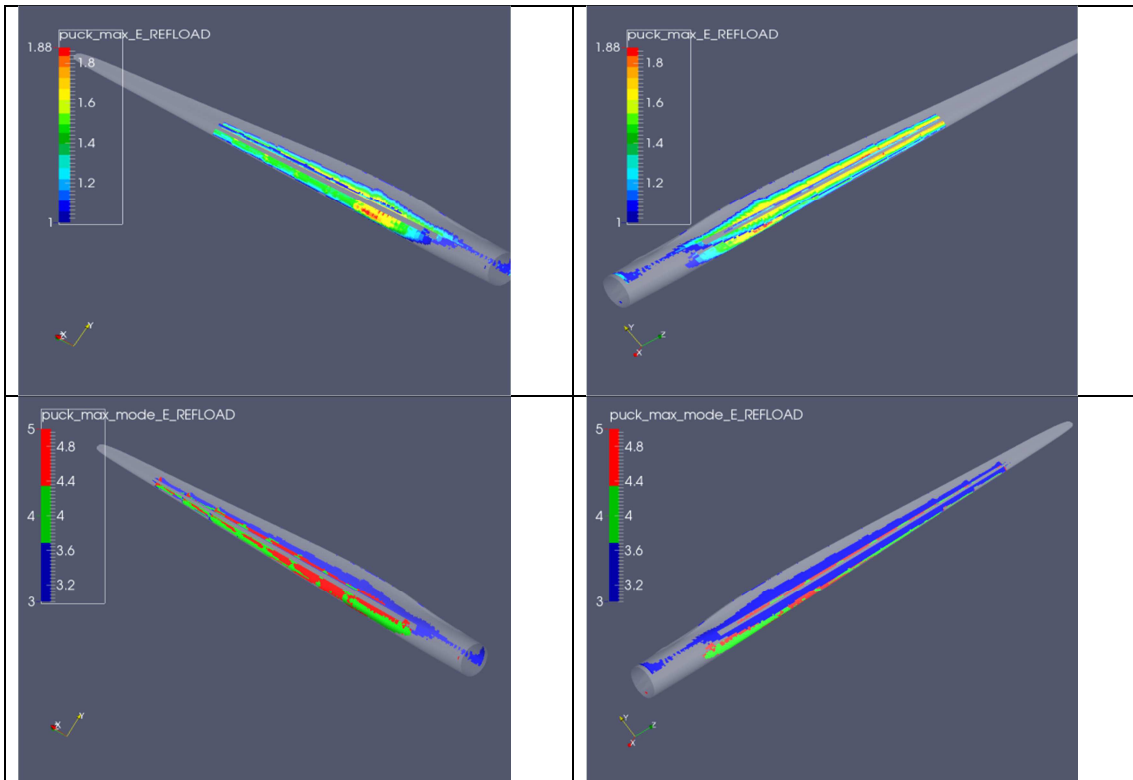


Table 6 Puck results BIAx

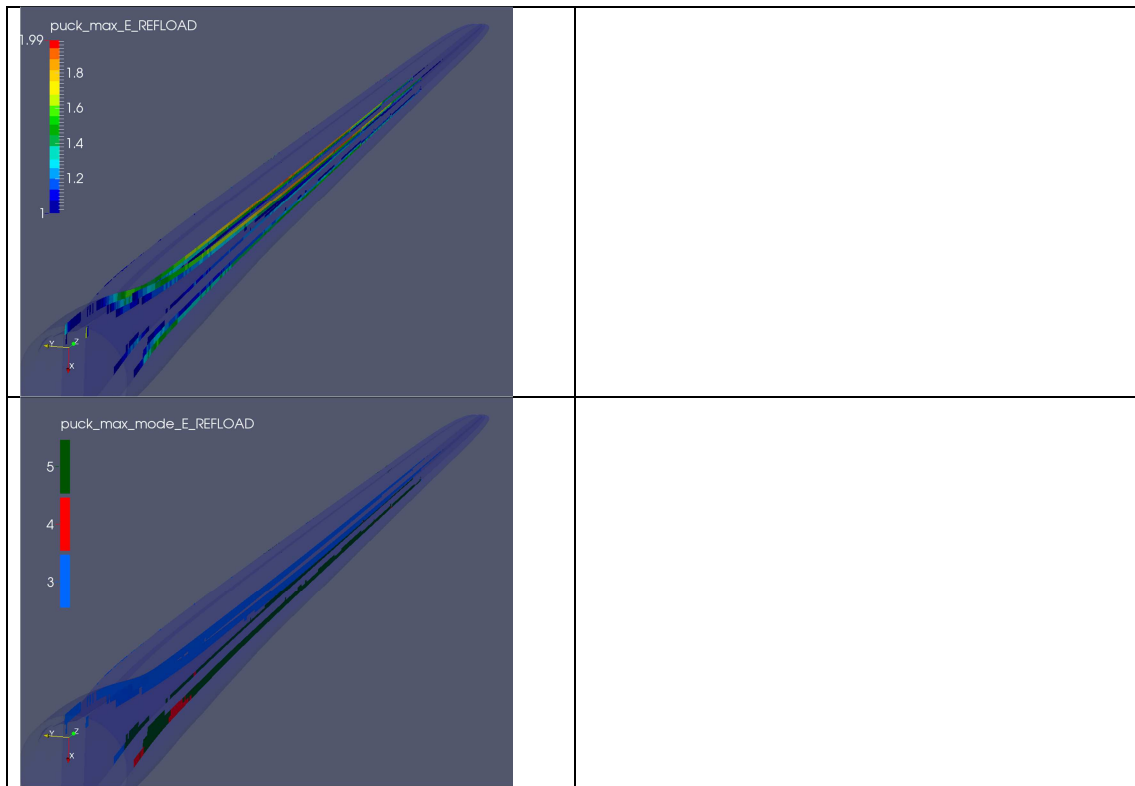


Table 7 Puck results BALSA

